UNIVERSIDAD AUTÓNOMA DE NUEVO LEÓN
FACULTAD DE ECONOMÍA
DIVISION DE ESTUDIOS DE POSGRADO

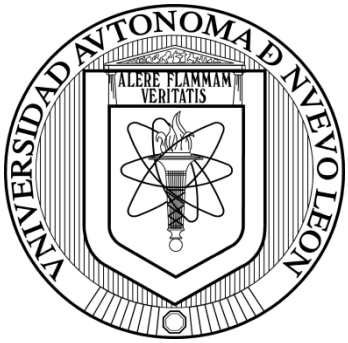

THREE ESSAYS ON THE IMPACT OF EXTERNALITIES

Por

JOSÉ EDUARDO CASTRO PÉREZ

Tesis presentada como requisito parcial para
obtener el grado de Doctorado en Ciencias Económicas

Julio, 2024

THREE ESSAYS ON THE IMPACT OF EXTERNALITIES

José Eduardo Castro Pérez

Comité de tesis:

Director principal	**DR. DANIEL FLORES CURIEL** Facultad de Economía, UANL
Sinodal	**DR. JULIO CÉSAR ARTEAGA GARCÍA** Facultad de Economía, UANL
Sinodal	**DR. EDGAR M. LUNA DOMÍNGUEZ** Facultad de Economía, UANL
Sinodal	**DRA. EVA O. ARCEO GÓMEZ** Centro de Investigación y Docencia Económicas, A.C.
Sinodal	**DRA. PAULINA OLIVA VALLEJO** Economics Department, U. of Southern California

DR. ERNESTO AGUAYO TÉLLEZ
Director de la División de Estudios de Posgrado
Facultad de Economía, UANL
Julio, 2024.

A mi esposa Mar y mis padres.

“Esa luz que ha iluminado al sabio espera
Tus brazadas, las más largas, la búsqueda es el camino
Esa luz no va a golpear jamás tus puertas
Anda y nada en sombras a su encuentro”.

—Los Espíritus, Esa luz.

Acknowledgments

Writing this thesis would not have been possible without the support and trust of many people and institutions. First, I thank my wife and my parents for their love, understanding and company throughout the preparation of this thesis.

I give special thanks to Dr. Daniel Flores, for directing my master's and doctoral theses. Thank you for listening and your genuine interest to each idea and/or research question that I have posed to you. Thank you for your time and comments that have greatly enriched me as a researcher and person. Thank you for your example, trust and patience. I couldn't choose a better mentor to direct my doctoral thesis. I hope we can continue working to approach the many research questions that remained left to be answered.

I thank Dr. Julio César Arteaga, for his trust and the opportunity to begin my master's studies at the Facultad de Economía, UANL back in 2013. Thanks to Dr. Ernesto Aguayo for his trust and support, and especially for giving me the opportunity to have my first approach to academic research, conducting a research stay abroad with Dr. José N. Martínez in 2014. I am also grateful to Dr. Pedro Villezca, together with the Graduate Academic Committee—integrated by Dr. Joana Chapa, Dr. Jorge Valero, and Dr. Daniel Flores—for allowing me to rejoin the Facultad de Economía, UANL to continue my doctoral studies in 2020.

I am fortunate to have studied at an excellent institution with a great administrative support team and exceptional professors with outstanding human quality, dedication, academic rigor, and passion for economics. I am grateful to all my professors for their teachings and tools provided that have allowed me to develop the competencies and skills to write this doctoral thesis. I especially thank Dr. Julio César Arteaga, Dr. Jorge Moreno, Dr. Edgar Luna, Dr. Leonardo Torre, Dr. Joana Chapa, Dr. Edgardo Ayala, Dr. Cynthia Caamal, and Dr. Lorenzo Blanco, for teaching me their courses during my doctoral studies.

Thanks to Dr. Eva Arceo and Dr. Paulina Oliva, for their indirect motivation and academic inspiration to write high-quality research articles on relevant topics with public policy implications for the country. Thank you also for accepting the invitation to join my Doctoral Thesis Committee.

I thank the National Council of Science and Technology (Conacyt) for their financial support provided through the national scholarship program that allowed me to carry out my doctoral studies. I also thank the transparency unit of the Ministry of the Environment in Nuevo León and Mexico City for responding to my requests for public information, giving me access to two databases essential for the completion of the first and third chapter of this thesis. I also thank Strava Metro for accepting a partnership that allowed me to access the main dataset used in the third chapter of this thesis.

This thesis, together with the results, conclusions, and recommendations derived from it, as well as any unnoticed errors or omissions, remain my exclusive responsibility.

Content

Chapter 1. The effects of Cadereyta's refinery temporary shutdown on air quality and mortality

Executive Summary

The Cadereyta refinery is the third largest of the six that exist in Mexico. It processes around 17% of the crude oil refined in the country (Mexican Ministry of Energy, 2021a). This oil is used to produce—mainly—gasoline and diesel. Unfortunately, the refinery emits air pollutants while these goods are produced, affecting the inhabitants of the Monterrey´s Metropolitan Area (MMA).

The harmful health effects generated by refineries have been studied mainly in developed countries. For example, it has been shown that refinery operations increase the number respiratory-related hospital admissions and visits (Burr et al., 2018; Du, 2023; Lavaine & Neidell, 2017), or cause longer stays (Lavaine, 2016). Their adverse consequences may be accentuated if the exposition is prolonged; particularly, for vulnerable groups such as newborns (Lavaine & Neidell, 2017) and elders (Lavaine, 2016).

Although gasoline and diesel production are important economic activities in the country, it is natural to ask how big is the externality that the Cadereyta refinery generates—in terms of air quality and health—for the inhabitants of the MMA. In this chapter, we take advantage of an unscheduled 6-day shutdown—occurred in July 2016—to assess the effects of Cadereyta's refinery on air quality and mortality in the MMA.

This chapter uses a regression discontinuity in time (RDiT) approach, comparing—through a time-series econometric model that controls for various factors—the concentration of pollutants and mortality registered in the days before and after the refinery shutdown, with the days in which the refinery was kept temporarily out of operations. This method has been widely used in similar studies.

According to our estimations, the temporary shutdown of the refinery caused a local reduction of 12.8% in sulfur dioxide concentrations. In addition, the concentrations of $PM_{2.5}$ and PM_{10} in the MMA decreased by 30%; even in areas located up to 60 km away from the refinery. On the other hand, we estimate that the 6-day shutdown prevented the deaths of 8 persons, which translates to a reduction of 2.4% in daily mortality from internal causes in the MMA. Those who benefited the most from the temporary absence of the Cadereyta refinery were children 5 years and younger, with a 9% reduction in daily mortality from internal causes.

As far as we know, this study is the first finding significant effects of oil refineries on particulate matter concentrations. This is important because previous studies on refineries have usually focused on sulfur dioxide and, therefore, consider that their polluting effects are local. This chapter shows that the dispersion of pollutants can extend the effects of refineries to areas far from the emission source. Even if an emitted primary pollutant such as sulfur

dioxide poses only a local risk, its subsequent conformation in secondary pollutant—as particulate matter—can travel long distances affecting remote areas.

The estimates from this chapter can be used to conduct a back of the envelope calculation of the refinery's effects on pollution and health on an annual basis. For instance, without the pollution emitted by the refinery, the official standards for the concentrations of particulate matter in the MMA would be met more frequently. Hence, if the concentrations of PM_{10} would have been reduced by 33.1% throughout 2016, the number of days above the maximum permissible limit would have changed from 212 to only 77 days. Similarly, a reduction of 27.1% in the concentrations of $PM_{2.5}$ would have reduced the number of days above the standard from 29 to 4. On the other hand, the estimated figures suggest that if pollutants emitted by the Cadereyta refinery could be eliminated, 471 premature deaths would be avoided annually in the MMA.

Full text

1.1. Introduction

Even the simplest economic activity requires some form of energy. In Mexico this need is predominantly attended with fossil fuels, namely: coal (3%), gas (47%) and oil (38%) (BP, 2022). Refineries have a key role fulfilling the increasing demand for energy. They transform crude oil into a variety of products that we use mainly for transportation—for example, gasoline and diesel—and industrial activities such as electricity generation, petrochemical manufacturing, construction, etc.

Unfortunately, refining oil conveys the emission of air pollutants that pose an external cost to surrounding communities. According to Adebiyi (2022), their effects can range from simple annoyances—such as fatigue and irritation of the eyes—to severe damages. Refineries have been proved to increase respiratory-related hospital admissions and visits (Burr et al., 2018; Du, 2023; Lavaine & Neidell, 2017) or cause longer stays (Lavaine, 2016). Their adverse consequences may be accentuated if the exposition is prolonged; particularly, for vulnerable groups such as newborns (Lavaine & Neidell, 2017) and elders (Lavaine, 2016). In addition, pollutants cause other external costs such as the reduction of work hours (Hanna & Oliva, 2015), changes in the values of properties (Lavaine, 2019), and even crime and aggressive online behavior (Du, 2023).

In this article, we use a regression discontinuity in time (RDiT) approach—taking advantage of an unscheduled 6-day shutdown—to assess the effects of Cadereyta's refinery on air quality and mortality in Monterrey´s Metropolitan Area (MMA)[1]. We argue that this

[1] The MMA is composed of 9 municipalities: Apodaca, García, General Escobedo, Guadalupe, Juárez, Monterrey, San Nicolás de los Garza, San Pedro Garza García, and Santa Catarina (State Government of Nuevo León, 2020). The municipality of Cadereyta is located next to Juárez. According to the latest population census, there are 4.6 million inhabitants in MMA (INEGI, 2020).

temporary shutdown—which occurred during July of 2016—created a neat natural experiment for several reasons. First, the event was not strategically planned by Petróleos Mexicanos (PEMEX). It was held for safety reasons in response to the reduction in water pressure of Ramos River. Second, it was short enough not to interrupt the supply of fuel, allowing drivers in the MMA to continue with their routinary journeys[2]. Third, it didn't affect other economic activities that may also impact pollution. For instance, the demand for transportation services by workers of the refinery was not affected because they kept attending to conduct administrative and cleaning tasks[3]. Similarly, it did not affect refined product prices, because they were set by the government. In summary, the only change was the abrupt temporal disruption of the refinery's productive process.

There are only a few studies that estimate Cadereyta's refinery contribution to air pollution: the bottom-up emissions inventories by State Government of Nuevo León (2008, 2016a) and the estimated annual emissions of sulfur dioxide obtained with satellite measurements from the ozone monitoring instrument (OMI) (Fioletov et al., 2016). However, emission inventories are costly, require a large amount of information—often self-reported by the refinery—and its reliability depends on many parameters that are difficult to estimate (SEMARNAT, 2013). More importantly, inventories only account for the emission of primary pollutants.

Previous studies about refineries have been mainly conducted in developed countries such as France, US, and Canada (Burr et al., 2018; Du, 2023; Lavaine, 2019, 2016; Lavaine & Neidell, 2017) and focus on their local impacts, no more than 20 km away from their location (Burr et al., 2018; Du, 2023; Hanna & Oliva, 2015; Lavaine, 2019, 2016; Lavaine & Neidell, 2017). Moreover, except for Du (2023)—who considers volatile organic compounds ($VOCs$)—these studies focus on sulfur dioxide (SO_2) concentrations. The idea that only nearby inhabitants are exposed and affected by the refinery is not correct. Even if an emitted primary pollutant such as sulfur dioxide poses only a local risk—as suggested by previous studies—its subsequent conformation in secondary pollutant—as particulate matter—can travel long distances affecting remote areas.

As expected, we find that the 6-day shutdown of the refinery led to a 12.8% local reduction of the concentrations of SO_2. However, it also diminished roughly 30% the concentrations of $PM_{2.5}$ and PM_{10} in the MMA, 60 km away from the refinery. Furthermore, it prevented the deaths of 8 persons, which translates to a reduction of 2.4% in daily mortality from internal causes in the MMA. The most benefited from the temporary shutdown of the refinery

[2] "Pemex garantiza abasto ante paro en refinería en Cadereyta", *El Horizonte*, July 22, 2016. Available at: https://www.elhorizonte.mx/finanzas/pemex-garantiza-abasto-paro-refineria-cadereyta/1672657

[3] "Refinería de Cadereyta deja de producir millones", *Milenio*, July 21, 2016. Available at: https://www.milenio.com/estados/refineria-de-cadereyta-deja-de-producir-millones

were children 5 years and younger, for whom daily mortality from internal causes was reduced 9%.

As far as we know, our work is the first finding significant effects of oil refineries on particulate matter concentrations, which provides insight into the extent to which pollutant dispersion can extend refinery externalities over areas far away from the emitting source. In addition, it is the first study estimating the effect on mortality for any of the refineries in Mexico. A back of the envelope calculation suggests that the permanent absence of the refinery could prevent 471 annual deaths from internal causes in the MMA. Additionally, it may substantially improve compliance with official standards for particulate matter in the city. Therefore, policymakers should correctly weigh the costs and benefits of the current fossil-fuel oriented energy strategy in Mexico.

1.2. Institutional context

Cadereyta's refinery was inaugurated in 1979. It is the third largest in the country and belongs to the state-owned monopoly PEMEX. It processes an average of 116 thousand barrels of oil per day, which is about 17% of the total crude oil refined in México between 2016 and 2021 (Mexican Ministry of Energy, 2021a). As shown in Figure 1.1, 70% of its refined products are gasoline and diesel. However, it also produces fuel oil, liquified and dry gas, jet fuel, asphalt, as well as other refined products.

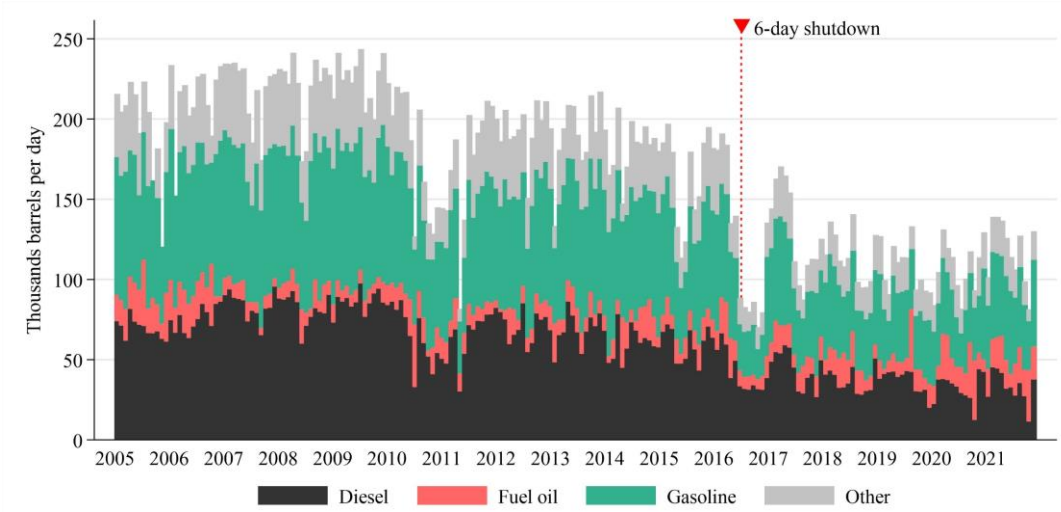

Figure 1.1. Refined products by the Cadereyta's refinery. *Source*: Prepared using monthly data from the Energy Information System of the Mexican Ministry of Energy (2021b).

The refinery is recognized as a big contributor to air and water pollution in the city. Its presence has been widely criticized since its inauguration. According to Flores Torres and Robles (2015), it was initially opposed by the population and farmers because it demanded a

large amount of water. After an oil spill that contaminated the San Juan River in 2014[4], a group of local stakeholders—including inhabitants of the surrounding communities—summoned federal and local authorities to inspect water discharges from the refinery[5]. Among other things, this group urged for air quality studies related to the operations of the refinery. Surprisingly, it was not until mid-2017 that a monitoring station was installed in the municipality of Cadereyta[6].

Mexican refineries are required to recover 90% of the sulfur contained in the crude oil, net of the sulfur allowed for their refined products[7]. Nonetheless, the Cadereyta's refinery has been included in a global catalog of large sources of sulfur dioxide (SO_2) detected from space with average annual emissions estimated at 37.98 thousand tons of SO_2 during the period 2005-2021 (Fioletov et al., 2016)[8]. Additionally, the refinery has been highlighted as one of the main sources of $PM_{2.5}$ in the MMA, based on chemical characterizations from downwind samples at the northwest and southwest of the MMA (Martínez et al., 2012; Martínez-Cinco et al., 2016).

Local authorities have also acted against the refinery. Nonetheless, all these actions have been discarded at the federal level. Refineries—as country-owned companies—are envisioned as a key asset to achieve gasoline and diesel self-sufficiency[9]. For instance, Mexico started the construction of a new refinery in the municipality of Paraíso, Tabasco. Furthermore, Mexico enunciated a national refining plan that includes the renovation of its 6 refineries, aiming an increase of the national supply of gasoline and diesel.

1.3. Related literature

Previous studies have demonstrated that exposition to air pollution results in adverse health effects. Symptoms can range from coughing (Du, 2023; Gupta & Spears, 2017) to more serious respiratory diseases that require hospital—or emergency department—admissions (Burr et al., 2018; Du, 2023; Lavaine & Neidell, 2017; Pope, 1989), a longer stay

[4] "Oil spill that fouled Mexican river will take months to clean up", *Reuters*, August 21, 2014. Available at: https://www.reuters.com/article/us-mexico-pemex-spill-idUSKBN0GL29620140821

[5] "A un año del derrame de un ducto de PEMEX en Cadereyta Jiménez, N.L, la contaminación causada por la Refinería sigue vigente", *Ciudadanos en Apoyo a los Derechos Humanos, A.C.*, August 17, 2015. Available at: https://cadhac.org/a-un-ano-del-derrame-de-un-ducto-de-pemex-en-cadereyta-jimenez-n-l-la-contaminacion-causada-por-la-refineria-sigue-vigente/

[6] "Inauguran estación de Monitoreo Ambiental en Cadereyta", Milenio, August 21, 2017. Available at: https://www.milenio.com/politica/inauguran-estacion-de-monitoreo-ambiental-en-cadereyta

[7] The percentage of sulfur to be recovered from the oil refining processes is established in the Mexican official norm NOM-148-SEMARNAT-2006. In addition, NOM-016-CRE-2016 establishes the required quality of petroleum products, which includes for example, the maximum content of sulfur in gasoline and diesel.

[8] The updated global catalogue was obtained from: https://so2.gsfc.nasa.gov/measures.html

[9] "AMLO promete que la autosuficiencia en gasolina y diésel vendrá… en 2023", *Forbes*, July 2, 2020. Available at: https://www.forbes.com.mx/economia-amlo-autosuficiencia-gasolina-diesel-2023/

at the hospital (Lavaine, 2016), and even to death (Brown & Tousey, 2020; Clancy et al., 2002; He et al., 2016; Pope et al., 1992, 2007).

The health effects of pollution are particularly harmful for vulnerable groups such as infants, children, and elders. Studies report that infants exposed to pollution, especially during the first and third quarter of pregnancy (Lavaine & Neidell, 2017), exhibit lower birth weight (Currie et al., 2015, 2022; Hill, 2018; Severnini, 2017; Yang & Chou, 2018), higher incidence of preterm birth (Casey et al., 2018; Parker et al., 2008; Yang & Chou, 2018), and higher mortality (Arceo et al., 2016; Barrows et al., 2019; Gutiérrez, 2015; He et al., 2016; Luechinger, 2014). Pre-school aged children have more visit to the hospital for respiratory-related diseases, as bronchitis and asthma (Komisarow & Pakhtigian, 2022; Pope, 1991), and face higher mortality risk (Martínez-Muñoz et al., 2020). Similarly, elders stay more at the hospital (Lavaine, 2016) and are more likely to die from pollution exposure (Anderson, 2020; Deryugina et al., 2019; He et al., 2016; Martínez-Muñoz et al., 2020).

Aguilar-Gómez et al. (2022) explain that pollution—through its effect on health—plays a key role in many other relevant areas of our life. For example, it impacts our labor productivity (Chang et al., 2019; He et al., 2019; Zivin & Neidell, 2012), labor supply (Hanna & Oliva, 2015), sports performance (Guo & Fu, 2019; Lichter et al., 2017; Mullins, 2018), school attendance (Komisarow & Pakhtigian, 2022; Ransom & Pope, 1992), cognitive function (la Nauze & Severnini, 2021), sleep (Heyes & Zhu, 2019), willingness to pay for housing (Currie et al., 2015; Davis, 2011; Galán González et al., 2021; Lavaine, 2019), and subjective well-being (Zhang et al., 2017). It can also lead to more road accidents (Sager, 2019) and crimes (Bondy et al., 2019; Burkhardt et al., 2019; Du, 2023; Herrnstadt et al., 2021).

Many of these studies use quasi-experimental research designs to estimate the health and non-health effects of pollution. As noted by Rich (2017), their advantage—with respect to observational studies—relays in its similarity with a controlled experiment. Our work relates mainly to studies that take advantage of the closing, suspension, expansion or opening of industrial plants to estimate their effects on pollution and other outcomes. These studies include diverse settings, such as: a steel mill in the Utah Valley (Parker et al., 2008; Pope, 1989, 1991; Pope et al., 1992; Ransom & Pope, 1992;); US copper smelters (Pope et al., 2007); coal-fired and nuclear power plants in the United States (Brown & Tousey, 2020; Casey et al., 2018; Davis, 2011; Davis & Hausman, 2016; Komisarow & Pakhtigian, 2022; Severnini, 2017; Yang & Chou, 2018), India (Barrows et al., 2019; Gupta & Spears, 2017), Germany (Bauer et al., 2017), and Mexico (Gutiérrez, 2015); as well as 1,600 industrial plants that emit toxic pollutants in the US (Currie et al., 2015).

Closer to our work, some studies assess the impact of oil refineries. For instance, Hanna and Oliva (2015) found that the permanent closure of the Azcapotzalco refinery reduced local concentrations of SO_2 (within 5 km from the refinery) almost 20% in Mexico City. Consequently, households near the refinery increased their labor supply in 3.5%. Similarly,

Lavaine (2016) finds that the permanent shutdown of the Flandres refinery reduced 30% the concentrations of SO_2 at Dunkirk in the north of France. The closure did not change monthly respiratory-related hospital admissions, but reduced their average duration in 1 day, especially for vulnerable groups as elders (more than 70 years), middle-aged adults (40-60 years) and young children (0-5 years). Finally, Burr et al. (2018) find an annual decrease in respiratory-related hospital admissions in the city of Oakville, Canada due to the permanent closure of the Petro-Canada Refinery.

The most recent studies focus on temporary and unexpected refinery shutdowns. For instance, Lavaine and Neidell (2017) examine a nationwide strike in France that resulted in an 18-day complete shutdown of 4 refineries in 2010. They find a highly localized (within 2 km from refineries) increase in weight and gestational age of newborns, particularly those exposed to the temporary shutdown during their first and third quarters of pregnancy. Additionally, monthly hospital admissions for asthma and bronchitis were locally reduced. More recently, Du (2023) studies the effects of unexpected refinery outages in the US. These pollution spikes trigger aggressive behaviors online, spreading violence to distant areas through social networks. Additionally, Du (2023) reports that unexpected refinery outages increase the number of hospital visits and spending on cough and sinus remedies from households near refineries (within 20 km). However, the author does not find a significant effect on daily mortality.

Our study is different from others for several reasons. First, except for Du (2023)—who measures volatile organic compounds ($VOCs$) within 20 km of the refineries using space observations—the rest of the studies focus on local sulfur dioxide (SO_2) concentrations. In contrast, our study takes into consideration that sulfur dioxide (SO_2) is a precursor of sulfate, an important component of secondary inorganic aerosol that can travel long distances and persist various days in the air (Weijers et al., 2010), which is one of the main constituents of $PM_{2.5}$ (Martínez et al., 2012; Martínez-Cinco et al., 2016). Therefore, our study contributes to the literature estimating—for the first time—the effect of refineries on particulate matter ($PM_{2.5}$ and PM_{10}), considering a wide geographical area (up to 60 km away from the refinery).

Second, unlike the nationwide strike studied by Lavaine and Neidell (2017), the temporary shutdown of the refinery did not affect other economic activities. Third, in contrast with the abnormal outages considered by Du (2023), our natural experiment did not cause excess pollutant emissions during its first day. Fourth, unlike refinery outages in the US (Chesnes, 2015; Kendix & Walls, 2010), the temporary shutdown we consider did not impact refined products prices because in Mexico gasoline and diesel prices were liberalized until 2017. Therefore, our setting keeps demand for transport unchanged. Fifth, we study the effects of the refinery temporary shutdown over a closer time window. For instance, our main results consider data within a 30-day window (i.e., including up to 30 days before and after the 6-day shutdown).

Sixth, like Du (2023), we explore the effect of the refinery on daily mortality. Nonetheless, Du (2023) concentrates on country-level general mortality of Medicare beneficiaries in the US. On the contrary, we obtain mortality data from administrative records (mostly, death certificates) and focus on mortality within the MMA. Furthermore, we disaggregate mortality by causes of death and age groups. Seventh, except for Burr et al. (2018) who use a segmented regression model with a yearly time series, all studies use panel data and report difference-in-difference estimates. Instead, we employ a regression discontinuity in time (RDiT) approach with hourly and daily time-series. Finally, except for Hanna and Oliva (2015), the impact of oil refineries has been studied mainly in developed countries such as France, US, and Canada. As suggested by Arceo et al. (2016) and Gupta and Spears (2017), these results may not be easily extrapolated to developing countries.

1.4. Impact on air quality

1.4.1. Data

We use hourly records of criteria pollutant concentrations and meteorological parameters that were compiled and facilitated by the Integrated Environmental Monitoring System (SIMA). The system is comprised of 14 monitoring stations distributed geographically—almost entirely—within the MMA. As shown in Figure 1.2, half of the stations are located within 40 km of the refinery's centroid. Whereas 6 stations are between 40 km and 60 km away. One of the stations—NO2—is in the municipality of Garcia, almost 70 km away from the refinery.

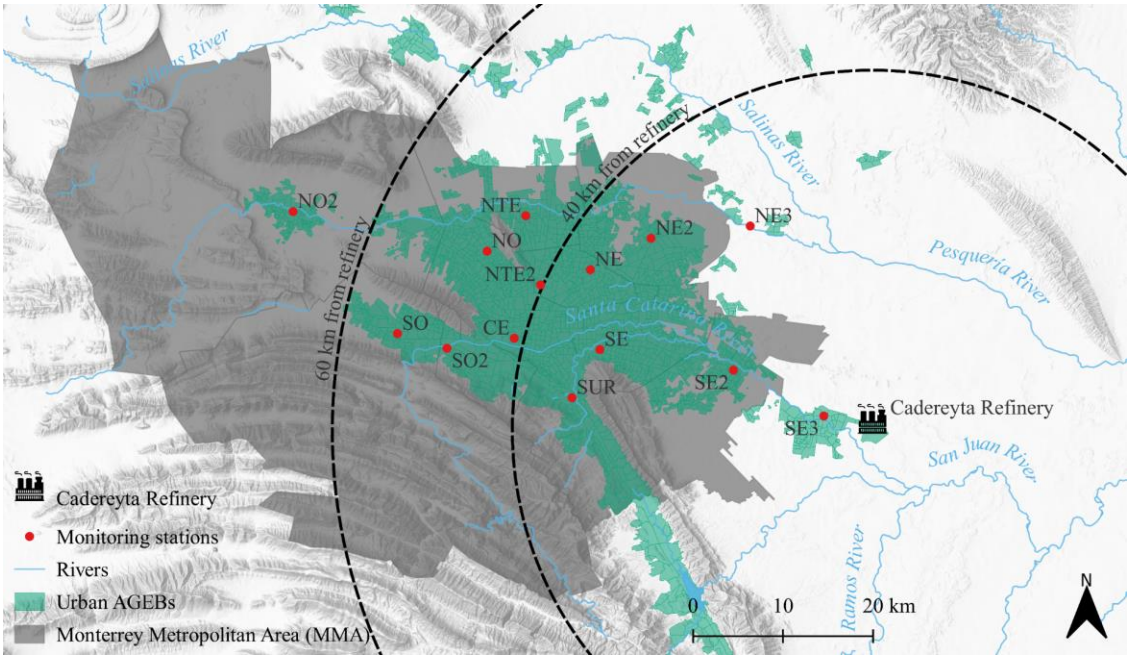

Figure 1.2. Map with locations of monitoring stations with respect to the Cadereyta's refinery. *Source*: Prepared with QGIS 3.22 using the location from monitoring stations of the Integrated Environmental Monitoring System (SIMA), urban area delimitation based on INEGI geostatistical framework, rivers' location extracted from OpenStreetMap, and an elevation basemap from Esri.

The pollutants we consider are carbon monoxide (CO), nitrogen dioxide (NO_2), ozone (O_3), particulate matter with aerodynamic diameter less than 10 micrometers (PM_{10}) and less than 2.5 micrometers ($PM_{2.5}$), and sulfur dioxide (SO_2). Meteorological parameters include temperature, relative humidity, wind speed and precipitation.

We focus on a period which is very close to the 6-day production shutdown that occurred from July 19 to July 24, 2016. Our main results are obtained with data from a total of 66 days between June 19 and August 23, including: 30 days before the event, 6 days during the refinery shutdown, and 30 days after the event. Hereinafter, we refer to this period as the 30-day window. However, an extension to our main methodology augments the 30-day window, including data one year before and after the refinery temporary shutdown. Specifically, from July 19 of 2015 to July 25 of 2017.

Not all monitoring station were reporting pollutant concentrations with the desired frequency during the period of this study. For this reason, our main results consider stations reporting at least 70% of the time within the 30-day window. That is, stations that compile and report at least 1,108 out of the 1,584 possible hourly records for each pollutant ($= 66\ days\ \times 24\ hours\ per\ day$)[10].

We construct aggregate measures for pollutants and meteorological parameters, averaging hourly records across stations based on their distance to the refinery (0-40 km, 40-60 km, or all stations). For example, in the case of PM_{10}, the first aggregate measure corresponds to an hourly average of PM_{10} across stations within 40 km of the refinery, reporting more than 70% of the time during the 30-day window. As Chen and Whalley (2012), we treat hourly pollutant records as missing when a station reports a 0 value. Conversely, if the stations do not report precipitation for a given hour, we treat it as a 0 (no rain).

Table 1.1. Descriptive statistics for aggregate measures

	0-40 km				40-60 km			
	30 days before and after the event		During 6-day shutdown		30 days before and after the event		During 6-day shutdown	
	Obs.	Mean	Obs.	Mean	Obs.	Mean	Obs.	Mean
CO	1440	0.51	144	0.51	1,440	0.52	144	0.46
(ppm)		(0.15)		(0.08)		(0.14)		(0.11)
NO_2	1,203	9.33	132	8.64	1,440	6.17	144	5.05
(ppb)		(3.81)		(2.16)		(2.28)		(1.76)
O_3	1,440	23.34	144	23.84	1,440	23.79	144	25.71
(ppb)		(13.22)		(9.95)		(17.19)		(14.69)
PM_{10}	1,440	52.26	144	38.86	1,440	54.91	144	37.56
$(\mu g/m^3)$		(20.65)		(11.59)		(24.55)		(13.82)
$PM_{2.5}$	1,142	33.11	114	20.69	1,328	22.03	126	16.29

[10] In fact, most of the stations we consider report with higher frequency, meaning at least 85% of the time. However, we opted for the 70% level so we can report results for $PM_{2.5}$.

$(\mu g/m^3)$		(23.34)		(11.76)		(11.73)		(9.71)
SO_2	1,437	5.48	144	5.04	1,433	6.94	144	6.89
(ppb)		(1.86)		(1.52)		(2.74)		(2.50)
Temperature	1,440	29.10	144	29.22	1,440	28.41	144	28.44
$(°C)$		(4.28)		(4.17)		(3.90)		(3.72)
Humidity	1,440	61.89	144	58.67	1,440	60.61	144	58.03
(%)		(18.56)		(17.13)		(16.71)		(15.31)
Wind speed	1,440	3.15	144	3.28	1,440	2.60	144	2.83
(m/s)		(1.30)		(1.19)		(1.17)		(1.11)
Precipitation	1,440	0.11	144	0.01	1,440	0.01	144	0.02
(mm/h)		(0.85)		(0.11)		(0.08)		(0.13)

Notes: Aggregates are obtained averaging measures across stations that report at least 70% of the time within the 30-day window. Standard deviations are in parentheses. Figures presented with rounding to 2 decimal places.

Table 1.1 summarizes aggregated measures before and after the 6-day shutdown and compares them with pollutants and meteorological parameters during the event. As we can see, the weather is almost identical during both periods. However, some pollutants—as PM_{10} and $PM_{2.5}$—exhibit substantial drops of about 40 to 48 per cent, respectively, during the refinery temporary shutdown. Other pollutants, such as sulfur and nitrogen dioxides, decrease marginally.

1.4.2. Empirical strategy

It is not easy to estimate the contribution of Cadereyta's refinery to pollutant concentrations in the MMA. There are many other sources of air pollution—changing with time—that cannot be fully accounted in a simple time series regression framework. Moreover, the refinery can strategically adjust its production to comply with regulations or avoid community complains, generating a reverse causality problem. In fact, it has been reported that emissions from the refinery are higher during the night and early morning when most of the inhabitants of the MMA sleep[11].

RDiT is a suitable empirical framework to overcome some of the difficulties of estimating the effect of Cadereyta's refinery on air pollution. As reviewed by Hausman and Rapson (2018), RDiT has been widely used to estimate the treatment effects of environmental and energy policies. Following this approach, we can take advantage of the 6-day unscheduled shutdown of the refinery comparing the concentration of criteria pollutants in the absence of the refinery with the concentration of the same pollutants when the refinery was operating under comparable conditions (30 days before and after the event).

[11] "Acelera la Refinería aire sucio de noche", *El Norte*, March 13, 2022. Available at: https://www.elnorte.com/aplicacioneslibre/preacceso/articulo/default.aspx?__rval=1&urlredirect=/acelera-la-refineria-aire-sucio-de-noche/ar2366530

Hence, our basic model regress pollutant concentrations, y_t, in natural logarithms on the indicator variable $RefineryShutdown_t$, which takes the value of 1 during the 6 days that the refinery stopped its production, and the value of 0 at any other time. This model is given by

$$lny_t = \beta_0 + \beta_1 RefineryShutdown_t + \beta_2 x_t + \beta_3 Trend_t + \sum_{j=1}^{4} \rho_j lny_{t-j} + u_t. \qquad (1)$$

As Chen and Whalley (2012) and Davis (2008), we consider a vector of control variables, x_t, that includes seasonal indicators for month, day of the week, and hour of the day. It also includes weather control variables, which consists of current and 1-hour lags of cubic functions for temperature, relative humidity, wind speed and precipitation. Because pollutant concentrations may persist in the atmosphere for more than one hour, we follow Chen and Whalley (2012) including 4 lags of the dependent variable for each pollutant. Furthermore, we report Newey-West standard errors which are consistent in the presence of heteroskedasticity and autocorrelation[12].

In contrast with Davis (2008) and Chen and Whalley (2012), who consider high order polynomial time trends and long-time windows around the events (driving restrictions and a subway line inauguration, respectively), we follow the recommendations of Gelman and Imbens (2019) and Hausman and Rapson (2018), specifying a local linear regression. That is, we consider observations within the 30-day window and only include a linear trend, instead of a high-order polynomial. This specification reduces the likelihood of overfitting and the omission of variables correlated with time that may induce bias.

To recover parameter β_1, which represents the short-term treatment effect of the refinery on air quality, we are assuming—as Chen and Whalley (2012) and Davis (2008)—that hourly pollutant concentrations reported during the 30 days before and after the event conform a valid control group. In other words, we are assuming that unobservable factors are comparable within the 30-day window.

Even though considering a short time window around the event is crucial for our identifying assumption to hold, there is a tradeoff between precision and bias (Hausman & Rapson, 2018). That is, a longer time window increases power but makes the presence of an unobserved factor correlated with time more likely. For this reason, to better control for seasonality, and to improve the precision of our estimates, we follow the recommendations of Hausman and Rapson (2018) specifying a two-step augmented local linear regression.

[12] We select the truncation parameter, $m = 9$, for the heteroskedasticity and autocorrelation consistent (HAC) variance of the estimated parameters based on the length of our time series, T. This number can be found rounding up the result of the following formula: $m = 0.75T^{1/3}$, as proposed by Stock and Watson (2020) for moderate amounts of autocorrelation.

We first regress pollutant concentrations, y_t, in natural logarithms on four lags of the dependent variable, seasonal indicators, and weather control variables, augmenting the 30-day window to consider data one year before and after the refinery temporary shutdown. This model is

$$lny_t = \delta_0 + \delta_1 x_t + \sum_{j=1}^{4} \rho_j lny_{t-j} + e_t. \quad (2)$$

Second, we regress the residuals saved from the first stage, $\hat{e}_t$, on the indicator variable $RefineryShutdown_t$ and a linear trend, just for the observations within the 30-day window. As suggested by Hausman and Rapson (2018), we report bootstrapped standard errors from 500 replications in this stage. The corresponding regression is given by

$$\hat{e}_t = \gamma_0 + \gamma_1 RefineryShutdown_t + \gamma_2 Trend_t + u_t. \quad (3)$$

We further present a set of robustness checks that support the results of our two main model specifications (local linear and augmented local linear). As a first check, we select the optimal number of lags for each pollutant based on the Bayesian Information Criterion (BIC). As a second one, we allow the existence of two separate linear trends for the periods before and after the temporary shutdown of the refinery. As a third check, we include additional controls such as the interactions between weekends and hours of the day, as well as two indicator variables that control for working days on the academic calendar of public education. Finally, we estimate a "donut" regression, removing observations occurring one day before and after the shutdown and restart of the Cadereyta's refinery. The logic is that the time in which the shutdown or restart of operations was reported may not coincide exactly with the time in which the events occurred. According to Lavaine and Neidell (2017), this can be important because closing (and reopening) a refinery can take from two days to one week. Discarding these observations allows us to effectively compare hours when the refinery was closed with hours when it operated normally.

Our approach has several advantages when compared with emission inventories. It requires less information, which implies a lower cost to implement it. In addition, pollution data comes from an independent source, which may better represent the operation conditions of the refinery, preventing false or inaccurate reports (Duflo et al., 2013). Another advantage is that it considers pollutants emitted from all points of the refinery, including processes leaks and spills which may be an important source of emission. Furthermore, it includes emissions within the refinery facilities as well as from other interrelated industrial activities. For example, it may include water treatment and other processes that can be conducted outside the refinery. More importantly, focusing on pollutant concentrations instead of primary emissions, our estimates include the contribution caused by the emission of primary pollutants, as well as their subsequent contribution to the conformation of secondary pollutants.

1.4.3. Results

In Table 1.2 we report the estimated effect of the temporary shutdown of the refinery on criteria pollutant concentrations based on model (1). We find a significant drop of about 30% in particulate matter, which is smaller than the one obtained comparing simple averages of treatment and control groups. However, it seems as if fine particles disperse less than coarse particles in the MMA. That is, stations within 40 km of the refinery report a higher (lower) reduction in concentrations of $PM_{2.5}$ (PM_{10}) than stations 40 to 60 km apart from the refinery.

It is important to say that whenever we refer to the effect (or the changes) caused by the refinery temporary shutdown on pollutant concentrations, we are considering the cumulative effect unless otherwise stated. As noted by Chen and Whalley (2012), given that we include lags of our dependent variables, the instant or short-term effect of the event has an indirect effect on pollutant concentrations in subsequent periods. Following Castro Pérez and Flores (2023), we can calculate the cumulative effect by dividing the instant (short-term) effect ($\hat{\beta}_1$) by 1 minus the sum of the estimated coefficients of the lagged dependent variables ($1 - \sum_{j=1}^{4} \hat{\rho}_j$).

Gases as nitrogen dioxide (NO_2) and sulfur dioxide (SO_2) also decreased in the MMA during the refinery temporary shutdown. However, the reduction of 10.5% in concentrations of NO_2 is only significant 40 to 60 km away from the refinery. In contrast, SO_2 concentrations are significantly reduced around 10% within 40 km from the refinery. Carbon monoxide (CO) and ozone (O_3) concentrations did not change significantly. This latter result supports our identification strategy because CO and O_3 have been mainly attributed to mobile and area sources such as vehicles and non-industrial economic activities (State Government of Nuevo León, 2016a).

Table 1.2. The effect of refinery temporary shutdown on pollutant concentrations: local linear regression

	a) Stations within 40 km					
	CO	NO_2	O_3	PM_{10}	$PM_{2.5}$	SO_2
Refinery shutdown	-0.0007	-0.0254*	0.0114	-0.0932***	-0.1950***	-0.0585***
	(0.0066)	(0.0148)	(0.0121)	(0.0211)	(0.0584)	(0.0214)
Obs.	1584	1295	1584	1584	825	1569
Adjusted R^2	0.8909	0.7702	0.9447	0.6683	0.5297	0.5542
BIC	-2924.37	-658.77	-1476.81	-44.61	1186.69	432.01
Cumul. effect	-0.0043	-0.0821	0.0482	-0.2961	-0.3437	-0.0945
	b) Stations within 40-60 km					
	CO	NO_2	O_3	PM_{10}	$PM_{2.5}$	SO_2
Refinery shutdown	-0.0165**	-0.0510***	0.0256	-0.0886***	-0.2055***	-0.0320*
	(0.0084)	(0.0178)	(0.0164)	(0.0203)	(0.0629)	(0.0193)
Obs.	1584	1584	1584	1584	1100	1565
Adjusted R^2	0.8997	0.7241	0.9467	0.8706	0.2314	0.6362

BIC	-3097.78	-410.41	-694.48	-776.28	1869.18	-239.02
Cumul. effect	-0.0501	-0.1047	0.0926	-0.3801	-0.2894	-0.1095
			c) All stations			
	CO	NO_2	O_3	PM_{10}	$PM_{2.5}$	SO_2
Refinery	-0.0113	-0.0111	0.0171	-0.0732***	-0.1776***	-0.0297**
shutdown	(0.0074)	(0.0126)	(0.0106)	(0.0174)	(0.0395)	(0.0137)
Obs.	1584	1584	1584	1584	1382	1584
Adjusted R^2	0.9151	0.7746	0.9666	0.8481	0.3711	0.5581
BIC	-3541.37	-1228.02	-2018.70	-1000.62	1665.07	-1105.49
Cumul. effect	-0.0417	-0.0311	0.0788	-0.3118	-0.2907	-0.0919

Notes: OLS regressions for the average hourly concentrations of each pollutant (columns) within the 30-day window. Hourly concentrations were calculated averaging across stations according to their distance to the refinery as long as they report at least 70% of the time within this period. Each regression includes a linear trend, 4 lags of the dependent variable for each pollutant, and controls for seasonal variables and current and 1-hour lags of cubic functions of weather variables. Newey-West standard errors in parenthesis. The symbols ***, **, * indicate significance at the 1%, 5%, and 10% levels, respectively.

We include a graphical representation of the pollutant concentrations reductions in Figure 1.3. We focus on particles as these pollutants seem to be the most affected. However, we also include sulfur dioxide because refineries are catalogued as one of their main sources (Fioletov et al., 2016). Both $PM_{2.5}$ and PM_{10} concentrations exhibit a clear decline during the 6 days in which the refinery stopped its production. More importantly, these reductions occurred both at stations near and far from the refinery, demonstrating how pollutants dispersion can cause externalities all over the MMA. In contrast, SO_2 concentrations seem to only be affected locally (within 40 km) by the refinery. This result matches previous findings in the literature (Burr et al., 2018; Hanna & Oliva, 2015; Lavaine, 2019, 2016; Lavaine & Neidell, 2017). In fact, Fioletov et al. (2016) estimate that the mean spread (or width) of the plume of SO_2 is 21.3 km.

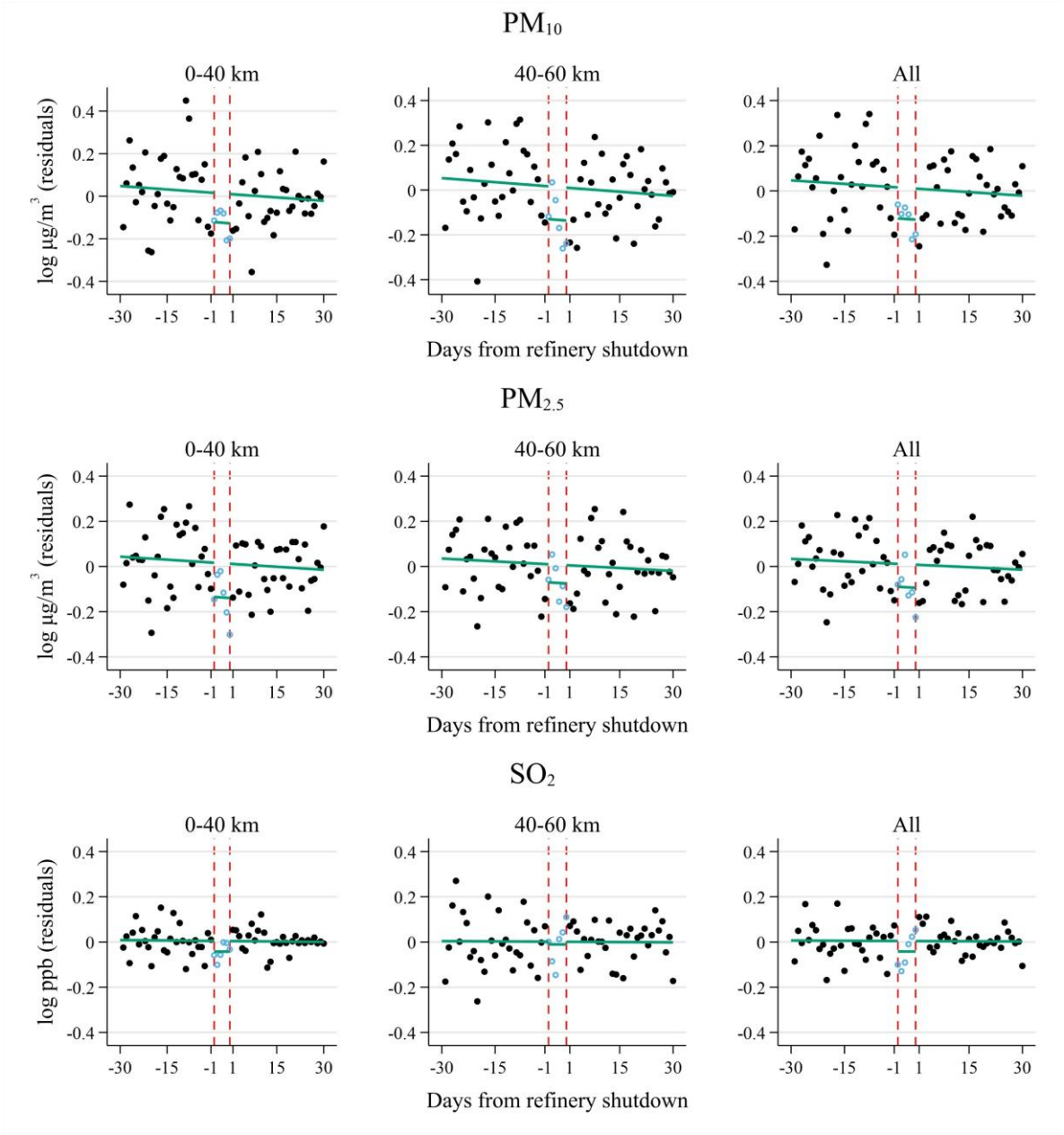

Figure 1.3. The short-term effect of Cadereyta's refinery temporary shutdown on PM_{10}, $PM_{2.5}$, and SO_2 concentrations. Points on the graphs correspond to residuals from a regression of average daily concentrations of each pollutant (in natural logarithms) on seasonal indicators for month and day of the week, and current and 1-hour lags of cubic functions of weather variables. The green lines were obtained regressing the residuals (points) on an indicator variable for the 6-day refinery shutdown and a linear trend. The dashed vertical red lines mark the shutdown and restart of the Cadereyta's refinery. Daily concentrations were calculated averaging across stations according to their distance to the refinery within the 30-day window.

As warned by Chen and Whalley (2012) and Davis (2008), it may be difficult to control seasonality of pollution concentrations with less than 2 years of data. For this reason, we

follow the recommendation of Hausman and Rapson (2018), presenting the results from the second stage of an augmented local linear regression in Table 1.3.

Our previous results do not change drastically. We still find a reduction of 32% for concentrations of particulate matter in the MMA. However, we now observe that both fine and coarse particles have a similar dispersion. The stations located within 40 to 60 km of the refinery show greater impacts than nearer stations. In the case of gases, we only capture significant changes at the 10% significance level if we consider all stations in the MMA. The reduction in concentrations remains around 10% for nitrogen dioxide but increase to 17% for sulfur dioxide. Finally, as expected, both carbon monoxide and ozone remain statistically unchanged.

Table 1.3. The effect of refinery temporary shutdown on pollutant concentrations: augmented regression

	a) Stations within 40 km					
	CO	NO_2	O_3	PM_{10}	$PM_{2.5}$	SO_2
Refinery shutdown	-0.0015	-0.0156	0.0140	-0.056***	-0.0844	-0.0275
	(0.0054)	(0.0176)	(0.0094)	(0.0207)	(0.0526)	(0.0286)
Obs.	1584	1295	1584	1584	825	1569
Adjusted R^2	-0.0011	0.0119	0.0005	0.0067	0.0053	0.0056
BIC	-3039.73	-660.15	-1618.00	-114.16	1035.18	405.09
Cumul. effect	-0.0691	-0.1005	0.0796	-0.2976	-0.2493	-0.2531
	b) Stations within 40-60 km					
	CO	NO_2	O_3	PM_{10}	$PM_{2.5}$	SO_2
Refinery shutdown	-0.0046	-0.0271	0.0184	-0.0677***	-0.1231**	-0.0146
	(0.0074)	(0.0185)	(0.0134)	(0.0176)	(0.0606)	(0.0164)
Obs.	1584	1584	1584	1584	1100	1565
Adjusted R^2	-0.0008	0.0022	0.0098	0.0140	0.0085	-0.0004
BIC	-3086.00	-467.82	-746.10	-918.90	1575.96	-497.90
Cumul. effect	-0.0784	-0.1185	0.1047	-0.4015	-0.2712	-0.0902
	c) All stations					
	CO	NO_2	O_3	PM_{10}	$PM_{2.5}$	SO_2
Refinery shutdown	-0.0024	-0.0225*	0.0101	-0.0548***	-0.113***	-0.0226*
	(0.0056)	(0.0127)	(0.0087)	(0.0136)	(0.0434)	(0.0119)
Obs.	1584	1584	1584	1584	1382	1584
Adjusted R^2	-0.0010	0.0113	0.0049	0.0118	0.0050	0.0098
BIC	-3510.69	-1298.38	-2066.96	-1151.26	1429.61	-1302.86
Cumul. effect	-0.0735	-0.1003	0.0748	-0.3536	-0.2834	-0.1721

Notes: This table shows results from the second stage of an augmented local linear regression. The dependent variable consists of residuals saved from regressing average hourly concentrations of each pollutant (columns) on lagged pollutant concentrations, seasonal indicators, and weather control variables considering data within 1 year (before or after) of the refinery temporary shutdown. Each regression for the second stage considers data within the 30-day window and includes a linear trend. Bootstrapped standard errors from 500

replications in parenthesis. The symbols ***, **, * indicate significance at the 1%, 5%, and 10% levels, respectively.

The results we present are hardly justified by changes in climate conditions, since they were practically unchanged within the 30-day window, and we have included flexible controls for these observed parameters in our regressions. Moreover, neither changes in the number of barrels that were processed nor changes in the production or input mix are much likely to have been the responsible for changes in pollutant concentrations because they didn't vary substantially during the months close to the 6-day unscheduled shutdown (July and August 2016). For example, the refinery went from processing 88,000 barrels per day in July to 85,500 in August. In July, 1.8 barrels of heavy crude oil were processed for each barrel of light crude oil, while in August this ratio was 2.5. Similarly, the production mix remain almost unchanged between July and August 2016, with gasoline and diesel representing 70% and 72%, respectively.

We discard other important events that could abruptly change pollutant concentrations in the MMA during the period. First, there were no environmental pre-emergencies or emergencies within the 30-day window (State Government of Nuevo León, 2016b, 2016c). Second, changes in gasoline prices were negligible, and we include monthly indicators to control for possible modifications in the demand for transportation. For example, according to Centro de Estudios de las Finanzas Públicas (2016) regular gasoline prices went from $13.16 pesos per liter in June (about 0.71 US dollars) to $13.4 in July (about 0.72 US dollars) and $13.96 in August (about 0.76 US dollars). Third, the operation of other important stationary sources of particulate matter—as companies dedicated to the extraction of nonmetallic minerals and quarrying at mountains in the MMA—didn't reported abrupt changes (as closures or new entries) within the 30-day window.

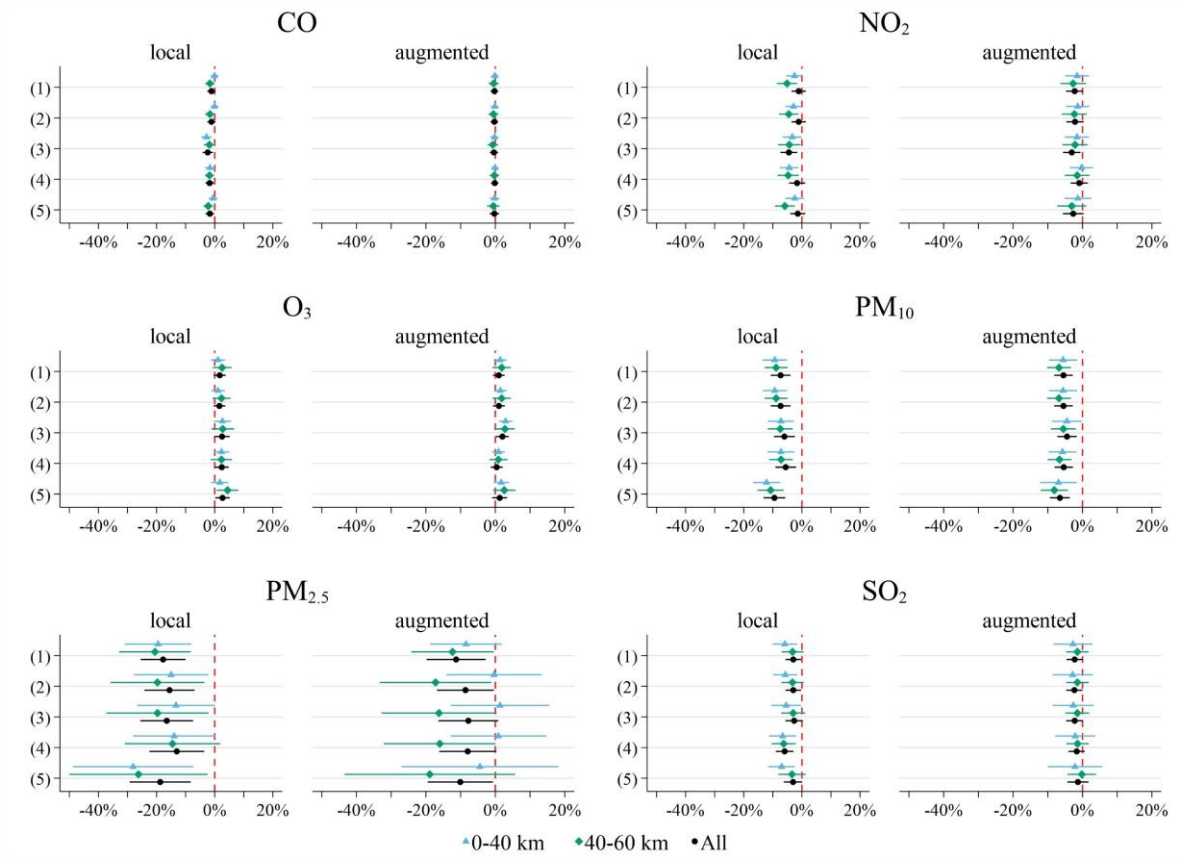

Figure 1.4. The short-term effect of Cadereyta's refinery temporary shutdown on pollutant concentrations: robustness checks. Each point corresponds to a separate estimate of the short-term effect of the refinery temporary shutdown on criteria pollutant concentrations. Lines denote 95% confidence intervals. We estimate 30 regressions for each pollutant (15 local linear and 15 augmented local linear). We present the short-term effect for our main model along with 4 robustness checks: (1) main model specifications, (2) selecting optimal number of lags with BIC, (3) including a separate trend posterior to the refinery temporary shutdown, (4) adding additional controls, (5) estimating a "donut" regression. All specifications consider the optimal number of lags as (2), except from our main model specifications (1).

In Figure 1.4, we test the robustness of the results in Tables 1.2 and 1.3 comparing them with four variations of our main model. These checks include: i) selecting the optimal number of lags according to the Bayesian Information Criterion (BIC); ii) including separate linear trends before and after the refinery temporary shutdown; iii) controlling for working days at public educational institutions, and interactions between weekends and hours of the day; and iv) estimating a "donut" regression. Essentially, we observe that the absence of the refinery consistently, significantly, and substantially reduced the concentrations of fine and coarse particulates ($PM_{2.5}$ and PM_{10}) and sulfur dioxide (SO_2).

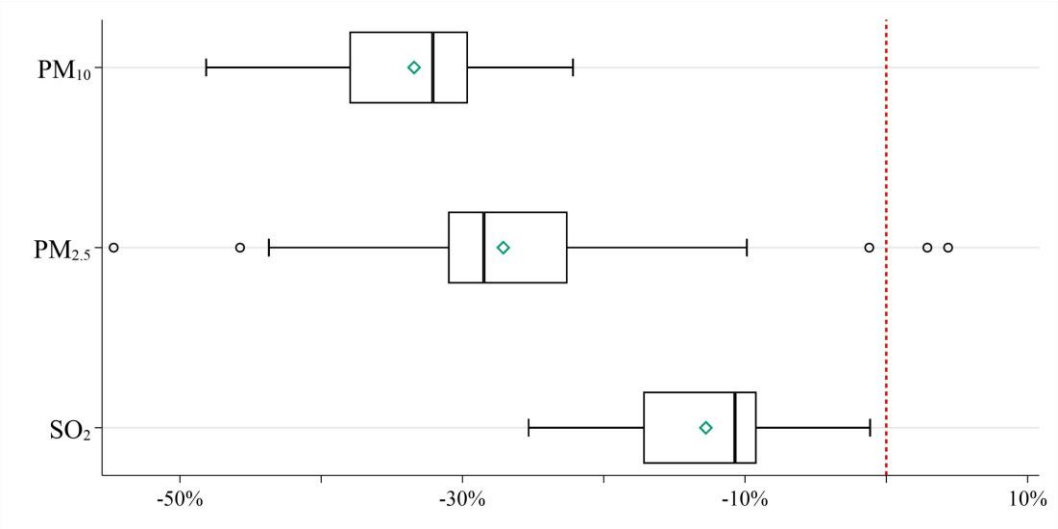

Figure 1.5. The cumulative effect of Cadereyta's refinery temporary shutdown on PM_{10}, $PM_{2.5}$, and SO_2 concentrations. Each box plot summarizes the estimated cumulative effects from the 30 regressions described in Figure 1.4. The green hollow diamond denotes the mean cumulative effect for each pollutant.

As we show in Figure 1.5, considering all different specifications for each of these 3 pollutants, we recover average (or median) cumulative effects that are very close to those we obtained with our base model. For instance, particulate matter was reduced on average 30.3% during the refinery absence, with concentrations of $PM_{2.5}$ and PM_{10} falling 27.1 and 33.4%, respectively. In the case of sulfur dioxide (SO_2), it was reduced on average 12.8%.

1.5. Impact on mortality

1.5.1. Data

We count the daily number of deaths in the MMA which occurred within the 30-day window from the statistics of registered deaths published by the National Institute of Statistics and Geography (INEGI)[13]. A few of these administrative records (10 out of the 21,467 deaths in 2016) didn't contain the specific day and/or month of death. We randomly assign this information assuming that they could have occurred in any month or day with the same probability.

Next, we disaggregate the daily number of deaths based on their causes and age groups. We use the classification of death causes proposed by Arceo et al. (2016) dividing the daily number of deaths into five non-mutually exclusive groups: i) all causes; ii) internal causes; iii) external causes; iv) respiratory causes; and v) non-respiratory causes[14]. Similarly, we

[13] Registered deaths statistics are available at: https://en.www.inegi.org.mx/programas/mortalidad/

[14] Akin Arceo et al. (2016), external causes include accidents, suicides, homicides, and other external causes detailed in the chapter 20 from the 10th revision of the International Statistical Classification of Diseases and Related Health Problems (ICD-10). Internal causes comprehend all causes except those classified as external. Respiratory causes contain deaths caused by diseases of the circulatory or respiratory systems (chapters 9 and

follow Martínez-Muñoz et al. (2020) separating the daily number of deaths into three age groups: i) all ages; ii) 65 years and older; and iii) 5 years and younger[15].

Table 1.4. Mean daily number of deaths in the MMA

Age\Causes	All	Internal	External	Respiratory	Non-respiratory
All ages					
During 6-day	55.33	48.83	6.50	21.33	34.00
shutdown	(8.80)	(7.81)	(1.76)	(5.05)	(6.90)
30 days before and	58.98	53.72	5.27	21.02	37.97
after the event	(9.72)	(9.19)	(2.71)	(5.28)	(7.45)
5 years and younger					
During 6-day	1.17	1.00	0.17	0.00	1.17
shutdown	(0.98)	(0.89)	(0.41)	(0)	(0.98)
30 days before and	2.65	2.47	0.18	0.10	2.55
after the event	(1.60)	(1.51)	(0.43)	(0.30)	(1.56)
65 years and older					
During 6-day	33.00	32.33	0.67	15.33	17.67
shutdown	(5.22)	(4.76)	(0.82)	(4.03)	(3.33)
30 days before and	34.07	33.30	0.77	15.48	18.58
after the event	(6.90)	(6.84)	(0.89)	(4.29)	(5.10)

Notes: As the unit of observation is the day, there are 6 observations during the 6-day refinery shutdown. Similarly, there are 60 observations for the period of 30 days before and after the event. Standard deviations are reported between parentheses. Figures presented with rounding to 2 decimal places.

In Table 1.4, we can compare the mean daily number of deaths—disaggregated according to their cause and age group—before and after the refinery temporary shutdown against the same disaggregated measure during the event. Although there appears to be a reduction in mortality for the various causes of death and age groups during the 6-day refinery shutdown, this change is only statistically significant for children (5 and younger) in deaths from all causes as well as from internal and non-respiratory causes. Surprisingly, the mean difference in the number of deaths due to respiratory and cardiovascular problems is not statistically significant for any age group.

However, as in the case of pollutant concentrations, before interpreting sample mean differences as valid causal estimates of the effect of the refinery on mortality, we must ensure that all other factors (observable and unobservable) are constant. Furthermore, we should

10 from ICD-10). Non-respiratory causes consist of all deaths except those from respiratory and cardiovascular diseases, including external causes.

[15] 3 out of the 3,871 death records within the 30-day window didn't specify age at the time of death because the birth date was missing. These records were only considered within the all-ages group.

incorporate the fact that the daily number of deaths may not be normally distributed which is particularly relevant for death causes and age groups with small sample means.

1.5.2. Empirical strategy

The daily count of deaths from a particular cause and age group that occurred in the MMA within the 30-day window, y_t, is strictly a nonnegative discrete integer. Therefore, as Martínez-Muñoz et al. (2020) and Pope et al. (1992, 2007), we consider that this count could be generated by the total number of realizations of a Poisson process—with parameter μ_t—in a day. Hence, the probability that y_t takes a particular value, conditional on a set of explanatory variables $\boldsymbol{x}_t$, is given by

$$f(y_t|\boldsymbol{x}_t) = \frac{e^{-\mu_t}\mu_t^{y_t}}{y_t!}, \qquad y_t = 0, 1, 2 \ldots \tag{4}$$

Initially, we propose that the mean number of deaths for a particular day t within the 30-day window depends on whether that day coincides with the 6-day refinery shutdown, as well as a linear time trend and other seasonal and weather control variables, x_t, including an indicator for the day of the week, month, and daily temperature in the MMA. Therefore,

$$\begin{gathered}\mu_t = \mathrm{E}(y_t|\boldsymbol{x}_t) = \exp(\boldsymbol{\beta}\boldsymbol{x}_t) \\ = \exp(\beta_0 + \beta_1 RefineryShutdown_t + \beta_2 x_t + \beta_3 Trend_t)\end{gathered} \tag{5}$$

Additionally, we examine the case in which the natural logarithm of the number of deaths in each of the past four days can also partially help explain changes in the conditional mean[16]. That is,

$$\mu_{t|t-1} = \mathrm{E}(y_t|\boldsymbol{x}_t, y_{t-1}, y_{t-2}, \ldots) = \exp\left(\boldsymbol{\beta}\boldsymbol{x}_t + \sum_{j=1}^{4} \rho_j ln y_{t-j}^*\right) \tag{6}$$

Following Cameron and Trivedi (2013), we estimate the static and autoregressive regression models (5) and (6) using the Poisson quasi-maximum likelihood estimator (QMLE). This estimator is consistent if (5) or (6) are correctly specified, even if—as in (4)—we incorrectly specified a Poisson density. As suggested by Cameron and Trivedi (2013), we use Newey-West standard errors for the static regression, and heteroskedastic-robust standard errors for the autoregressive model.

Our main interest is estimating the impact of Cadereyta's refinery on mortality. That is, if on average the temporary shutdown of the refinery caused a reduction in the number of deaths

[16] Given that the natural logarithm of zero—a possible number of deaths in a day—is undefined, we follow Cameron and Trivedi (2013) replacing zeros with a constant, $c = 0.5$. This transformation is represented as y_t^*.

in the MMA. Hence, we focus on average treatment effects (ATE), which according to Greene (2017) can be computed for the static model as

$$ATE = \frac{1}{T}\sum_{t=1}^{T}\left[\exp\left(\hat{\beta}_0 + \hat{\beta}_1 + \hat{\beta}_2 x_t + \hat{\beta}_3 Trend_t\right) - \exp\left(\hat{\beta}_0 + \hat{\beta}_2 x_t + \hat{\beta}_3 Trend_t\right)\right] \quad (7)$$

The first exponential term corresponds to the prediction of the number of deaths for a particular day t within the 30-day window assuming that the Cadereyta's refinery was shutdown (i.e. $RefineryShutdown_t = 1$). In contrast, the second exponential term assumes that the refinery was operating (i.e. $RefineryShutdown_t = 0$). ATE is calculated averaging the difference of the two terms over all days within the 30-day window. This formula can be easily extended to the autoregressive model.

1.5.3. Results

We present the average treatment effects in Table 1.5. In general, our results for most of the causes of death and age groups point to a reduction of mortality. This is consistent with a large body of literature that attributes higher mortality to increases of pollutant concentrations (Anderson, 2020; Arceo et al., 2016; Barrows et al., 2019; Brown & Tousey, 2020; Clancy et al., 2002; Deryugina et al., 2019; Gutiérrez, 2015; He et al., 2016; Luechinger, 2014; Martínez-Muñoz et al., 2020; Pope et al., 1992, 2007).

Table 1.5. Average treatment effects of Cadereyta's refinery temporary shutdown on mortality

Age\Causes	All	Internal	External	Respiratory	Non-respiratory
Static model					
All ages	-5.2271***	-6.8935***	2.0000**	-0.3157	-4.8912***
	(1.6596)	(1.5870)	(0.8121)	(1.4023)	(1.2459)
5 years and younger	-1.3995***	-1.3310***	-0.0811	-0.1083	-1.2793***
	(0.2888)	(0.2461)	(0.0823)		(0.2962)
65 years and older	-1.5469	-1.7028	0.2274	-0.7392	-0.7894
	(1.2341)	(1.2169)	(0.4820)	(1.0866)	(1.0517)
Autoregressive model					
All ages	-6.1788*	-8.5733**	3.0663**	-0.3341	-6.0242***
	(3.4554)	(3.4453)	(1.4586)	(2.0681)	(2.2220)
5 years and younger	-1.5430***	-1.4084***	-0.2530*	-0.1795	-1.4809***
	(0.4296)	(0.3858)	(0.1310)		(0.4046)
65 years and older	-1.9828	-2.1595	0.2131	-0.6071	-0.5817
	(2.3667)	(2.3429)	(0.5540)	(1.5112)	(1.8136)

Notes: Average treatment effects (ATE) calculated from estimates of the static and autoregressive models of (5) and (6) via Poisson quasi-maximum likelihood estimator (QMLE) with corrected standard errors. We report standard errors obtained by the delta method in parenthesis, except for children's (5 years and younger) deaths from respiratory causes because it was not possible to estimate the variance-covariance matrix. The symbols ***, **, * indicate significance at the 1%, 5%, and 10% levels, respectively.

We find that the unscheduled 6-day shutdown of the refinery prevented the death from internal causes of around 8 individuals in any age group. This number is at least 2 times greater than what we obtained using estimates from Martínez-Muñoz et al. (2020), which are comparable for the MMA. Martínez-Muñoz et al. (2020) report that each increment of $10\,\mu g/m^3$ of $PM_{2.5}$ concentrations is associated with a short-term increase of between 1.42 and 1.65 per cent in the daily number of deaths from internal causes in the MMA. Hence, according to Martínez-Muñoz et al. (2020), the reduction of 27.1% in concentrations of $PM_{2.5}$ caused by the 6-day refinery shutdown, should prevented between 3.13 and 3.64 deaths.

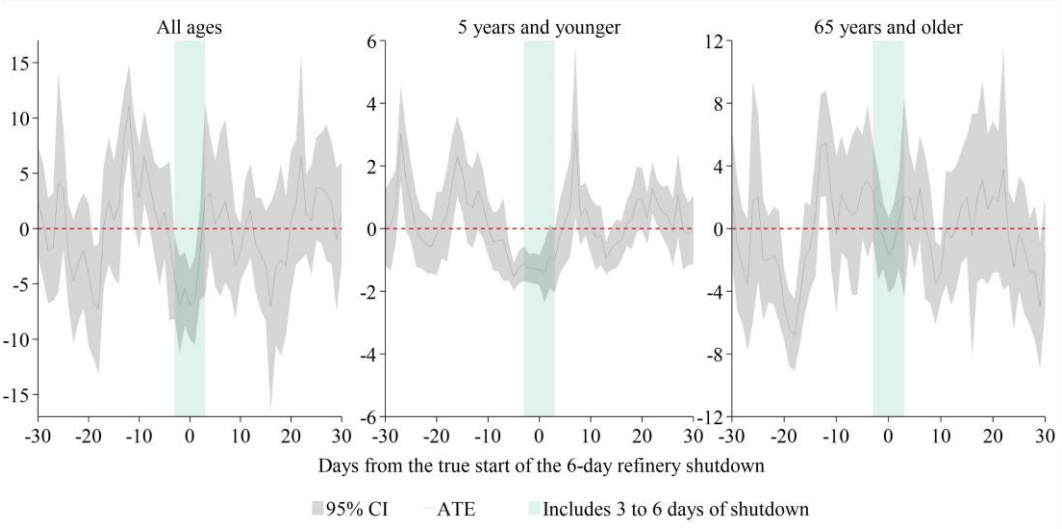

Figure 1.6. Falsification test for the effect of Cadereyta's refinery temporary shutdown on mortality from internal causes. The solid line correspond to the average treatment effect (ATE) of the refinery temporary shutdown starting on different—mostly false—dates on mortality from internal causes. Each false start is identified with respect to day 0, which corresponds to the truth start of the refinery temporary shutdown. Hence, ATEs from days -3 to 3 contain at least 3 days of the truth 6-day shutdown. ATEs and 95% confidence intervals (CI) are calculated from estimates of the static model (5) via Poisson QMLE with corrected standard errors.

In Figure 1.6, we show that this result can hardly be explained by luck or coincidence with some other unobserved event simultaneous to the refinery temporary shutdown. Specifically, we performed a falsification test presuming that the 6-day refinery shutdown started on different—mostly false—dates within the 30-day window. As can be seen in Figure 1.6, the number of deaths from internal causes from all ages are statistically lower largely on the truth start of the refinery temporary shutdown, and the days close to it (which include at least 3 out of the 6 days of the refinery shutdown).

Surprisingly, we do not find significant improvements in mortality associated to respiratory and cardiovascular diseases as commonly reported in the literature (Anderson, 2020; Arceo et al., 2016; Brown & Tousey, 2020; Clancy et al., 2002; Gutiérrez, 2015; He et al., 2016; Martínez-Muñoz et al., 2020; Pope et al., 1992). However, the sign of the average

treatment effect is negative as expected. Perhaps the 6-day reduction of pollutant concentrations was very brief to capture the gradual effects of pollution on respiratory and circulatory systems. For this reason, our result should only be taken as a short-term estimate. Alternatively, a significant change may be more difficult to observe in July—when the refinery temporarily stopped its production—than during the months with lower temperatures (e.g., December and January) because deaths from respiratory and cardiovascular diseases are less common in summer. This latter hypothesis may explain why when we separate deaths caused by diseases of the respiratory system from those associated with the circulatory system (see Table A1.4. from the Appendix), only the latter show a—not statistically significant—negative sign.

A second contradictory result is that there were 2 or 3 additional deaths from external causes as accidents, suicides and homicides during the 6-day refinery shutdown. This latter result contrasts with what we would have expected based on the literature that positively relates crime (including violent crime, such as homicides) with pollution (Bondy et al., 2019; Burkhardt et al., 2019; Du, 2023; Herrnstadt et al., 2021) or studies that suggest a positive relationship between car accidents and pollution (Sager, 2019). Hence, we recommend taking this result with caution.

In relation to our results for vulnerable age-groups, we find that the 6-day refinery shutdown prevented on average 1.37 children's (5 years and younger) deaths from internal causes. This represents a reduction of 9% ($= 1.37/(2.47 \times 6)$) considering that on average 2.5 children's deaths occur each day from these causes. This number is much larger than the 2.4% reduction for all deaths from internal causes. Hence, consistent with previous studies (Arceo et al., 2016; Barrows et al., 2019; Gutiérrez, 2015; He et al., 2016; Luechinger, 2014; Martínez-Muñoz et al., 2020), our result confirm that children face a higher risk of death from pollution. This result is robust to the falsification test we present in Figure 1.6. Finally, elders have also been identified as a vulnerable group to the effect of pollution (Anderson, 2020; Deryugina et al., 2019; He et al., 2016; Martínez-Muñoz et al., 2020). However, in our study the mortality of elders was not significantly impacted by the refinery temporary shutdown.

1.6. Discussion

We could go further extending our results by saying that around 471 annual deaths ($= (7.73/6) \times 365.25$) from internal causes could be avoided annually if the refinery is shutdown permanently. Based on an estimate of the value of a statistical life (VSL) reported by de Lima (2020) this is equivalent to $109 million US dollars (MUSD) in 2016 ($= 471 \times \$232{,}290$)[17]. However, according to an average of the estimates reported by Trejo-

[17] Applying a questionnaire to citizens of the Mexico Valley Metropolitan Area, de Lima (2020) calculates a VSL of $210,880 US dollars in 2010. This is equivalent to $232,290 US dollars in 2016.

González et al. (2019) and INECC (2014)[18], this corresponds to $820 MUSD in 2016 ($= 471 \times \$1.74$ MUSD). These amounts represent between 2 and 16 per cent of the annual revenue obtained by Cadereyta's refinery in 2016[19].

Additionally, a permanent reduction in particle concentrations of the same magnitude as those estimated for the 6-day refinery shutdown would substantially improve compliance with official standards in the MMA (see Figure A1.5 from the Appendix). For example, if the concentrations of PM_{10} were reduced 33.1% during all 2016, the number of days with any monitoring station above the standard would change from 212 (80%) to just 77 out of the 366 days (21%). Similarly, a reduction of 27.1% in the concentrations of $PM_{2.5}$ would have reduced the number of days above the standard from 29 to 4.

Nevertheless, we should recognize that our approach has some limitations. It is important to remember that we estimated the effect of the 6-day refinery shutdown on air quality and mortality conditional on a set of weather and operational characteristics, which are not necessarily held fixed in other regions, subsequent years, or seasons within 2016. Although we have demonstrated the validity of our results within the 30-day window, extrapolating our results could lead us to either underestimate or overestimate the effect of a permanent refinery shutdown.

1.7. Conclusions

In this article, we demonstrate the importance of including direct as well as indirect effects from emissions when evaluating the impact of oil refineries and other important sources of pollution. Moreover, our contribution provides insight into the extent to which pollutant dispersion can extend refinery externalities over distant areas. Even if an emitted primary pollutant poses only a local risk, its subsequent conformation as secondary pollutant can travel long distances affecting inhabitants far from the emitting source.

Specifically, we take advantage of an unforeseen 6-day shutdown at the Cadereyta's refinery to estimate its effects on air quality and mortality in the MMA. As in other quasi-experimental studies that focus on oil refineries (Burr et al., 2018; Hanna & Oliva, 2015;

[18] Both Trejo-González et al. (2019) and INECC (2014) adjust estimates of VSL for OECD countries or US, based on Mexico's gross domestic product (GDP) or gross national income (GNI) per capita. Trejo-González et al. (2019) reports a VSL of $1.643 MUSD in 2015, while INECC (2014) calculates a VSL of $1.65 MUSD in 2010. We respectively multiply these figures by 1.02 and 1.09 to account for inflation, and then calculate their average which is equal to $1.74 MUSD in 2016.

[19] PEMEX's income statements include consolidated revenue for the industrial transformation segment (which considers the refining activities of all its subsidiaries) for $41,216.58 MUSD in 2016. However, they do not report disaggregated revenues by subsidiary. Therefore, we assume that the revenue of Cadereyta's refinery approximates a proportion similar to its contribution in the number of barrels of crude oil that were processed, which is equivalent to 12.78% in 2016. With this, we calculate a sales income of 5,269.78 MUSD in 2016. We consider an average exchange rate of 18.7 MXN/USD for 2016, according to Banco de México. PEMEX's income statements are available at: https://www.pemex.com/ri/finanzas/Documents/dcf_efd_da_1612_e.pdf

Lavaine, 2019, 2016; Lavaine & Neidell, 2017), we find that, on average, the temporary shutdown reduced local concentrations (within 40km from the refinery) of sulfur dioxide by 12.8%. However, unlike these studies, we recognize that SO_2 is a precursor of particles that disperse to distant regions (Martínez et al., 2012; Martínez-Cinco et al., 2016; Weijers et al., 2010). Consequently, we report that the refinery contributes, respectively, with 27.1 and 33.4 percent of the concentrations of $PM_{2.5}$ and PM_{10} in the MMA (up to 60 km away from the refinery).

In contrast with the null effects on mortality caused by unplanned oil refinery outages in the US (Du, 2023), we find that the 6-day shutdown prevented 8 deaths from internal causes, which is equivalent to a 2.4% reduction in daily deaths. This effect is comparable to the 2.5% reduction in mortality in the southwest states of United States attributed to the temporal closure—caused by a nationwide strike—of cooper smelters in July 1967 (Pope et al., 2007). As in previous studies (Arceo et al., 2016; Barrows et al., 2019; Gutiérrez, 2015; He et al., 2016; Luechinger, 2014; Martínez-Muñoz et al., 2020), we find that children are more vulnerable to the health effects of pollution than adults. According to our results, on average, the Cadereyta's refinery temporary shutdown reduced daily deaths from internal causes in children 5 years old and younger by 9% in the MMA.

In addition, our results suggest that future studies comparing outcomes close to a major stationary source of pollution, as an oil refinery, with outcomes from areas further away must consider that the control group could also be affected by unconsidered secondary pollutants. Hence, they could underestimate the effects of pollution.

Finally, given that the reported health and air quality effects of the Cadereyta's refinery are substantial, future studies should be carried out to assess whether recent refinery investments have been effective to reduce pollutant emissions. In addition, our study should be considered by policymakers to correctly weigh the costs and benefits of the current energy strategy (based on fossil fuels) in Mexico.

References

Adebiyi, F. M. (2022). Air quality and management in petroleum refining industry: A review. *Environmental Chemistry and Ecotoxicology*, *4*, 89–96. https://doi.org/10.1016/j.enceco.2022.02.001

Aguilar-Gómez, S., Dwyer, H., Zivin, J. G., & Neidell, M. (2022). This is air: The "nonhealth" effects of air pollution. *Annual Review of Resource Economics*, *14*, 403-425. https://doi.org/10.1146/annurev-resource-111820-021816

Anderson, M. L. (2020). As the wind blows: The effects of long-term exposure to air pollution on mortality. *Journal of the European Economic Association*, *18*(4), 1886–1927. https://doi.org/10.1093/jeea/jvz051

Arceo, E., Hanna, R., & Oliva, P. (2016). Does the effect of pollution on infant mortality differ between developing and developed countries? Evidence from Mexico City. *The Economic Journal*, *126*(591), 257–280. https://doi.org/10.1111/ecoj.12273

Barrows, G., Garg, T., & Jha, A. (2019). The health costs of coal-fired power plants in India. *IZA Discussion Paper Series*, 12838. https://www.iza.org/publications/dp/12838/the-health-costs-of-coal-fired-power-plants-in-india

Bauer, T. K., Braun, S. T., & Kvasnicka, M. (2017). Nuclear power plant closures and local housing values: Evidence from Fukushima and the German housing market. *Journal of Urban Economics*, *99*, 94–106. https://doi.org/10.1016/j.jue.2017.02.002

Bondy, M., Roth, S., & Sager, L. (2019). Crime is in the air: The contemporaneous relationship between air pollution and crime. *Journal of the Association of Environmental and Resource Economists*, *7*(3), 555–585. https://doi.org/10.1086/707127

BP. (2022). *bp Statistical Review of World Energy 2022*. https://www.bp.com/en/global/corporate/energy-economics/statistical-review-of-world-energy.html

Brown, J. P., & Tousey, C. (2020). Death of coal and breath of life: The effect of power plant closure on local air quality. *The Federal Reserve Bank of Kansas City Research Working Papers*, 20-15. https://doi.org/10.18651/RWP2020-15

Burkhardt, J., Bayham, J., Wilson, A., Carter, E., Berman, J. D., O'Dell, K., Ford, B., Fischer, E. V., & Pierce, J. R. (2019). The effect of pollution on crime: Evidence from data on particulate matter and ozone. *Journal of Environmental Economics and Management*, *98*, 102267. https://doi.org/10.1016/j.jeem.2019.102267

Burr, W., Dales, R., Liu, L., Stieb, D., Smith-Doiron, M., Jovic, B., Kauri, L., & Shin, H. (2018). The Oakville oil refinery closure and its influence on local hospitalizations: A natural experiment on sulfur dioxide. *International Journal of Environmental Research and Public Health*, *15*(9), 2029. https://doi.org/10.3390/ijerph15092029

Cameron, A. C., & Trivedi, P. K. (2013). *Regression analysis of count data* (2nd ed., Econometric Society Monographs). Cambridge: Cambridge University Press. https://doi.org/10.1017/CBO9781139013567

Casey, J. A., Karasek, D., Ogburn, E. L., Goin, D. E., Dang, K., Braveman, P. A., & Morello-Frosch, R. (2018). Retirements of coal and oil power plants in California: Association with reduced preterm birth among populations nearby. *American Journal of Epidemiology*, *187*(8), 1586–1594. https://doi.org/10.1093/aje/kwy110

Castro Pérez, J. E., & Flores, D. (2023). The effect of retail price regulation on the wholesale price of electricity. *Energy Policy*, *173*, 113408. https://doi.org/10.1016/j.enpol.2022.113408

Centro de Estudios de las Finanzas Públicas. (2016). *Precios de las gasolinas en México, 2016*. https://www.cefp.gob.mx/publicaciones/nota/2016/agosto/notacefp0222016.pdf

Chang, T. Y., Graff Zivin, J., Gross, T., & Neidell, M. (2019). The effect of pollution on worker productivity: Evidence from call center workers in China. *American Economic Journal: Applied Economics*, *11*(1), 151–172. https://doi.org/10.1257/app.20160436

Chen, Y., & Whalley, A. (2012). Green infrastructure: The effects of urban rail transit on air quality. *American Economic Journal: Economic Policy*, *4*(1), 58–97. https://doi.org/10.1257/pol.4.1.58

Chesnes, M. (2015). The impact of outages on prices and investment in the U.S. oil refining industry. *Energy Economics*, *50*, 324–336. https://doi.org/10.1016/j.eneco.2015.05.008

Clancy, L., Goodman, P., Sinclair, H., & Dockery, D.W. (2002). Effect of air-pollution control on death rates in Dublin, Ireland: An intervention study. *The Lancet*, *360*(9341), 1210–1214. https://doi.org/10.1016/S0140-6736(02)11281-5

Currie, J., Davis, L., Greenstone, M., & Walker, R. (2015). Environmental health risks and housing values: Evidence from 1,600 toxic plant openings and closings. *American Economic Review*, *105*(2), 678–709. https://dx.doi.org/ 10.1257/aer.20121656

Currie, J., Greenstone, M., & Meckel, K. (2022). Hydraulic fracturing and infant health: New evidence from Pennsylvania. *Science Advances*, *3*(12), e1603021. https://doi.org/10.1126/sciadv.1603021

Davis, L., & Hausman, C. (2016). Market impacts of a nuclear power plant closure. *American Economic Journal: Applied Economics*, *8*(2), 92–122. https://doi.org/10.1257/app.20140473

Davis, L. W. (2011). The effect of power plants on local housing values and rents. *The Review of Economics and Statistics*, *93*(4), 1391–1402. https://doi.org/10.1162/REST_a_00119

Davis, L. W. (2008). The effect of driving restrictions on air quality in Mexico City. *Journal of Political Economy*, *116*(1), 38–81. https://doi.org/10.1086/529398

de Lima, M. (2020). The value of a statistical life in Mexico. *Journal of Environmental Economics and Policy*, *9*(2), 140–166. https://doi.org/10.1080/21606544.2019.1617196

Deryugina, T., Heutel, G., Miller, N. H., Molitor, D., & Reif, J. (2019). The mortality and medical costs of air pollution: Evidence from changes in wind direction. *American Economic Review*, *109*(12), 4178–4219. https://doi.org/10.1257/aer.20180279

Du, X. (2023). Symptom or culprit? Social media, air pollution, and violence. *CESifo Working Paper*, 10296. https://ssrn.com/abstract=4380957

Duflo, E., Greenstone, M., Pande, R., & Ryan, N. (2013). Truth-telling by third-party auditors and the response of polluting firms: Experimental evidence from India. *The Quarterly Journal of Economics*, *128*(4), 1499–1545. https://doi.org/10.1093/qje/qjt024

Fioletov, V. E., McLinden, C. A., Krotkov, N., Li, C., Joiner, J., Theys, N., Carn, S., & Moran, M. D. (2016). A global catalogue of large SO2 sources and emissions derived from the ozone monitoring instrument. *Atmospheric Chemistry and Physics*, *16*(18), 11497–11519. https://doi.org/10.5194/acp-16-11497-2016

Flores Torres, O., & Robles, M. Y. (2015). *La industria del gas en Monterrey: historia de leyes y oportunidades* (1940-2013), in: Roux, R., & Flores Torres, O. (Eds.), Los hidrocarburos en el noreste de México (pp. 125-137). Universidad Autónoma de Tamaulipas & El Colegio de Tamaulipas. http://www.coltam.edu.mx/wp-content/uploads/2016/09/2015-HIDROCARBUROS-EN-EL-NORESTE-DE-MEXICO-.pdf

Galán González, J. R., Martínez Herrera, J. R., Chapa Cantú, J. C., Ramírez Díaz, K. I., & Hutchinson Tovar, S. (2021). La contaminación del aire y su efecto en el precio de la vivienda del AMM. *Revista de Economía*, Facultad de Economía, Universidad Autónoma de Yucatán, *38*(96), 9–46. https://doi.org/10.33937/reveco.2021.173

Gelman, A., & Imbens, G. (2019). Why high-order polynomials should not be used in regression discontinuity designs. *Journal of Business & Economic Statistics*, *37*(3), 447–456. https://doi.org/10.1080/07350015.2017.1366909

Greene, W. H. (2017). *Econometric analysis* (8th ed.). Pearson, New York, NY.

Guo, M., & Fu, S. (2019). Running with a mask? The effect of air pollution on marathon runners' performance. *Journal of Sports Economics*, *20*(7), 903–928. https://doi.org/10.1177/1527002518822701

Gupta, A., & Spears, D. (2017). Health externalities of India's expansion of coal plants: Evidence from a national panel of 40,000 households. *Journal of Environmental Economics and Management*, *86*, 262–276. https://doi.org/10.1016/j.jeem.2017.04.007

Gutiérrez, E. (2015). Air quality and infant mortality in Mexico: Evidence from variation in pollution concentrations caused by the usage of small-scale power plants. *Journal of Population Economics*, *28*, 1181–1207. https://doi.org/10.1007/s00148-015-0539-y

Hanna, R., & Oliva, P. (2015). The effect of pollution on labor supply: Evidence from a natural experiment in Mexico City. *Journal of Public Economics*, *122*, 68–79. https://doi.org/10.1016/j.jpubeco.2014.10.004

Hausman, C., & Rapson, D. S. (2018). Regression discontinuity in time: Considerations for empirical applications. *Annual Review of Resource Economics*, *10*, 533–552. https://doi.org/10.1146/annurev-resource-121517-033306

He, G., Fan, M., & Zhou, M. (2016). The effect of air pollution on mortality in China: Evidence from the 2008 Beijing Olympic Games. *Journal of Environmental Economics and Management*, *79*, 18–39. https://doi.org/10.1016/j.jeem.2016.04.004

He, J., Liu, H., & Salvo, A. (2019). Severe air pollution and labor productivity: Evidence from industrial towns in China. *American Economic Journal: Applied Economics*, *11*(1), 173–201. https://doi.org/10.1257/app.20170286

Herrnstadt, E., Heyes, A., Muehlegger, E., & Saberian, S. (2021). Air pollution and criminal activity: Microgeographic evidence from Chicago. *American Economic Journal: Applied Economics*, *13*(4), 70–100. https://doi.org/10.1257/app.20190091

Heyes, A., & Zhu, M. (2019). Air pollution as a cause of sleeplessness: Social media evidence from a panel of Chinese cities. *Journal of Environmental Economics and Management*, *98*, 102247. https://doi.org/10.1016/j.jeem.2019.07.002

Hill, E. L. (2018). Shale gas development and infant health: Evidence from Pennsylvania. *Journal of Health Economics*, *61*, 134–150. https://doi.org/10.1016/j.jhealeco.2018.07.004

INECC. (2014). *Valoración económica de los beneficios a la salud de la población que se alcanzarían por la reducción de las PM2.5 en tres zonas metropolitanas mexicanas*. https://www.gob.mx/cms/uploads/attachment/file/195224/2014_CGCSA_Beneficos_econ_micos_al_reducir_PM2.5.pdf

INEGI. (2020). *Census of Population and Housing 2020*. http://en.www.inegi.org.mx/programas/ccpv/2020/ (accessed 8 April 2022).

Kendix, M., & Walls, W. D. (2010). Estimating the impact of refinery outages on petroleum product prices. *Energy Economics*, *32*(6), 1291–1298. https://doi.org/10.1016/j.eneco.2010.05.016

Komisarow, S., & Pakhtigian, E. L. (2022). Are power plant closures a breath of fresh air? Local air quality and school absences. *Journal of Environmental Economics and Management*, *112*, 102569. https://doi.org/10.1016/j.jeem.2021.102569

la Nauze, A., & Severnini, E. (2021). Air pollution and adult cognition: Evidence from brain training, *IZA Discussion Paper Series*, 14353. https://www.iza.org/publications/dp/14353/air-pollution-and-adult-cognition-evidence-from-brain-training

Lavaine, E. (2019). Environmental risk and differentiated housing values: Evidence from the north of France. *Journal of Housing Economics*, *44*, 74–87. https://doi.org/10.1016/j.jhe.2019.02.001

Lavaine, E. (2016). Impact of energy production on respiratory outcomes: Evidence from the Flandres refinery in France. *Économie & Prévision*, *208-209*, 157–175. https://doi.org/10.3917/ecop.208.0157

Lavaine, E., & Neidell, M. (2017). Energy production and health externalities: Evidence from oil refinery strikes in France. *Journal of the Association of Environmental and Resource Economists*, *4*(2), 447–477. https://doi.org/10.1086/691554

Lichter, A., Pestel, N., & Sommer, E. (2017). Productivity effects of air pollution: Evidence from professional soccer. *Labour Economics*, *48*, 54–66. https://doi.org/10.1016/j.labeco.2017.06.002

Luechinger, S. (2014). Air pollution and infant mortality: A natural experiment from power plant desulfurization. *Journal of Health Economics*, *37*, 219–231. https://doi.org/10.1016/j.jhealeco.2014.06.009

Martínez, M. A., Caballero, P., Carrillo, O., Mendoza, A., & Mejia, G. M. (2012). Chemical characterization and factor analysis of PM2.5 in two sites of Monterrey, Mexico. *Journal of the Air & Waste Management Association*, *62*(7), 817–827. https://doi.org/10.1080/10962247.2012.681421

Martínez-Cinco, M., Santos-Guzmán, J., & Mejía-Velázquez, G. (2016). Source apportionment of PM2.5 for supporting control strategies in the Monterrey Metropolitan Area, Mexico. *Journal of the Air & Waste Management Association*, *66*(6), 631–642. https://doi.org/10.1080/10962247.2016.1159259

Martínez-Muñoz, A., Hurtado-Díaz, M., Cruz, J. C., & Riojas-Rodríguez, H. (2020). Mortalidad aguda asociada con partículas suspendidas finas y gruesas en habitantes de la Zona Metropolitana de Monterrey. *Salud Pública de México*, *62*(5), 468–476. https://doi.org/10.21149/11184

Mexican Ministry of Energy. (2021a). *Energy Information System: Manufacture of petroleum products*. https://datos.gob.mx/busca/dataset/elaboracion-de-productos-petroliferos-gas-licuado-gasolina-b-querosenos-turbosina-diesel-combus

Mexican Ministry of Energy. (2021b). *Energy Information System: Crude oil process by refinery*. https://datos.gob.mx/busca/dataset/proceso-de-petroleo-crudo-por-refineria-para-obtener-los-diferentes-tipos-de-petroleo

Mullins, J. T. (2018). Ambient air pollution and human performance: Contemporaneous and acclimatization effects of ozone exposure on athletic performance. *Health Economics*, *27*(8), 1189–1200. https://doi.org/10.1002/hec.3667

Parker, J. D., Mendola, P., & Woodruff, T. J. (2008). Preterm birth after the Utah Valley steel mill closure: A natural experiment. *Epidemiology*, *19*(6), 820-823. https://doi.org/10.1097/EDE.0b013e3181883d5d

Pope, C. A. (1991). Respiratory hospital admissions associated with PM10 pollution in Utah, Salt Lake, and Cache Valleys. *Archives of Environmental Health: An International Journal*, *46*(2), 90–97. https://doi.org/10.1080/00039896.1991.9937434

Pope, C. A. (1989). Respiratory disease associated with community air pollution and a steel mill, Utah Valley. *American Journal of Public Health*, *79*(5), 623–628. https://doi.org/10.2105/AJPH.79.5.623

Pope, C. A., Rodermund, D. L., & Gee, M. M. (2007). Mortality effects of a copper smelter strike and reduced ambient sulfate particulate matter air pollution. *Environmental Health Perspectives*, *115*(5), 679–683. https://doi.org/10.1289/ehp.9762

Pope, C. A., Schwartz, J., & Ransom, M. R. (1992). Daily mortality and PM10 pollution in Utah Valley. *Archives of Environmental Health: An International Journal*, *47*(3), 211–217. https://doi.org/10.1080/00039896.1992.9938351

Ransom, M. R., & Pope, C. A. (1992). Elementary school absences and PM10 pollution in Utah Valley. *Environmental Research*, *58*(1-2), 204–219. https://doi.org/10.1016/S0013-9351(05)80216-6

Rich, D. Q. (2017). Accountability studies of air pollution and health effects: Lessons learned and recommendations for future natural experiment opportunities. *Environment International*, *100*, 62–78. https://doi.org/10.1016/j.envint.2016.12.019

Sager, L. (2019). Estimating the effect of air pollution on road safety using atmospheric temperature inversions. *Journal of Environmental Economics and Management*, *98*, 102250. https://doi.org/10.1016/j.jeem.2019.102250

SEMARNAT. (2013). *Guía metodológica para la estimación de emisiones de fuentes fijas. México*.

Severnini, E. (2017). Impacts of nuclear plant shutdown on coal-fired power generation and infant health in the Tennessee Valley in the 1980s. *Nature Energy*, *2*, 17051. https://doi.org/10.1038/nenergy.2017.51

State Government of Nuevo León. (2020). *Coordination agreement for the recognition and integration of the Monterrey Metropolitan Area*. http://sistec.nl.gob.mx/Transparencia_2015/Archivos/AC_0001_0007_00168665_000001.pdf

State Government of Nuevo León. (2016a). *Programa de gestión para mejorar la calidad del aire del estado de Nuevo León 2016-2025*. https://www.gob.mx/cms/uploads/attachment/file/250974/ProAire_Nuevo_Leon.pdf

State Government of Nuevo León. (2016b). *Reporte de Calidad del Aire y Meteorología del Área Metropolitana de Monterrey: Julio 2016*. http://aire.nl.gob.mx/docs/reportes/mensuales/07_Reporte_Julio_2016.pdf

State Government of Nuevo León (2016c). *Reporte de Calidad del Aire y Meteorología del Área Metropolitana de Monterrey: Agosto 2016*. http://aire.nl.gob.mx/docs/reportes/mensuales/08_Reporte_Agosto_2016.pdf

State Government of Nuevo León. (2008). *Programa de Gestión para Mejorar la Calidad del Aire del Área Metropolitana de Monterrey 2008-2012*. https://www.gob.mx/cms/uploads/attachment/file/69303/3_ProAire_AMM_2008-2012.pdf

Stock, J. H., & Watson, M. W. (2020). *Introduction to Econometrics* (4th ed.). Pearson Education.

Trejo-González, A. G., Riojas-Rodriguez, H., Texcalac-Sangrador, J. L., Guerrero-López, C. M., Cervantes-Martínez, K., Hurtado-Díaz, M., de la Sierra-de la Vega, L.A., & Zuñiga-Bello, P. E. (2019). Quantifying health impacts and economic costs of PM2.5 exposure in Mexican cities of the National Urban System. *International Journal of Public Health*, *64*, 561–572. https://doi.org/10.1007/s00038-019-01216-1

Weijers, E. P., Sahan, E., ten Brink, H. M., Schaap, M., Matthijsen, J., Otjes, R. P., & van Arkel, F. (2010). *Contribution of secondary inorganic aerosols to PM10 and PM2.5 in the Netherlands; measurements and modelling results*. https://www.pbl.nl/en/publications/Contribution-of-secondary-inorganic-aerosols-to-PM10-and-PM2-5-in-the-Netherlands

Yang, M., & Chou, S.-Y. (2018). The impact of environmental regulation on fetal health: Evidence from the shutdown of a coal-fired power plant located upwind of New Jersey. *Journal of Environmental Economics and Management*, *90*, 269–293. https://doi.org/10.1016/j.jeem.2018.05.005

Zhang, X., Zhang, X., & Chen, X. (2017). Happiness in the air: How does a dirty sky affect mental health and subjective well-being? *Journal of Environmental Economics and Management*, *85*, 81–94. https://doi.org/10.1016/j.jeem.2017.04.001

Zivin, J. G., & Neidell, M. (2012). The Impact of Pollution on Worker Productivity. *American Economic Review*, *102*(7), 3652–3673. https://doi.org/10.1257/aer.102.7.3652

Appendix

Table A1.1. Monitoring stations considered for each pollutant

	0-40 km							40-60 km						> 60 km
	NE	NE2	NE3	SE	SE2	SE3	SUR	CE	NTE	NTE2	NO	SO	SO2	NO2
CO	✓✓			✓✓				✓✓	✓✓		✓✓	✓✓	✓✓	
NO_2					✓			✓✓			✓✓			
O_3	✓✓			✓✓							✓✓	✓✓	✓✓	✓✓
PM_{10}	✓✓	✓✓		✓✓	✓✓			✓✓	✓✓		✓✓	✓✓	✓✓	✓✓
$PM_{2.5}$		✓										✓	✓	
SO_2	✓✓			✓✓	✓✓				✓✓		✓✓			

Notes: This table indicates the stations considered to construct aggregate measures for each of the six pollutants we analyze. Stations are grouped according to their distance to the Cadereyta's refinery. Checkmarks indicate if the monitoring station (column) reports at least 70% (✓) or 85% (✓✓) of the time within the 30-day window for a certain pollutant (row).

Table A1.2. The effect of refinery shutdown on pollutant concentrations: local linear regression for stations SE2 and NO2

	a) Station SE2 (Juárez)	
	PM_{10}	SO_2
Refinery shutdown	-0.1218***	-0.0427**
	(0.027)	(0.0188)
Observations	1540	1203
Adjusted R^2	0.5008	0.6901
BIC	981.89	-690.33
Cumulative effect	-0.3185	-0.1392
	a) Station NO2 (García)	
	PM_{10}	SO_2
Refinery shutdown	-0.1804***	-
	(0.0287)	-
Observations	1541	-
Adjusted R^2	0.7818	-
BIC	1000.16	-
Cumulative effect	-0.4187	-

Notes: This table strengthen our base results that indicate that pollutants dispersion can extend the externalities from the refinery to the MMA, affecting air quality at both near and far distances. We present OLS regressions for the hourly concentrations of each pollutant (columns) within the 30-day window registered at stations SE2 (Juárez) and NO2 (García). SE2 is the nearest station from the refinery (17 km away) that was operating and reporting at least 70% of the time within the 30-day window. Conversely, NO2 station is far from the refinery, almost 70 km away. Each regression includes a linear trend, 4 lags of the dependent variable for each pollutant, and controls for seasonal variables and current and 1-hour lags of cubic functions of weather variables. Newey-West standard errors in parenthesis. The symbols ***, **, * indicate significance at the 1%, 5%, and 10% levels, respectively.

Table A1.3. The short-term effect of the 6-day refinery shutdown on pollutant concentrations: Testing for the presence of a pollution spike on day 1

	a) Stations within 40 km					
	CO	NO_2	O_3	PM_{10}	$PM_{2.5}$	SO_2
Day 1	-0.0049	0.0034	0.0050	-0.0678**	-0.1948*	-0.0124
	(0.0116)	(0.0281)	(0.0262)	(0.0332)	(0.1087)	(0.0292)
Days 2-6	0.0001	-0.0275*	0.0127	-0.0986***	-0.1950**	-0.0679***
	(0.0073)	(0.0151)	(0.0129)	(0.0228)	(0.0627)	(0.0234)
	b) Stations within 40-60 km					
	CO	NO_2	O_3	PM_{10}	$PM_{2.5}$	SO_2
Day 1	-0.0286*	0.0227	-0.0242	-0.0766*	-0.2490**	-0.0589
	(0.0151)	(0.0470)	(0.0221)	(0.0438)	(0.1037)	(0.0385)
Days 2-6	-0.0143	-0.066***	0.0354**	-0.0912***	-0.1975***	-0.0268
	(0.0091)	(0.0157)	(0.0177)	(0.0210)	(0.0710)	(0.0205)
	c) All stations					
	CO	NO_2	O_3	PM_{10}	$PM_{2.5}$	SO_2
Day 1	-0.0199	0.0111	-0.0019	-0.0553	-0.2041***	-0.0344
	(0.0143)	(0.0233)	(0.0151)	(0.0337)	(0.0642)	(0.0300)
Days 2-6	-0.0096	-0.0157	0.0210*	-0.0772***	-0.1720***	-0.0287**
	(0.0079)	(0.0133)	(0.0117)	(0.0182)	(0.0427)	(0.0143)

Notes: In this table we discard that the Cadereyta's refinery caused a pollution spike during the first day of the shutdown, differing from the unplanned outages studied by Du (2023). Therefore, our results are not diluted by an opposite effect at the onset of the 6-day shutdown. Local linear regressions are identical to the ones presented in Table 1.2 from the article, but instead of including a unique indicator variable for the 6-day refinery shutdown, we include two indicator variables that distinguish the first day from following 5 days in order to test for the potential presence of a pollution spike on day 1. Newey-West standard errors in parenthesis. The symbols ***, **, * indicate significance at the 1%, 5%, and 10% levels, respectively.

Table A1.4. Average treatment effects of Cadereyta's refinery temporary shutdown on mortality caused by diseases of the circulatory and respiratory systems

Age\Causes	Circulatory system	Respiratory system
Static model		
All ages	-0.2363	0.0136
	(1.2764)	(0.5274)
5 years and younger		-0.0884
65 years and older	-0.7191	0.1168
	(0.9584)	(0.4437)
Autoregressive model		
All ages	-0.3869	0.0145
	(1.5946)	(0.7643)
5 years and younger	-0.0152	0.1219

65 years and older	-0.4730	0.0594
	(1.1204)	(0.6854)

Notes: Average treatment effects (ATE) calculated from estimates of the static and autoregressive models of (5) and (6) via Poisson quasi-maximum likelihood estimator (QMLE) with corrected standard errors. We report standard errors obtained by the delta method in parenthesis, except for children's (5 years and younger) deaths because it was not possible to estimate the variance-covariance matrix. The symbols ***, **, * indicate significance at the 1%, 5%, and 10% levels, respectively.

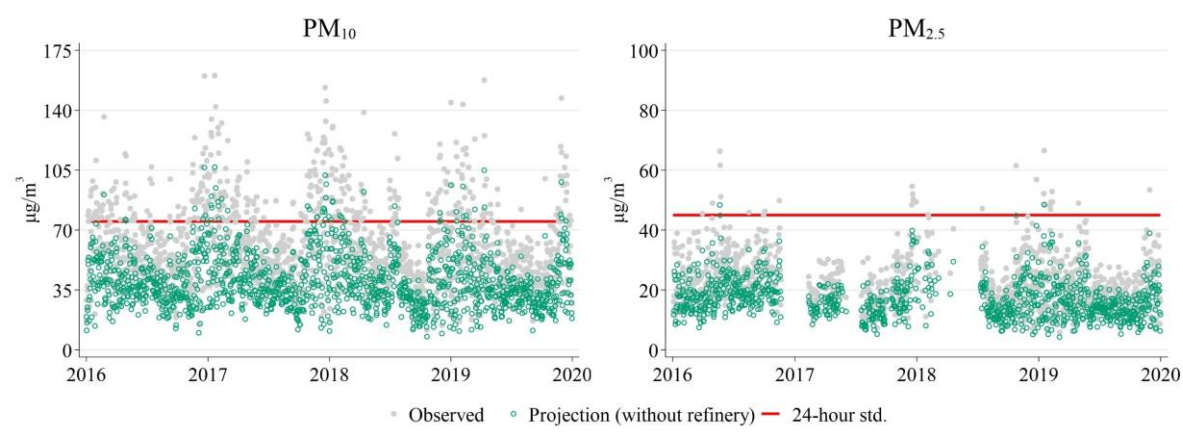

Figure A1.5. 24-hour average particle concentrations in the MMA with and without the refinery. In this figure, we show that a permanent reduction in particle concentrations of the same magnitude as those estimated for the 6-day refinery shutdown would substantially improve compliance with official standards in the MMA. To maintain comparability across time, we only consider hourly records from stations NE, NE2, SE, SE2, CE, NTE, NO, SO, SO2, and NO2 for PM_{10}. Similarly, we only consider stations NE2, SO, and SO2 for $PM_{2.5}$. To include a station in the calculation of the 24-hour average for each day, we require that it reports at least 70% of the hourly records (16 out of 24). 24-hour standards for $PM_{10} = 75\ \mu g/m^3$ and $PM_{2.5} = 45\ \mu g/m^3$ according to NOM-025-SSA1-2014 (valid in Mexico for this period).

Chapter 2. Congestion and severe road accidents: An hourly econometric study for Mexico City

Executive Summary

Road congestion generates evident external costs for the inhabitants of Mexico City. On average, individuals require 59% more time to complete their weekday trips compared to what it would take under free flow conditions. This amounts to about 154 hours a year—or 19 workdays—just considering weekday travel. Congestion is also linked to other external costs that often go unnoticed or are attributed to distinct causes. Such is the case of pollution and road accidents.

As the number of vehicles on the road increases, and we require more time to complete our trips, are there more or fewer road accidents? Is this relationship sensitive to the day of the week or the level of congestion? The existing literature is divided between articles that associate congestion with road accidents either positively or negatively. Furthermore, there is still a debate regarding the functional form of this relationship. Congestion and its effects on road accidents have been primarily studied on high-speed roads or cities in high-income countries where data is usually available. Apart from two articles, there is no research available on this topic for highly congested cities in developing countries and, particularly, studies considering traffic congestion in the whole city instead of specific high-speed roads.

This chapter answers these questions by analyzing the case of Mexico City. To overcome the lack of information on hourly vehicle flows or other traffic-related measures, we construct a congestion index using hourly travel times reported by Uber. The congestion index represents the additional percentage of time it takes to travel by car from one geographical zone (AGEB) to another compared to the time it would take without congestion. This measure can be aggregated depending on the relevant dimension of the study. This chapter focuses on the time of the day dimension, calculating an hourly congestion index by quarter that distinguishes between weekdays and weekends. However, it also includes a base spatial analysis that aggregates the congestion index by region.

In addition, this chapter uses a database of severe road accidents occurred in the urban areas of Mexico City, which is built from emergency reports confirmed by the authority at the scene. This allows calculating—without measurement error—the average number of severe road accidents per day occurring at a certain hour in a quarter, considering the 24 hours of the day. In total, the database includes 128,020 severe road accidents for the period 2016-2019. This database also permits evaluating the sensitivity of the relationship between congestion and accidents for different road users and the specific regions where these severe road accidents occurred. To do this, we separated severe road accidents into those that affect only vulnerable road users (pedestrians, cyclists, and motorcyclists) from those that only involve car occupants (single or multi-car severe road accidents).

We estimate panel fixed effects and time series models to study the relationship between severe road accidents and the congestion index in Mexico City for the quarters in the period from 2016 to 2019. Thus, unlike previous studies, we use different estimation methods and report specific results for Mexico City, using a more reliable dataset that focuses on severe road accidents. Furthermore, our analysis distinguishes the relationship between severe road accidents and congestion that exists on weekdays and weekends, which is essential to determine the functional form of the relationship. Finally, it evaluates the sensitivity of the results for the different road users involved in severe road accidents (vulnerable users and car occupants) and the regions where these accidents occur in Mexico City (center, northeast, northwest, southeast, and southwest).

The results indicate that congestion and severe road accidents are positively related. Highly congested cities such as Mexico City could prevent between 1,717 and 3,716 severe road accidents per year if congestion is reduced roughly 30%. Distinguishing between congestion patterns on weekdays and weekends is important. While there is a positive linear relation during weekends, the relationship can be either linear or quadratic (concave) during weekdays. This article is the first to address this distinction.

Finally, it is worth mentioning that both vulnerable road users and car occupants are affected with increased congestion during weekdays. For weekends, this positive relationship only holds for severe road accidents that involve pedestrians, cyclists, and motorcyclists. Moreover, the positive relationship between congestion and severe road accidents seems to be driven mainly by the central region of Mexico City. Hence, policymakers could reduce the number of accidents evaluating and implementing transportation policies that reduce the vehicular flow toward the city center.

Full text

2.1. Introduction

Road congestion takes away one of our most valuable endowments: time. In the Valley of Mexico, this burden represents the equivalent of 17 workdays for users of automobiles and 21 workdays for users of public transportation (IMCO & Sin Tráfico, 2019). Besides the opportunity cost, congestion generates other important costs. For instance, it indirectly impairs our health causing depression, fatigue, and irritability (Calatayud et al., 2021). Moreover, it increases pollution, leading to more infant mortality associated with respiratory and cardiovascular diseases (Arceo et al., 2016). In addition, recent studies suggests that as more cars circulate on the roads and the time required to complete our trips increases, there are more accidents (Green et al., 2016; Sánchez González et al., 2021; Shi et al., 2016; Sun et al., 2016). Nevertheless, there are some studies that suggest the opposite (Albalate & Fageda, 2021; Pasidis, 2019; Shefer, 1994), at least for some levels of congestion. Moreover, the underlying functional form—linear or quadratic—is still being debated.

Congestion and its effects on road accidents have been primarily studied on high-speed roads (for example, highways (Pasidis, 2019; Romem & Shurtz, 2016), motorways (Wang et al., 2009), and urban expressways (Shi et al., 2016; Sun et al., 2016)) or cities in high-income countries such as groups of European cities (Albalate & Fageda, 2021), London (Green et al., 2016; Dickerson et al., 2000; Noland & Quddus, 2005; Tang & van Ommeren, 2021; Wang et al., 2009), Adelaide (Retallack & Ostendorf, 2020), and Florida (Shi et al., 2016) where the data is usually available. Except for one study about the urban expressways in Shanghai (Sun et al., 2016) and another about 10 Latin American cities (Sánchez González et al., 2021), there is no research available on this topic for highly congested cities in developing countries and, particularly, studies considering traffic congestion in the whole city instead of specific high-speed roads.

2.2. On the relationship between congestion and road accidents

There is no consensus on the relationship between congestion and road accidents. Results seem to depend on the method, location, data aggregation and definition of the relevant variables of these studies. However, a recent literature review conducted by Retallack and Ostendorf (2019) suggests that the most common finding is a positive relation. Moreover, they report that this relationship is not linear for more than half of the reviewed studies. This tends to occur more in studies that consider many observations and use data with greater granularity.

Following Shefer (1994), empirical studies started testing the possible existence of a trade-off between congestion and road safety. That is, an increase in traffic flow—under uncongested conditions—results in more severe accidents due to an increase in exposure. However, as traffic density increases, speeds gradually fall reaching a point where the relationship turns negative. In line with this idea, Noland and Quddus (2005) used a negative binomial model to study the relationship between two proxies of congestion and accidents for over 15,000 spatial units (enumeration districts) in London. They did not find sufficient evidence to support an improvement in safety due to congestion.

More recent works adopted direct measures of traffic congestion such as the travel time—or travel speed—based indexes described by Taylor et al. (2000). These studies consider spatial dependency but ignore the time of the day dimension. They use a Bayesian approach assigning accidents to high-speed road segments over a time span. For example, Wang et al. (2009) rejected the hypothesis proposed by Shefer (1994), concluding that the level of congestion has no impact on the frequency of road accidents in M25 London orbital motorway. With a similar approach, Sun et al. (2016) find that congestion increases the risk of an accident on urban expressways in Shanghai, China. The authors attribute this result to the increased interaction caused by drivers frequently changing lanes and the reduced distance between vehicles due to congestion. Shi et al. (2016) separate accidents into peak and non-peak hours, recognizing that congestion can be both time and location specific. They use a Bayesian ridge regression to find that congestion—measured by a travel speed-based

index or road occupancy—is related to a higher frequency of crashes—more likely rear-end crashes—only during peak-hours on the urban expressway State Road 408 in Central Florida.

A related strand of literature tests for the existence of an accident externality of driving. These works follow Walters (1961), who according to Small and Chu (2003) established "the standard way" economist consider congestion. That is, the time required to complete a trip elevates more than proportionally as the number of vehicles flowing per hour rises. As traffic demand increases above the road capacity—and congestion becomes apparent—there is a fall in traffic flow accompanied with a rise in travel time that grows at a decreasing rate. This conception is comparable to Taylor et al. (2000) who define the level of congestion as the excess travel time incurred by a driver when completing a trip.

Using traffic flow as the explanatory variable, Dickerson et al. (2000), Edlin and Karaca-Mandic (2006) and Romem and Shurtz (2016) confirm the existence of a negative accident externality of driving, which is only relevant for high levels of traffic flow in London, United States, and Israel, respectively. That is, traffic volume increases the risk and costs of having an accident more than proportionally when traffic is high. Similarly, Retallack and Ostendorf (2020) find a positive linear relationship between traffic flow and accident frequency that increases quadratically at higher rates in Adelaide, Australia. Consistent with the previous results, Green et al. (2016) find a general drop in both the number of accidents and the probability of having an accident due to the reduced traffic flow attributable to the daily congestion charge imposed in London since 2003. In contrast, Tang and van Ommeren (2022) find a positive externality concluding that an additional driver decreases the risk and severity of accidents due to the reduction in drivers' speed and increased awareness under congested scenarios.

According to Edlin and Karaca-Mandic (2006), the probability of an accident increases with traffic density because for an accident to occur vehicles should be close to each other. However, Edlin and Karaca-Mandic (2006) and Jansson (1994) warn that congestion caused by excess driving—or more drivers on the road—might reduce risk and average costs (severity) of accidents to the point where accident frequency is reduced. Hence, akin to Tang and van Ommeren (2022), high congestion may dilute or reverse the accident externality of driving.

Additionally, as recognized by Jansson (1994), the accident externality may also impact other road users. The author hypothesizes that additional cars on the road translates into greater risk for "unprotected" or vulnerable users, as pedestrian, cyclist, and motorcyclist. In fact, the literature reviewed by Lindberg (2001) suggests that accidents between motor vehicles and vulnerable user increase at a decreasing rate with traffic volume in urban areas.

Shi et al. (2016) argue that traffic volume cannot replace a direct congestion measure, which they find more appropriate. The most recent studies consider non-linear functional forms to model the relationship between congestion and traffic accidents. Moreover, they

take advantage of the growing availability of big datasets obtained from crowd-sources and government agencies. These datasets include direct information about traffic congestion conditions even in real time. Consequently, the greater data granularity has introduced endogeneity as a potential threat when investigating this relationship. As recognized by Taylor et al. (2000), road capacity can change over time generating non-recurrent traffic congestion caused by accidents, weather conditions and other irregular factors. Pasidis (2019) confirms a short 15-minute small negative effect of personal injury accidents on traffic congestion for highways in England. Conversely, the author concludes that the probability of an accident falls—decreasing marginally—as congestion increases.

Albalate and Fageda (2021) employed a negative binomial panel model using a yearly congestion index obtained from actual GPS anonymous travel-times and found evidence to support a U-shape relationship for 129 large cities in Europe for the period 2008-2017. According to their results, an increase in congestion reduces deaths in accidents up to the point where congestion represents 30%. The authors suggest that a possible explanation for the positive relationship after the threshold level is that drivers try to avoid congestion by taking alternative routes that are generally less prepared to receive high traffic volumes.

Lastly, Sánchez González et al. (2021) estimated a Poisson panel model with fixed effects for 10 Latin-American cities, including Mexico City. Using 2019 hourly disaggregated data obtained from Waze mobile application, they construct an aggregate delay measure at the city level based on a neural network model and found a positive non-linear—decreasing marginally—effect of congestion on road accidents.

There are several differences between our work and Sánchez González et al. (2021) which are worth emphasizing. First, we use different estimation methods and report specific results for Mexico City. Second, we employ an accident database with greater reliability that allows us to consider the 24 hours of the day, instead of a subperiod (7:00 to 21:00 hrs.). Third, we focus on severe road accidents, which are less likely to have measurement errors. Fourth, our work distinguishes between weekdays and weekends, which is key to determine the functional form of the relation between congestion and accidents. Fifth, our work tests for differences in the relationship between accidents and congestion for different road users and regions within Mexico City.

2.3. Data

2.3.1. Traffic congestion using Uber movement aggregated data

Uber is a leading mobile application that connects car drivers with individuals needing transportation services all over the world. This mobile application records trips from the drivers' mobile GPS with a high frequency (every 4 seconds), generating a set of positions (latitude and longitude pairs) along with their corresponding date and time. Uber assigns

these observations to the appropriate geographic zone—AGEB in the case of Mexico City[1]—as a within-zone average, so that zone-to-zone travel times can be calculated (Uber Technologies, Inc., 2022).

Uber aggregates all trips and reports AGEB-to-AGEB hourly average travel times for each quarter of the period 2016-2019—distinguishing between weekdays and weekends—in Mexico City if there were enough trips in the quarter and the count of distinct drivers is large enough to keep their privacy. We referred to this dataset as the Uber movement aggregated data. It is important to note that we do not have access to the quantity of AGEB-to-AGEB trips nor the count of distinct drivers that conducted these trips.

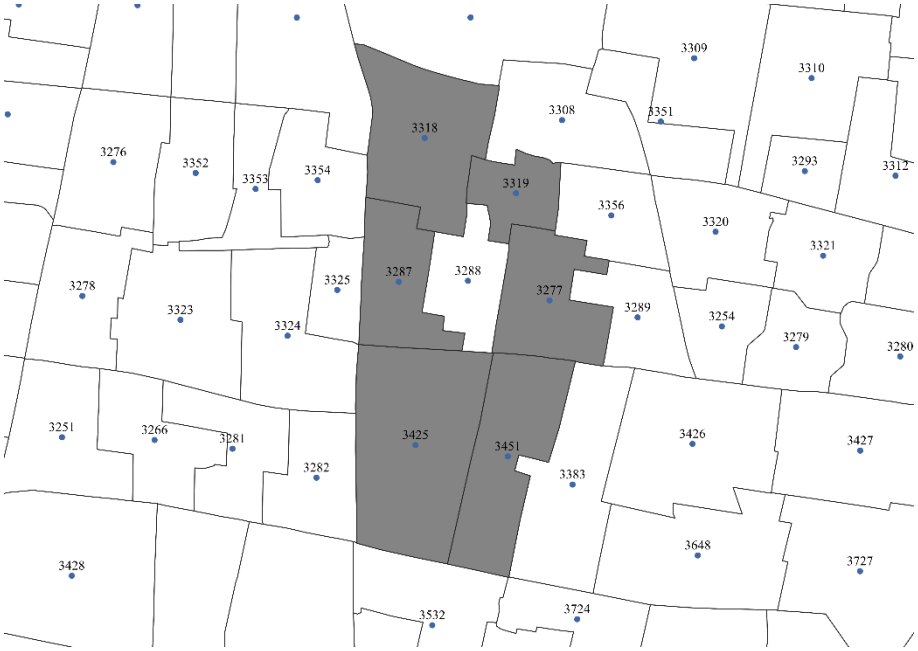

Figure 2.1. Neighbors' identification using queen criterion. The figure exemplifies the criteria used to identify neighbors. According to queen criterion, the set of polygons {3318, 3319, 3277, 3451, 3425, & 3287} are neighbors of the polygon 3288. Each point corresponds to the centroid of the polygon (AGEB). *Source:* Prepared by the authors using QGIS 3.16.

We identified the set of contiguity-based spatial neighbors from a total of 2,431 urban AGEBs in Mexico City using the queen criterion (see Figure 2.1). As Pearson et al. (2017), we define two polygons as neighbors if they share a boundary (a side or an edge). A total of 14,424 neighbors' pairs were registered (see Figure 2.2)[2].

[1] In Mexico, municipalities are subdivided for geostatistical purposes in basic geographic areas (AGEBs). The geostatistical limits are set by the National Institute of Statistics and Geography (INEGI). Urban AGEBs pertain to localities with more than 2,500 inhabitants and consist generally of 1 to 50 squares whose land is used for housing, commerce, industry, and services (INEGI, 2010).

[2] One of the 2,431 urban AGEBs in Mexico City does not have a neighbor according to the queen criterion. This zone is omitted in the following calculations.

Figure 2.2. 2,431 AGEBs' centroids linked to its neighbors in Mexico City. The figure shows 14,424 neighbor pairs represented as line segments joining two points—AGEB centroids—for Mexico City. Urban AGEBs are defined as neighbors if they share a boundary. *Source:* Prepared by the authors using "spdep" and "maptools" packages in R and data from the Mexico City geostatistical framework published by INEGI (2020).

For each neighbor pair, we recovered—due to availability—about 95% of the hourly average travel times from the origin AGEB i to its destination neighbor j, $j \in N(i)$ using Uber movement aggregated data. Akin to Arbia (2014), we denote $N(i)$ as the set of neighbors of location i. Later, we referred to $J(i)$ as the number of neighbors in the set $N(i)$. The complete dataset includes 461,568 observations (14,424 neighbors' pairs per 16 quarters distinguishing weekdays from weekends).

Following Taylor et al. (2000), we computed 10,527,503 hourly congestion indexes (CI_{ijhqw}) that represent the excess travel time $\left(T_{ijhqw} - \min\left(T_{ijqw}\right)\right)$ required to get from AGEB i to its neighbor AGEB j for a certain hour of the day, h, with respect to the minimum average travel time $\left(\min\left(T_{ijqw}\right)\right)$ required to complete the same AGEB-to-AGEB trip in that quarter, q, in weekdays or weekends, w. That is,

$$CI_{ijhqw} = \left(\frac{T_{ijhqw}}{\min\left(T_{ijqw}\right)} - 1\right) \times 100; \qquad \begin{array}{c} i = 1,2,\dots,2431; \\ j = 1,\dots,J(i)\ with\ J(i) = \#\{N(i)\}; \\ h = 0,\ 1,\ 2,\dots,23; \\ q = 2016\ 1Q,\dots,2019\ 4Q; \\ w = weekdays\ or\ weekends. \end{array}$$

Our congestion index is based on travel times obtained from crowd-sourced data. In this sense, it is comparable to the ones used by Kreindler (2016), Albalate and Fageda (2021), or Sánchez González et al. (2021). These measures have the virtue of considering all types of roads in places that otherwise could not be studied due to the lack of data. Kreindler (2016) uses travel time excess delay calculated from 150 routes across Delhi using Google Maps API. Similarly, Albalate and Fageda (2021) employs the TomTom yearly congestion index for 129 European cities in 2008-2017, while Sánchez González et al. (2021) construct an aggregate time delay measure for 10 major Latin-American cities using high-frequency data collected from Waze.

The measure of traffic congestion can be aggregated depending on the relevant dimension of the study. In this paper, we focus mostly on the time of the day dimension. However, we also extend our main model, including a base spatial analysis, leaving space-time specifications for further research. Regarding the time of the day dimension, we averaged the congestion indexes on each AGEB with respect to their set of neighbors and then over all the 2,431 AGEBs, resulting in an hourly measure by quarter that distinguishes between weekdays and weekends:

$$CI_{hqw} = \frac{1}{2431}\sum_{i=1}^{2431}\frac{\sum_{j=1}^{J(i)} CI_{ijhqw}}{J(i)}, \qquad J(i) = \#\{N(i)\}.$$

For the space dimension, we again averaged congestion indexes on each AGEB with respect to their set of neighbors but then proceed to average them by regions. For this, AGEBs were subset in 5 regions, r, depending on the municipality in which the origin AGEB i is located: CE (center), NE (northeast), NW (northwest), SE (southeast) and SW (southwest)[3]. Here, the number of AGEBs located in the subset from region r is $\#\{R(r)\}$. The regional traffic congestion index is:

$$CI_{rhqw} = \frac{1}{\#\{R(r)\}}\sum_{i=1}^{\#\{R(r)\}}\frac{\sum_{j=1}^{J(i)} CI_{ijrhqw}}{J(i)}, \;\; i \in R(r);\; r = CE, NE, NW, SE, SW.$$

Our measure has certain advantages over previous comparable congestion indexes. First, it was calculated from actual travel times registered by Uber drivers when completing their trips, instead of a prediction based on historical and current data as Kreindler (2016). Second, the reliability of our accident dataset (which we will explain in detail in the following subsection) allows us to consider the 24 hours of the day instead of a subperiod, for example 7:00 to 21:00 hrs. as Sánchez González et al. (2021). Third, it provides us with a more

[3] Regional classification of municipalities in Mexico City: CE (Iztacalco, Benito Juárez, Cuauhtémoc, and Venustiano Carranza); NE (Gustavo A. Madero); NW (Azcapotzalco and Miguel Hidalgo); SE (Tláhuac, Iztapalapa, Xochimilco, and Milpa Alta); and SW (Coyoacán, La Magdalena Contreras, Cuajimalpa de Morelos, Álvaro Obregón, and Tlalpan).

disaggregated measure than the yearly index used by Albalate and Fageda (2021). Specially, it allows us to distinguish between the significantly different congestion patterns of weekdays and weekends (see Figure 2.3), as well as the different regional traffic congestion patterns in Mexico City (see Figure 2.4). Finally, Uber travel times are open and freely available for 51 cities around the world in contrast to the comparable sources.

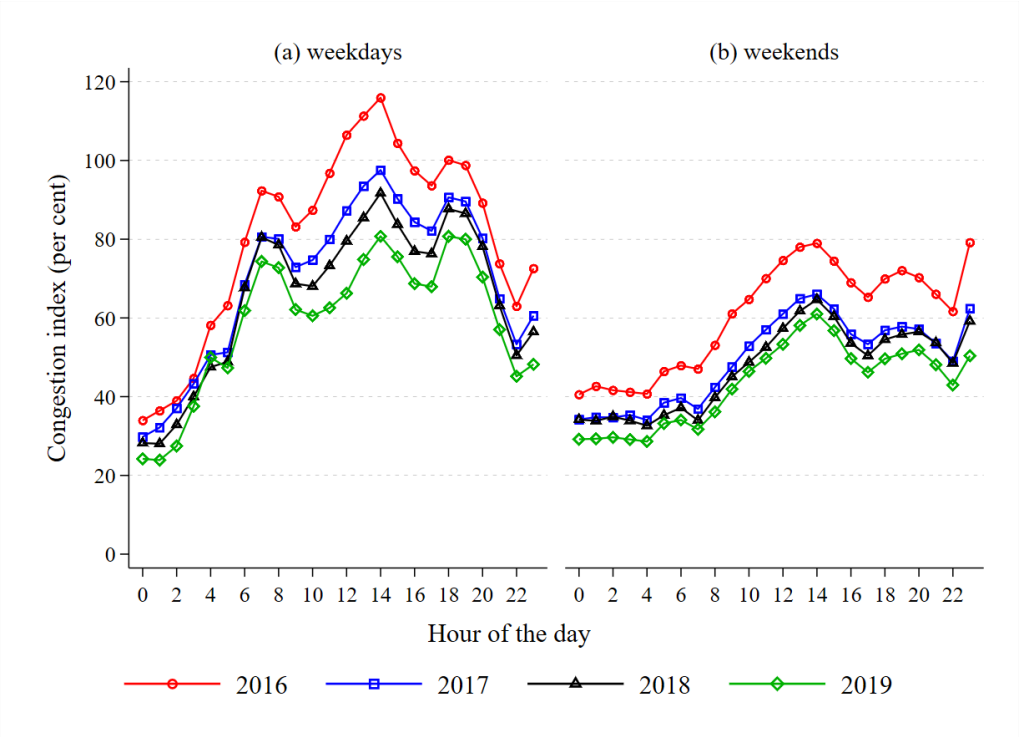

Figure 2.3. Average hourly congestion by year in Mexico City. Congestion is measured through an index that represents the excess travel time as a per cent of the average minimum travel time achieved under free flow conditions. *Source:* Prepared by the authors using data retrieved from Uber Movement, © 2022 Uber Technologies, Inc, https://movement.uber.com

Figure 2.3 shows the average hourly congestion index for weekdays and weekends in Mexico City, which has been ranked as the 2nd or 3rd most congested city in America—8th or 13th in the World—between 2017 and 2019 (TomTom, 2019). Inhabitants of the capital city required 59% more time—on average—to complete their weekdays' travels compared to the minimum time it would take under free flow conditions in 2019. That is, a daily 30-minute commute would result in a 48-minute trip because of traffic jams. Apart from a lower level of congestion (43%), weekends exhibit a distinct pattern throughout the day. There are 3 visible peaks for 2019 weekdays occurring at 7 a.m. (74%), 2 p.m. (81%), and 6 p.m. (81%). In contrast, the traffic congestion peak on weekends occurs almost solely at 2 p.m. (61%).

Differences in regional congestion patterns are worth emphasizing too. As shown in Figure 2.4, CE and SE regions are the most congested during weekdays. Their congestion indexes were nearly 6 percentage points higher than region NW (the least congested in Mexico City) in 2019. That is, an individual who conducted daily 60-minute commutes

throughout 2019 on these regions (CE and SE) instead of in region NW would spend around 16 more hours to complete their trips. Similarly, regions SE and NW are—respectively—the most and least congested during weekends, however, their congestion indexes differ in almost 20 percentage points.

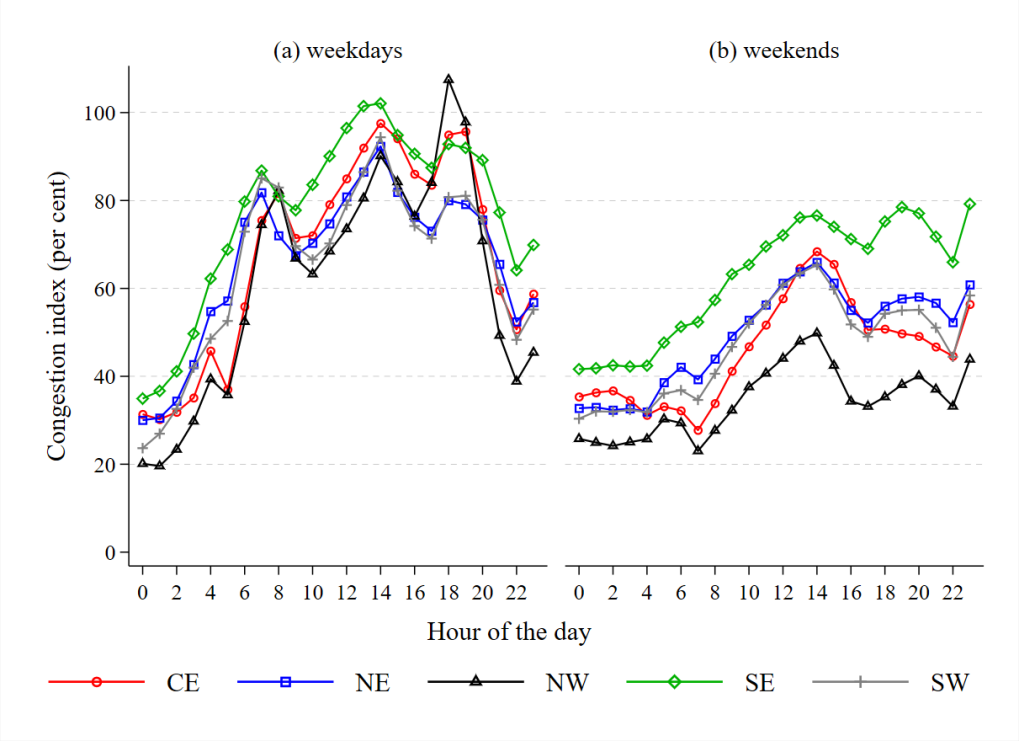

Figure 2.4. Average hourly congestion by region in Mexico City (2016-2019). *Source:* Prepared by the authors using data retrieved from Uber Movement, © 2022 Uber Technologies, Inc, https://movement.uber.com

Despite its advantages, our measure of traffic congestion does not come without limitations. As Kreindler (2016), our aggregated measure is an unweighted average. As mentioned before, Uber does not report how many trips were completed between each neighbor pair. Hence, we are implicitly giving all of them the same importance. Nonetheless, if we compare our congestion index with a weighted index, as the one used by Albalate and Fageda (2021), we find a similar reported level of congestion for 2019. While TomTom (2019) reports 52%, a combination of our weekdays and weekends data results in 55% $\left(\approx 0.59 \times (261/365) + 0.43 \times (104/365)\right)$. Additionally, because we don't have information at the trip level, we assume that travels completed between neighbor pairs are evenly distributed throughout the space for the distinct hours of the day. Otherwise, trip distance varies, and our measure would not be unitless. Finally, it has been proved that traffic regularities take place at short intervals. For example, Geroliminis and Daganzo (2008) aggregate vehicle-counts every 5 minutes. Unfortunately, we cannot calculate our congestion index for such short intervals because Uber only reports aggregated travel times by hour of the day.

The reader should also note that by characterizing Mexico City's congestion from Uber travel times, we are presuming that Uber drivers don't display a less reckless behavior than the average representative driver, even at night. Fortunately, as noted by Taylor et al. (2000), if similar trips are repeated many times by different drivers, it is less likely that our measure is influenced by the driver's particular driving style.

2.3.2. Severe road accidents

C5 is a state office that receives and captures incidents such as medical and general emergencies or crimes through help buttons, security cameras, emergency calls to 911, reports in the media, and social networks in Mexico City. Each report is uniquely identified and confirmed at the scene. The institution shares an open large dataset with all road incidents since 2014 including the date and time the reports were received and closed, the exact location, and a general description of confirmed events[4].

Our study is limited to severe road accidents, which we define initially as confirmed road reports where a dead body was found or there were injured persons. Unfortunately, not all confirmed reports include a general accident description that makes a distinction between various levels of severity. Hence, we also include events which descriptions suggests some form of personal injury and/or severity. For example, reports where there was an arrest, or a person or vehicle was overturned, trapped, or crushed. We also consider accidents involving pedestrians, motorcycles, bicycles, and trains. Only severe road accidents occurring up to 1 meter away from an urban AGEB area were considered. In total, our dataset incudes 128,020 severe road accidents for the period 2016-2019.

Given that each report is confirmed by the authority at the scene, it provides us with a reliable source of information for the 24 hours of the day. However, it is still possible that some road accidents are not reported by its nature. For example, drivers may decide to continue with their trips and not report an accident if they are in a hurry and the event was not severe. An advantage of limiting our work to severe road accidents is that such accidents are more likely to be reported and recorded (Green et al., 2016).

We grouped and counted these severe reports by the date and time they were received, obtaining an hourly measure by quarter for the 2016-2019 period. For comparability, we divide the total reports in each time frame by the number of weekdays or weekends in the quarter. Our measure then represents the average number of severe road accidents per day occurring at a certain hour in a quarter.

[4] This information is available at: https://datos.cdmx.gob.mx/dataset/incidentes-viales-c5

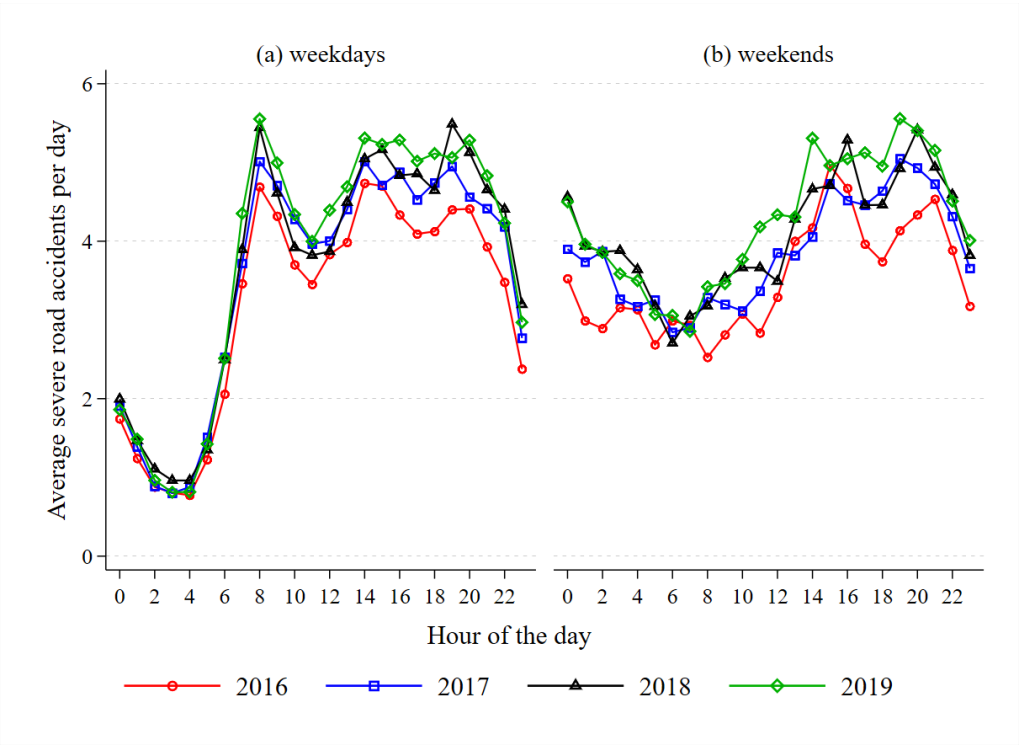

Figure 2.5. Average hourly severe road accidents per day by year in Mexico City. *Source:* Prepared by the authors using reported road incidents by C5.

As shown in Figure 2.5, road accidents occur more frequently on weekends. While on average 3.93 severe road accidents per hour are reported on weekends, only 3.54 occur on weekdays. Nonetheless, the pattern throughout the day is also distinct as seen by the statistically higher variance present on weekdays. After an initial drop in the number of severe road events at the first hours of the day, weekdays exhibit a steep 6-fold increase from a minimum of 0.84 severe accidents per hour at 3 a.m. to a maximum of 5.17 at 8 a.m. Comparable to the levels of congestion through the day, severe road accidents exhibit 2 additional peaks at 2 p.m. (5.03 accidents per hour) and 7 p.m. (4.97) on weekdays. In contrast, weekends present a lower variance with the highest levels of severe road accidents per hour occurring from 3 to 4 p.m. (4.86) and 7 to 8 p.m. (4.97).

Because the accident externality of driving can impact road users in a differentiated way, especially under highly congested scenarios, we separate severe road accidents into those that affect only vulnerable road users (pedestrians, cyclists, and motorcyclist) from those that only involve car occupants (single or multi-car severe accidents)[5]. We also disaggregate severe road accidents based on the region where they occurred because, as suggested by

[5] We do not include train accidents in this classification because we cannot distinguish whether train accidents affected only vulnerable users or car occupants. However, as shown in Table 2.1, our classification includes 98.5% of severe road accidents.

Lindberg (2001), urban traffic can be substantially different in terms of accident risk within a city (for example, if one compares the center vs. the periphery).

Table 2.1. Average hourly severe road accidents per day by region in Mexico City (2016-2019)

	a) Weekdays					
	CE	NE	NW	SE	SW	All regions
All users	1.2588	0.3949	0.4396	0.6788	0.7678	3.5400
	(0.5801)	(0.1901)	(0.2264)	(0.2965)	(0.3578)	(1.5608)
Vulnerable users	0.54702	0.16317	0.17846	0.31411	0.30290	1.5056
	(0.3174)	(0.1023)	(0.1202)	(0.1731)	(0.1856)	(0.8338)
Car occupants	0.6860	0.2294	0.2535	0.3613	0.4541	1.9842
	(0.2777)	(0.1056)	(0.1229)	(0.1495)	(0.1911)	(0.7580)
	a) Weekends					
	CE	NE	NW	SE	SW	All regions
All users	1.2541	0.4506	0.4007	0.8863	0.9341	3.9257
	(0.3285)	(0.1740)	(0.1536)	(0.2690)	(0.2966)	(0.8935)
Vulnerable users	0.4845	0.1711	0.1359	0.3774	0.3380	1.5069
	(0.2268)	(0.1118)	(0.0927)	(0.1909)	(0.1909)	(0.6419)
Car occupants	0.7318	0.2769	0.2540	0.5068	0.5811	2.3507
	(0.1931)	(0.1136)	(0.1101)	(0.1703)	(0.1851)	(0.4437)

Notes: Standard deviation reported within parentheses. Figures presented with rounding to 4 decimal places.
Source: Prepared by the authors using reported road incidents by C5.

Table 2.1 shows descriptive statistics for severe road accidents in Mexico City, distinguishing between the regions where accidents were reported and the road users who were severely affected. A salient observation is that around 35% of the severe road accidents occurred in the CE region of Mexico City. Additionally, consistent with what we would expect based on Jansson (1994) and Lindberg (2001), the most congested regions (CE and SE) appear to pose a greater risk for vulnerable users.

2.4. Empirical framework

For our main specification, we use a panel fixed effects model. As Pasidis (2019), who uses 15-minute periods within the day as cross-sectional units, we treat the hour of the day—separating weekdays from weekends—as our unit of observation. Hence, the basic model is

$$Severe_{hqw} = \alpha + \gamma_1 \cdot CI_{hqw} + \gamma_2 \cdot CI_{hqw}^2 + \beta \cdot X_{hqw} + \sum_{j=2}^{4} \theta_j \cdot quarter_{j,q} + \sum_{j=2017}^{2019} \lambda_j \cdot year_{j,q} + \sum_{h=1}^{23} \sum_{w=0}^{1} \phi_{hw} \cdot \upsilon_{hw} + \varepsilon_{hqw} \quad (1)$$

The dependent variable is the average number of hourly severe road accidents per day ($Severe_{hqw}$). The model includes the congestion index (CI_{hqw}) and a quadratic term (CI_{hqw}^2).

The sum $\gamma_1 + 2\gamma_2\overline{CI}_{hqw}$ represents how a one percentage point increase in congestion affects the average number of hourly severe road accidents per day. The proposed model includes a constant (α) and a vector of observable variables (X_{hqw}) that change with time: average millimeters of rain in the last hour, average minutes of astronomical, nautical, and civil twilight, and average minutes of night[6]. Note that we include time fixed effects for quarters and years, as well as unit fixed effects which allow the existence of unobservable characteristics that vary with the hour of the day and day of the week, but do not change through the quarters (υ_{hw}).

This model has two potential estimation problems. First, units (i.e., hours of the day) may be mutually dependent. That is, accidents occurring at a certain hour of the day could be correlated with accidents occurring in previous hours. Second, congestion may be an endogenous variable because accidents can cause traffic jams (Pasidis, 2019). Nonetheless, we argue—as Albalate and Fageda (2021)—that given the form in which we have aggregated our traffic congestion index, it only captures the recurrent patterns of traffic.

If accidents are correlated, the estimated standard errors will be inconsistent. We employ the test for cross-sectional dependence proposed by Pesaran (2021) and reject that units are cross-sectionally independent ($CD = 12.411; p = 0.0000$). Hence, we report the Driscoll and Kraay (1998) standard errors that are robust to the presence of heteroskedasticity and general forms of temporal and spatial correlation (i.e., cross-sectional dependence).

Because the count of hourly severe road accidents by quarter is a discrete nonnegative integer, the literature suggests using Poisson or negative binomial panel models. However, these models also assume that observations are independent of one another (Hilbe, 2014). Fortunately, Hoechle (2006) contributed with a Stata implementation of Driscoll and Kraay (1998) standard errors for panel fixed effects model. Therefore, we opted for the previously proposed model.

As mentioned earlier, we believe that accidents are not causing traffic congestion as measured by our index. Akin to the argument posed by Albalate and Fageda (2021), a sole accident occurring at a certain road segment and date/hour in Mexico City will hardly affect our aggregated congestion index because it was constructed based on many Uber trips distributed across the whole city in a quarter. We confirm this insight conducting both Durbin-Wu-Hausman ($F(1, 14) = 1.07; p = 0.3175$) and the C-statistic test for endogeneity ($\chi^2(1) = 1.329; p = 0.2489$). We cannot reject that our congestion index is an exogenous variable using the lagged congestion index (same hour of the day from the previous quarter)

[6] Daylight control variables were constructed from daily sunrise and sunset times available at timeanddate.com. These start and end times consider clock adjustment due to daylight saving which shifts Mexico City time zone from UTC-6 to UTC-5 the first Sunday from April and back to UTC-6 the last Sunday from October. The weather dataset that includes hourly rain volume for the centroid of the Cuauhtémoc municipality (historical center of Mexico City) was acquired from OpenWeather.

as an instrument. The instrument we selected to conduct the latter tests is comparable to Albalate and Fageda (2021), who employs lags of congestion as regressors, and Sánchez González et al. (2021), who use their aggregate delay measure lagged one week in an instrumental variable framework.

As shown in Figure 2.6, congestion seems to contribute differently to the increase in severe road accidents depending on the day of the week. Hence, the proposed panel model was also estimated separately for weekdays and weekends. That is, we allow both the intercept and the slope to differ conditional on the day of the week.

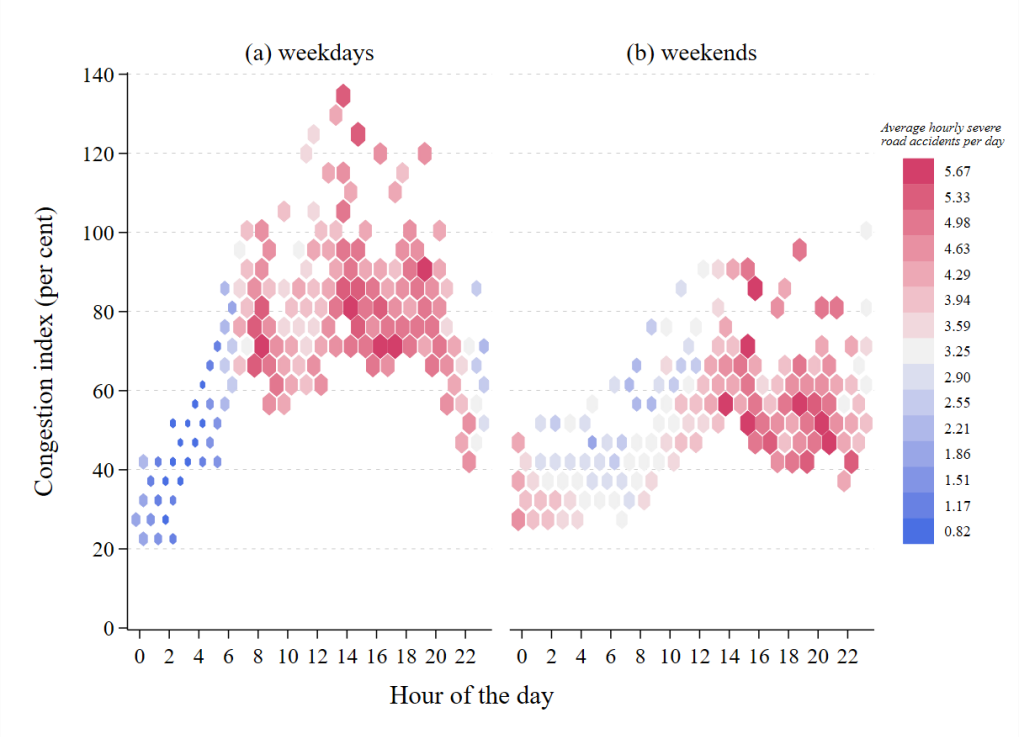

Figure 2.6. Congestion and severe road accidents by hour of the day. Data is arranged in hexagons according to their distribution by hour of the day (24 bins) and congestion index (24 bins). The color and size of the hexagons represents the average hourly severe road accidents per day within the hexagon. *Source:* Prepared by the authors using the "heatplot" package by Jann (2019) in Stata, reported road incidents by C5 and travel times retrieved from Uber Movement, © 2022 Uber Technologies, Inc.

Similarly, to test whether the relationship between severe accidents and congestion changes for distinct road users, we extend our basic model (1) running separate regressions for vulnerable road users and car occupants[7]. We would expect to observe a positive

[7] Although we confirm that error terms from the separate models are correlated (see Breusch–Pagan test in Table A2.1 from Appendix), we opted not to use a more efficient estimator such as the seemingly unrelated regression (SUR) estimator since our units of observation (hours of the day) are mutually dependent. Additionally, as indicated by Cameron and Trivedi (2010), SUR estimates (see Table A2.1 from the Appendix)

relationship between congestion and severe accidents from vulnerable users (Jansson, 1994; Lindberg, 2001). The relationship between severe road accidents from car occupants and congestion is more questionable. Severe accidents might be reduced with congestion if accident risk and costs (severity) are inversely related to congestion, and these are reduced substantially (Edlin & Karaca-Mandic, 2006; Jansson, 1994). Conversely, the studies from Dickerson et al. (2000), Retallack and Ostendorf, 2020, and Romem and Shurtz (2016) support an increasing positive relationship between accidents and traffic flow (the traffic volume externality, as Lindberg (2001) denominates it), which may also include an increment of severe road accidents. Therefore, the sign of the relationship for car occupant depends on which of these two outcomes predominates.

To test the robustness of our main specification, we first employ an auto-regressive distributed lags model that takes exogeneity as given from previous results but allow us to explicitly model the temporal (hourly) dependencies in our data. We reconfigure our dataset as two time series (separating weekdays from weekends) treating quarters as days. That is, the first quarter of 2016 is defined as the first day ($t = 1$ for the 00:00 hrs.), the second quarter would be our second day ($t = 25$ for the 00:00 hrs.), and so on. As a result, we end with two hourly time series of 384 realizations (24 hours for 16 days).

$$\begin{aligned} Severe_t = \alpha &+ \sum_{j=1}^{p} \phi_j \cdot Severe_{t-j} + \sum_{j=0}^{q_1} \gamma_{1j} \cdot CI_{t-j} + \sum_{j=0}^{q_2} \gamma_{2j} \cdot CI_{t-j}^2 + \sum_{k=1}^{K} \sum_{j=0}^{q_k} \beta_{kj} \cdot x_{k,t-j} \\ &+ \sum_{j=1}^{22} \omega_j \cdot hour_{j,t} + \sum_{j=2}^{4} \theta_j \cdot quarter_{j,t} + \sum_{j=2017}^{2019} \lambda_j \cdot year_{j,t} + \tau \cdot trend_t \\ &+ \varepsilon_t \end{aligned} \quad (2)$$

Both average hourly severe road accidents ($Severe_t$) and the congestion index (CI_t) are confirmed as stationary series around a linear trend using a modified Dickey-Fuller test ($Z(t)$ ranging from -7.96 to -6.05 with $p = 0.0000$ for both variables on weekdays and weekends). According to Wooldridge (2012), detrending and seasonally adjusting our variables is equivalent to including a linear trend and seasonal dummies for hour of the day, quarter, and year as we have proceeded in (2). Daylight and rain variables, represented by $x_{k,t}$, are included as control variables[8]. The optimal number lags (i.e., the p and q_s) are selected minimizing the Bayesian Information Criterion (BIC).

Moreover, as shown in Figures 2.3 and 2.5, there is a substantial difference between the congestion and accident patterns occurring around working hours (06:00 to 20:00 hrs.) and

are equivalent to our equation-by-equation estimates (see Table 2.3) because they contain the same set of regressors.

[8] In practice, we have restricted daylight control variables to only have a contemporaneous effect on the average hourly severe road accidents. In contrast, average rain in the last hour is unrestricted to have a dynamic effect on the dependent variable.

those present at night and early morning (21:00 to 05:00 hrs.). For this reason, we conduct a robustness test subsetting our panel data to test if the relationship found for the complete model remains for the two time-windows. This procedure can also serve to discard possible problems while characterizing average driving behavior through Uber drivers' performance, especially at night. We could not conduct the same test for our time-series because we ended up with an unevenly spaced series.

Finally, we test whether our results extend to the various regions of Mexico City, or they are driven to a greater or lesser extent by some regions. To do this, we run separate regressions for severe road accidents in each region using the regional congestion index as an explanatory variable. In Figure A2.3 from the Appendix, we present an alternative spatial analysis (geographically weighted regression (GWR)) that allows us to explore the spatial relationship between congestion and severe road accidents for vulnerable users in Mexico City.

2.5. Results

As expected, we find a positive relationship between congestion and average hourly severe road accidents if we estimate equation (1). Nevertheless, the functional form depends on the set of days of the week that we consider in the regressions (see Table 2.2). We obtain a positive linear relation if we use all the data. That is, we assume that congestion affects the number of severe road accidents equally during weekdays and weekends. If this is the case, increasing the congestion index by 1 percentage point results in 128 more severe road accidents per year ($\approx 0.0146 \times 24 \times 365$). We also obtain a positive linear relation if we run a separate regression for the weekends. However, if we estimate equation (1) solely for weekdays, the relation between accidents and congestion is still positive but the functional form is quadratic.

Table 2.2. Marginal effect of congestion on severe road accidents: Panel fixed effects models by days of the week

	All days		Weekdays		Weekends	
Congestion index	0.0146***	0.0296*	0.0107**	0.0445**	0.0203**	0.0273
	(0.0037)	(0.0139)	(0.0036)	(0.0167)	(0.0079)	(0.0298)
Congestion index²	-	-0.0001	-	-0.0002*	-	-0.0000
		(0.0001)		(0.0001)		(0.0002)
Rain in last hour	0.2866*	0.2711*	0.2274*	0.2044*	0.3431	0.3323
	(0.1375)	(0.1337)	(0.1125)	(0.1074)	(0.2216)	(0.2195)
Civil twilight	0.0133**	0.0123**	-0.0076	-0.0087	0.0331**	0.0326**
	(0.0053)	(0.0057)	(0.0081)	(0.0083)	(0.0137)	(0.0134)
Nautical twilight	-0.0059	-0.0064	0.0066	0.0062	-0.0188	-0.0190
	(0.0063)	(0.0065)	(0.0166)	(0.0166)	(0.0201)	(0.0207)
Astronomical twilight	0.0189***	0.0179***	0.0097	0.0081	0.0276**	0.0272**
	(0.0043)	(0.0046)	(0.0089)	(0.0088)	(0.0108)	(0.0109)
Night	0.0024	0.0017	0.0003	-0.0008	0.0042	0.0038

	(0.0046)	(0.0048)	(0.0035)	(0.0034)	(0.0073)	(0.0083)
Within R^2	0.3841	0.3871	0.4673	0.4820	0.3569	0.3572
Observations	768	768	384	384	384	384

Notes: All models include unit and time fixed effects. Driscoll and Kraay standard errors are reported within parentheses. Figures presented with rounding to 4 decimal places. *p<0.1, **p<0.05, ***p<0.01. *Source:* Prepared by the authors using the "xtscc" program by Hoechle (2006) in Stata.

As suggested by Figure 2.7, congestion and accidents should be studied separately for weekdays and weekends. To our knowledge, the present work is the first that makes such distinction when studying this relationship. Authors like Noland and Quddus (2005) have restricted their studies to weekdays warning that weekend patterns could be very different. Meanwhile, Sánchez González et al. (2021) have considered different intercepts, modelling a unique slope for distinct days of the week.

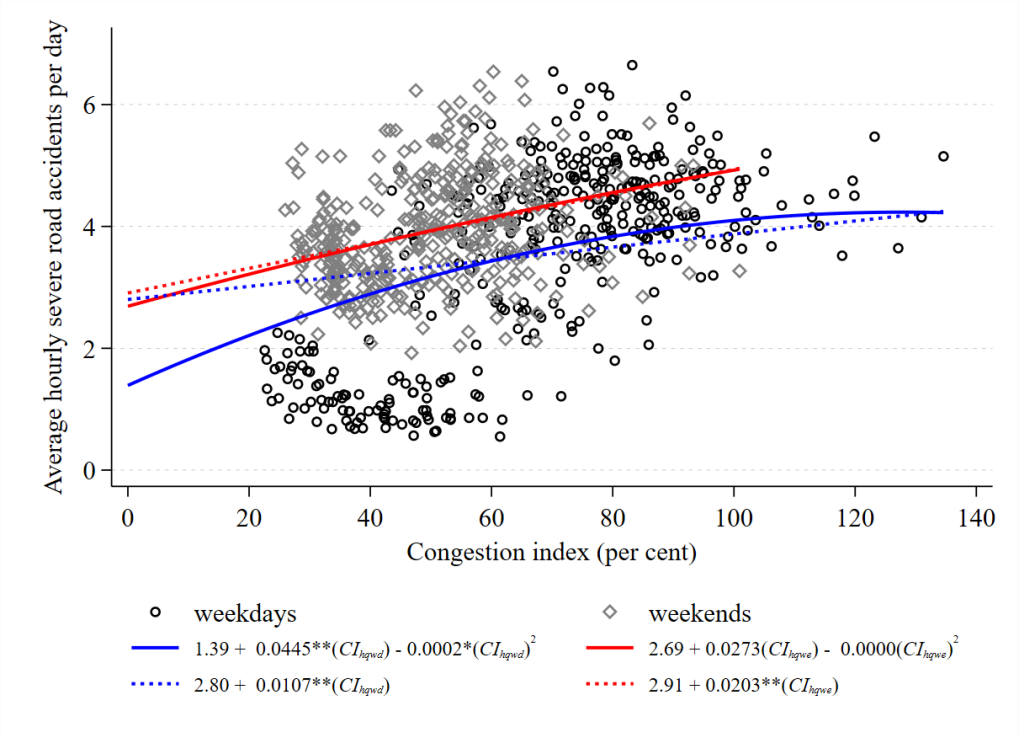

Figure 2.7. Fitted panel fixed effects models for weekdays and weekends. This figure compares the estimated models (lines) presented in Table 2.2 with respect to the actual data (points). CI_{hqwd} represents the hourly congestion index by quarter for weekdays, while CI_{hqwe} corresponds to weekends. Significance levels for the estimated congestion index coefficient are represented as: *p<0.1, **p<0.05, ***p<0.01. The line-intercepts corresponds to the sum of the constant (including unit and time fixed effects) and the estimated control variables evaluated at their means.

If the relationship is linear, reducing congestion by one standard deviation (that is, 17.74 p.p.) from 2019 average levels would result in a decrement of 1,194 severe road accidents per year (5.9%) on weekdays. On the other hand, a quadratic relationship could entail an expected reduction of 2,998 accidents (16.3%). Comparably, reducing congestion by one

standard deviation on weekends (that is, 10.93 p.p.) would result in an expected reduction of 554 (6.2%) severe road accidents per year in Mexico City.

The quadratic relationship that we find for weekdays implies that congestion increases severe road accidents at a marginal decreasing rate. Despite the differences in methodologies, this result is consistent with Sánchez González et al. (2021) previous finding. Therefore, the relationship becomes negative for congestion levels greater than 127.94% ($\approx 0.0445/(2 \times 0.0002)$). However, as shown in Figure 2.7, congestion in Mexico City is rarely in such a high range; with only 2 out of the 384 weekdays observations in this range. Therefore, we can say that the relationship is predominantly positive.

Regarding the set of daylight and rain control variables shown in Table 2.2, we find that a light rain of 5 mm in the last hour is associated with one additional severe road accident during weekdays. Similarly, 30 additional minutes of civil or nautical twilight instead of daylight results in 1 additional severe accident during weekends. It is important to note that the negative effects of the absence of daylight on severe road accidents are especially important for vulnerable users. In contrast, rain represents a greater risk factor for car occupants (see Table 2.3).

As shown in Table 2.3, we still find a positive relationship if we run separate regressions for vulnerable road users and car occupants. As expected, severe road accidents for vulnerable users increase with traffic congestion throughout the days of the week. While the positive relation is linear for weekends, the functional form for weekdays could be either linear or quadratic. For their part, car occupants are involved in a greater number of severe accidents as congestion increases during weekdays. Although the number of accidents increases at a decreasing rate with congestion, it would require congestion levels above 179.27% ($\approx 0.01545/(2 \times 0.000043)$) for the relationship to change. That is, even if the risk and severity of severe accidents falls with congestion, it would not be enough to offset the effect of the greater number of vehicles circulating on the roads.

Table 2.3. Marginal effect of congestion on severe road accidents from vulnerable users and car occupants: Panel fixed effects models by days of the week

	a) Vulnerable users					
	All days		Weekdays		Weekends	
Congestion index	0.0085***	0.0193*	0.0040*	0.0243*	0.0148***	0.0308*
	(0.0026)	(0.0097)	(0.0021)	(0.0130)	(0.0044)	(0.0147)
Congestion index²	-	-0.0001	-	-0.0001	-	-0.0001
		(0.0000)		(0.0001)		(0.0001)
Rain in last hour	0.1004	0.0892	0.2217**	0.2078***	-0.0098	-0.0345
	(0.1019)	(0.0965)	(0.0751)	(0.0699)	(0.1588)	(0.1514)
Civil twilight	0.0072*	0.0064	0.0083*	0.0076	0.0057	0.0045
	(0.0038)	(0.0038)	(0.0045)	(0.0046)	(0.0081)	(0.0078)
Nautical twilight	0.0044	0.0040	0.0070	0.0067	0.0017	0.0011

	(0.0044)	(0.0044)	(0.0066)	(0.0065)	(0.0105)	(0.0108)
Astronomical twilight	0.0138***	0.0130***	0.0138***	0.0129***	0.0128**	0.0118**
	(0.0031)	(0.0032)	(0.0037)	(0.0040)	(0.0051)	(0.0053)
Night	0.0033	0.0028	0.0073***	0.0066***	-0.0007	-0.0015
	(0.0028)	(0.0028)	(0.0021)	(0.0018)	(0.0056)	(0.0059)
Within R^2	0.5360	0.5390	0.5729	0.5832	0.5320	0.5348
Observations	768	768	384	384	384	384
b) Car occupants						
	All days		Weekdays		Weekends	
Congestion index	0.0058**	0.0070	0.0071***	0.0155**	0.0040	-0.0066
	(0.0026)	(0.0060)	(0.0019)	(0.0053)	(0.0065)	(0.0179)
Congestion index²	-	-0.0000	-	-0.0000*	-	0.0001
		(0.0000)		(0.0000)		(0.0001)
Rain in last hour	0.1768**	0.1756**	0.0015	-0.0042	0.3391***	0.3554***
	(0.0656)	(0.0667)	(0.0706)	(0.0716)	(0.0902)	(0.0874)
Civil twilight	0.0059	0.0058	-0.0171***	-0.0174***	0.0283**	0.0291**
	(0.0061)	(0.0062)	(0.0047)	(0.0047)	(0.0128)	(0.0128)
Nautical twilight	-0.0099**	-0.0099**	0.0016	0.0015	-0.0215	-0.0211
	(0.0043)	(0.0043)	(0.0118)	(0.0118)	(0.0153)	(0.0154)
Astronomical twilight	0.0048*	0.0047	-0.0053	-0.0057	0.0154*	0.0161*
	(0.0027)	(0.0028)	(0.0059)	(0.0057)	(0.0080)	(0.0082)
Night	-0.0003	-0.0004	-0.0058*	-0.0061*	0.0049*	0.0055*
	(0.0022)	(0.0024)	(0.0032)	(0.0033)	(0.0024)	(0.0027)
Within R^2	0.1726	0.1726	0.3112	0.3143	0.1497	0.1513
Observations	768	768	384	384	384	384

Notes: All models include unit and time fixed effects. They also include a constant and a set of daylight and rain control variables. Driscoll and Kraay standard errors within parentheses. Figures are rounded to 4 decimal places. *p<0.1, **p<0.05, ***p<0.01. *Source:* Prepared by the authors using "xtscc" program by Hoechle (2006) in Stata.

Our results are qualitatively identical (see Figure 2.8) if we reconfigure our dataset as a time series and estimate an auto-regressive distributed lags model as specified in equation (2). As seen in Table 2.4, we still find a positive linear relationship on weekends. However, we cannot distinguish if the relationship is linear or quadratic on weekdays. While both the Akaike Information Criterion (AIC) and a higher adjusted R^2 suggests that the quadratic specification is better, the Bayesian Information Criterion (BIC) supports a positive linear relationship.

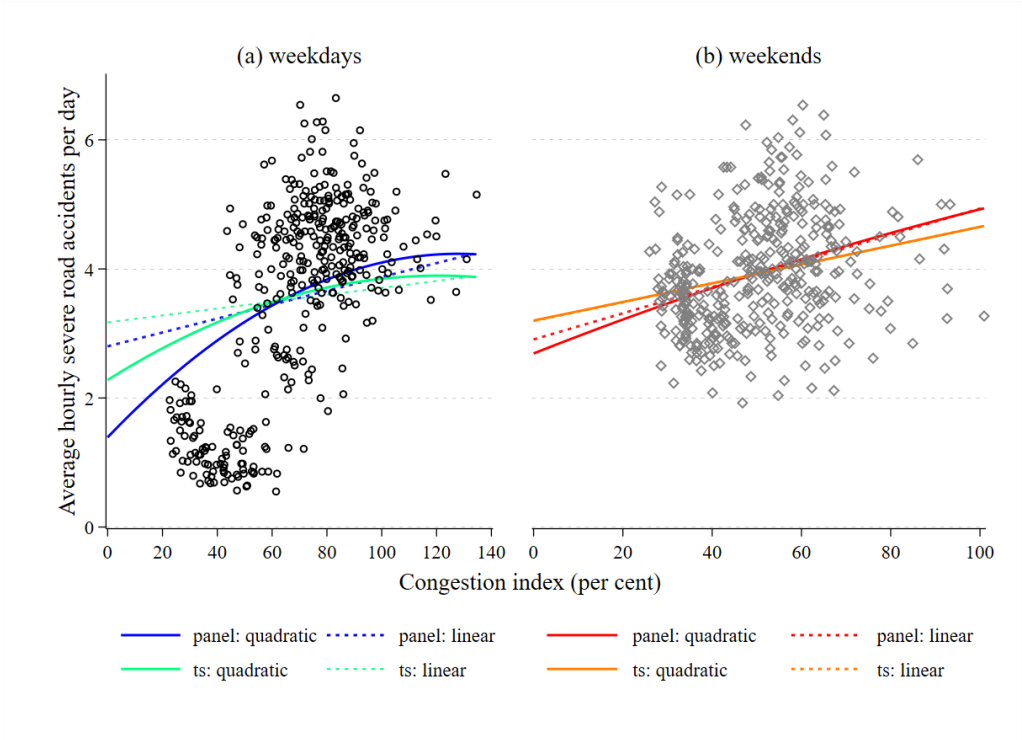

Figure 2.8. Comparison between panel fixed effects model and time series auto-regressive distributed lag models. This figure compares the estimated models (lines) from Table 2.2 and Table 2.4 with respect to the actual data (points). Line-intercepts correspond to the sum of the constant (including seasonal dummies by hour, quarter, and year) and the estimated control variables evaluated at their means.

Quantitatively, the estimated coefficients in our time series are of smaller magnitude than in the panel data. However, they only represent short-term effects. Given the autoregressive process followed by the number of hourly severe road accidents, a marginal change in our congestion index affects the dependent variable further in subsequent periods. Akin to Chen and Whalley (2012), we find the multiplier for the total effect iteratively substituting the corresponding lagged values of equation (2) into the original equation until it converges[9]. Employing numerical simulation, we report the corresponding multiplier for each estimated

[9] In practice, we used a simplified version of equation (2): $Severe_t = \alpha + \sum_{j=1}^{p} \phi_j \cdot Severe_{t-j}$, where $Severe_t$ represents average hourly severe road accidents per day. We program a numerical simulation setting an arbitrary initial condition very close to zero for the dependent variable, $Severe_0 = 0.0000001$. Similarly, we define an arbitrary value for $\alpha = 0.2$. Next, we iteratively simulate the simplified version of equation (2) using the estimated coefficients for $Severe_{t-1}$ and $Severe_{t-2}$ (reported in Table 2.4). To obtain the multipliers, we solve for μ the following equation: $Severe_\tau = \alpha\mu$, where τ represents a period in which the dependent variable has reached convergence.

model in Table 2.4. The cumulative effect of congestion represents the product of the multiplier and the estimated short-term coefficients[10].

The magnitudes for the cumulative effects of congestion of our time series setup suggests a very similar influence on severe road accidents than the one estimated with the panel models. Reducing congestion by one standard deviation on weekdays would result in an expected reduction of 1,170 severe road accidents per year if the relation is linear (24 less than with panel data) or 3,364 accidents if the relationship is quadratic (366 more than before). Similarly, reducing congestion by one standard deviation on weekends would result in a reduction of 516 severe road accidents (5.4%).

Table 2.4. Marginal effect of congestion on severe road accidents: Time series auto-regressive distributed lag models

	Weekdays		Weekends	
Average hourly severe road	0.3143***	0.3059***	0.2291***	0.2291***
accidents per day$_{t-1}$	(0.0521)	(0.0506)	(0.0473)	(0.0481)
Average hourly severe road	0.1783***	0.1779***	-	-
accidents per day$_{t-2}$	(0.0585)	(0.0573)		
Congestion index$_t$	0.0053*	0.0268**	0.0146**	0.0144
	(0.0029)	(0.0111)	(0.0063)	(0.0212)
(*Congestion index$_t$*)^2	-	-0.0001*	-	0.0000
		(0.0001)		(0.0001)
Rain in last hour$_t$	0.1058	0.0966	0.2716	0.2719
	(0.1258)	(0.1264)	(0.2187)	(0.2222)
Rain in last hour$_{t-1}$	0.5134***	0.5080***	-	-
	(0.1332)	(0.1330)		
Civil twilight$_t$	-0.0133	-0.0139	0.0322**	0.0323**
	(0.0097)	(0.0097)	(0.0142)	(0.0142)
Nautical twilight$_t$	0.0194	0.0189	-0.0146	-0.0146
	(0.0134)	(0.0133)	(0.0158)	(0.0159)
Astronomical twilight$_t$	0.0125	0.0116	0.0251**	0.0251**
	(0.0088)	(0.0087)	(0.0110)	(0.0111)
Night$_t$	0.0047	0.0039	0.0027	0.0027
	(0.0036)	(0.0037)	(0.0060)	(0.0062)
Adjusted R^2	0.9618	0.9621	0.7202	0.7193
AIC	207.63	204.68	544.06	546.06
BIC	361.29	362.28	689.85	695.79
Observations	380	380	380	380
Multiplier (μ)	1.9707	1.9374	1.2972	1.2972
Cumulative effect	0.0105	0.0223	0.0189	0.0188

[10] More precisely, the cumulative effect of congestion represents $\gamma_{10} \times \mu$ for linear specifications. Meanwhile, it represents $(\gamma_{10} + 2\gamma_{20}\overline{CI}_t) \times \mu$ for quadratic specifications.

Notes: The optimal number of lags was selected based on the Bayesian information criterion (BIC). All models include a constant, a trend, and a set of seasonal dummies by hour of the day, quarter, and year. Newey-West standard errors within parentheses. Figures presented with rounding to 4 decimal places. *p<0.1, **p<0.05, ***p<0.01. *Source:* Prepared by the authors using "ardl" module by Kripfganz and Schneider (2016) in Stata.

Moreover, we test whether the results presented so far hold if we limit our observations to a subset of hours. Estimating (1) separately for working hours (06:00 to 20:00 hrs.) and night and early morning (21:00 to 05:00 hrs.), we confirm a robust positive linear relationship for weekends (see Table 2.5). In contrast, the functional form that best describes the relationship between congestion and severe road accidents on weekdays seems to be strongly influenced by the time of day that we analyze. While our results point to a linear relationship from 6:00 to 20:00 hrs., the functional form seems to be quadratic from 21:00 to 5:00 hrs. This robustness exercise can be seen graphically in Figure 2.9.

Table 2.5. Marginal effect of congestion on severe road accidents: Panel fixed effects models by days of the week and hour of the day

	Weekdays			
	6:00 – 20:00 hrs.		*21:00 – 5:00 hrs.*	
Congestion index	0.0198***	0.0487**	-0.0001	0.0503***
	(0.0050)	(0.0202)	(0.0056)	(0.0113)
Congestion index²	-	-0.0001	-	-0.0004***
		(0.0001)		(0.0001)
Within R^2	0.6152	0.6197	0.3775	0.4166
Observations	240	240	144	144
	Weekends			
	6:00 – 20:00 hrs.		*21:00 – 5:00 hrs.*	
Congestion index	0.0201*	0.0160	0.0129*	0.0045
	(0.0113)	(0.0408)	(0.0074)	(0.0266)
Congestion index²	-	0.0000	-	0.0001
		(0.0002)		(0.0002)
Within R^2	0.3665	0.3666	0.3934	0.3938
Observations	240	240	144	144

Notes: All models include unit and time fixed effects. They also incorporate a set of daylight and rain control variables. The constant is omitted for weekends due to collinearity. Driscoll and Kraay standard errors are reported within parentheses. Figures presented with rounding to 4 decimal places. *p<0.1, **p<0.05, ***p<0.01. *Source:* Prepared by the authors using the "xtscc" program by Hoechle (2006) in Stata.

The quadratic relationship for weekdays occurring from 21:00 to 5:00 hrs. could be partially supported by Shefer (1994) hypothesis. In our case, as there are relatively few vehicles on the roads from 21:00 to 5:00 hrs., increasing traffic flow at these hours on weekdays results in more severe road accidents. However, the increase in density gradually decreases speeds reaching a point where the relationship becomes negative. According to our results, that point is reached when the congestion index is 61.47%.

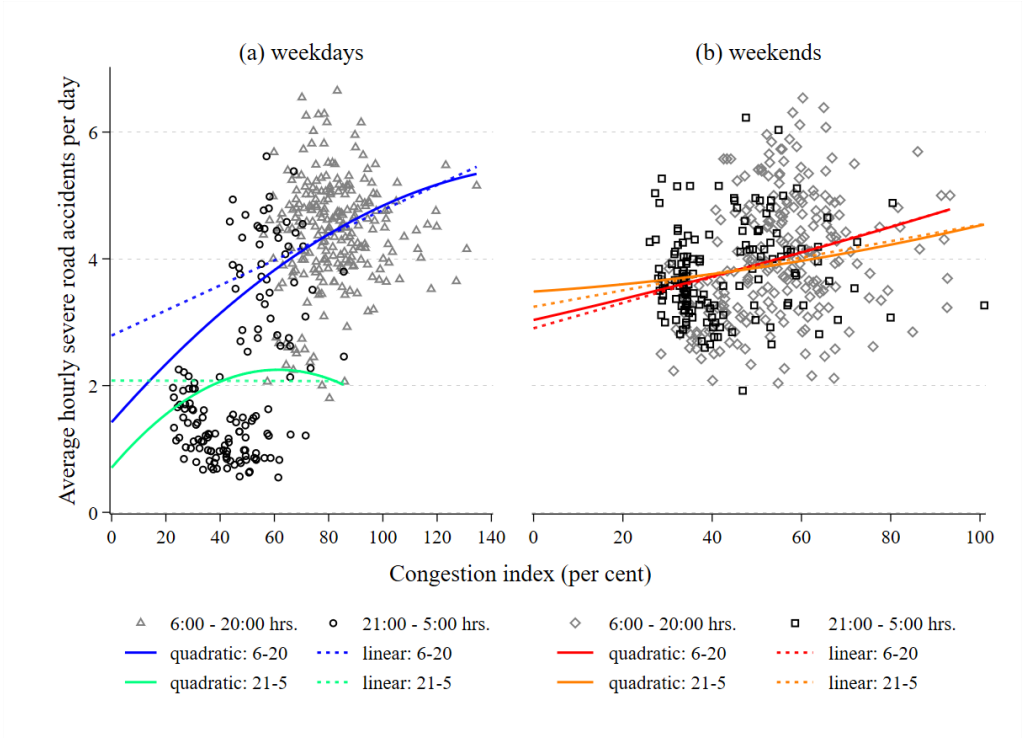

Figure 2.9. Fitted panel fixed effects models for weekdays and weekends distinguishing by hour of the day. This figure compares the 8 estimated models (lines) presented in Table 2.5 with respect to the actual data (points). The line-intercepts correspond to the sum of the constant (including unit and time fixed effects) and the estimated control variables evaluated at their means.

The last result should be taken with caution for at least three reasons. First, our ability to explain the variation in our dependent variable—as shown by the R^2—is substantially reduced for weekdays from 21:00 to 5:00 hrs. compared to the estimated model for 6:00 to 20:00 hrs. Second, predictions of the model for these hours include negative fitted values which are not appropriate given the nature of the dependent variable. It is important to note that neither of the other estimated panel or time series models we reported before predicted negative fitted values. Lastly, another important distinction from Shefer (1994) is that we have included various levels of severity while the original hypothesis was about fatalities on the roads.

Finally, in Table 2.6 we show that the positive relation between severe road accidents and congestion during weekdays is driven by the most congested and extensive regions, especially the CE region. Reducing congestion by one standard deviation (35%) from 2019 average levels in this region would result in a reduction of 1,017 severe road accidents per year (12.14%) on weekdays. Hence, severe road accidents in CE region increase less than proportionally with traffic congestion. Nevertheless, our results indicate that this relationship is not statistically significant during weekends.

Table 2.6. Marginal effect of congestion on severe road accidents: Panel models by days of the week and region

a) Weekdays										
	CE		NE		NW		SE		SW	
Congestion index	0.0042***	0.0127**	-0.0004	0.0023	-0.0007	0.0023	0.0022***	0.0048	0.0040***	0.0035
	(0.0013)	(0.0051)	(0.0008)	(0.0023)	(0.0010)	(0.0024)	(0.0004)	(0.0031)	(0.0012)	(0.0029)
Congestion index²	-	-0.0001*	-	-0.0000	-	-0.0000	-	-0.0000	-	0.0000
		(0.0000)		(0.0000)		(0.0000)		(0.0000)		(0.0000)
Within R^2	0.3244	0.3314	0.0998	0.1032	0.1885	0.1916	0.2756	0.2771	0.3303	0.3304
Observations	384	384	384	384	384	384	384	384	384	384
Mean congestion (2019)	61.89	61.89	55.98	55.98	55.54	55.54	61.45	61.45	57.35	57.35
Area (km^2)	116.18	116.18	87.91	87.91	79.95	79.95	244.70	244.70	267.91	267.91
b) Weekends										
	CE		NE		NW		SE		SW	
Congestion index	0.0049	0.0153	0.0021**	-0.0004	0.0009	0.0057	0.0040**	-0.0041	0.0089**	0.0068
	(0.0032)	(0.0114)	(0.0007)	(0.0035)	(0.0022)	(0.0073)	(0.0014)	(0.0045)	(0.0037)	(0.0095)
Congestion index²	-	-0.0001	-	0.0000	-	-0.0001	-	0.0000*	-	0.0000
		(0.0001)		(0.0000)		(0.0001)		(0.0000)		(0.0001)
Within R^2	0.2240	0.2279	0.0892	0.0901	0.1485	0.1500	0.1256	0.1313	0.1857	0.1858
Observations	384	384	384	384	384	384	384	384	384	384
Mean congestion (2019)	41.94	41.94	41.51	41.51	31.05	31.05	51.15	51.15	40.99	40.99
Area (km^2)	116.18	116.18	87.91	87.91	79.95	79.95	244.70	244.70	267.91	267.91

Notes: Each model includes unit and time fixed effects. Additionally, models incorporate a constant and a set of daylight and rain control variables (not reported). Regional classification of municipalities in Mexico City: CE (Iztacalco, Benito Juárez, Cuauhtémoc, and Venustiano Carranza); NE (Gustavo A. Madero); NW (Azcapotzalco and Miguel Hidalgo); SE (Tláhuac, Iztapalapa, Xochimilco, and Milpa Alta); and SW (Coyoacán, La Magdalena Contreras, Cuajimalpa de Morelos, Álvaro Obregón, and Tlalpan). Driscoll and Kraay standard errors are reported within parentheses. Figures presented with rounding to 4 decimal places. *p<0.1, **p<0.05, ***p<0.01. *Source:* Prepared by the authors using the "xtscc" program by Hoechle (2006) in Stata.

The previous result is useful in terms of transportation policy, as it would suggest migrating from a congestion abatement approach that applies throughout the whole territory of Mexico City, such as the driving restrictions imposed by the program *Hoy No Circula*, to an approach focused on the CE region of Mexico City. Two options that could be evaluated are the input's adaptive control approach proposed by Daganzo (2006), or the establishment of a congestion charge—as the London Congestion Charge—that penalizes car trips to the center of the city during peak hours (Green et al., 2016).

2.6. Discussion

In this section we discuss some hypotheses that may explain the positive relationship we found between congestion and severe road accidents in Mexico City. Additionally, we relate our work to the literature that explores the existence of an accident externality of driving.

Given the absence of available and comparable information of traffic flows in Mexico City, we assume the existence of a macroscopic fundamental diagram (MFD) that relates flow, density, and speed in Mexico City comparable to the one presented by Geroliminis and Daganzo (2008) for Yokohama (Japan). For this, we need three important assumptions. We are confident that, although the magnitudes of the these back of the envelope calculations are sensitive to the assumptions presented below, the fundamental relationships between these variables, as well as the conclusions, would persist.

First, we assume that the distances between the centroids of AGEBs are proportional to the average distances traveled from AGEB-to-AGEB by Uber drivers. With this, we can obtain the average speed at which cars circulate in Mexico City at different times and quarters of the 2016-2019 period. As shown in Figure 2.10a, the greater the congestion, the lesser the speed at which vehicles circulate.

Second, we assume that the relationship between traffic flow and speed observed in Yokohama (Japan)—once we express these variables as deviations from their means—is the same for Mexico City. Specifically, we estimate that the standardized traffic flow (expressed as the number of standard deviations from its mean) for Mexico City, z_{flow}, bears the following relationship to the standardized speed, z_{speed}[11]:

[11] This equation was estimated with data extracted from Figure 1f in Geroliminis and Daganzo (2008), using PlotDigitizer (https://plotdigitizer.com/).

$$z_{flow} = 0.342 - 1.352z_{speed} - 0.277z_{speed}^2 + 0.152z_{speed}^3$$

It is important to note that our congestion measure is positively related with the traffic flow for a wide range of values, up to the point where road capacity is reached (see Figure 2.10b). From this point on, grater congestion implies a drop in traffic flow.

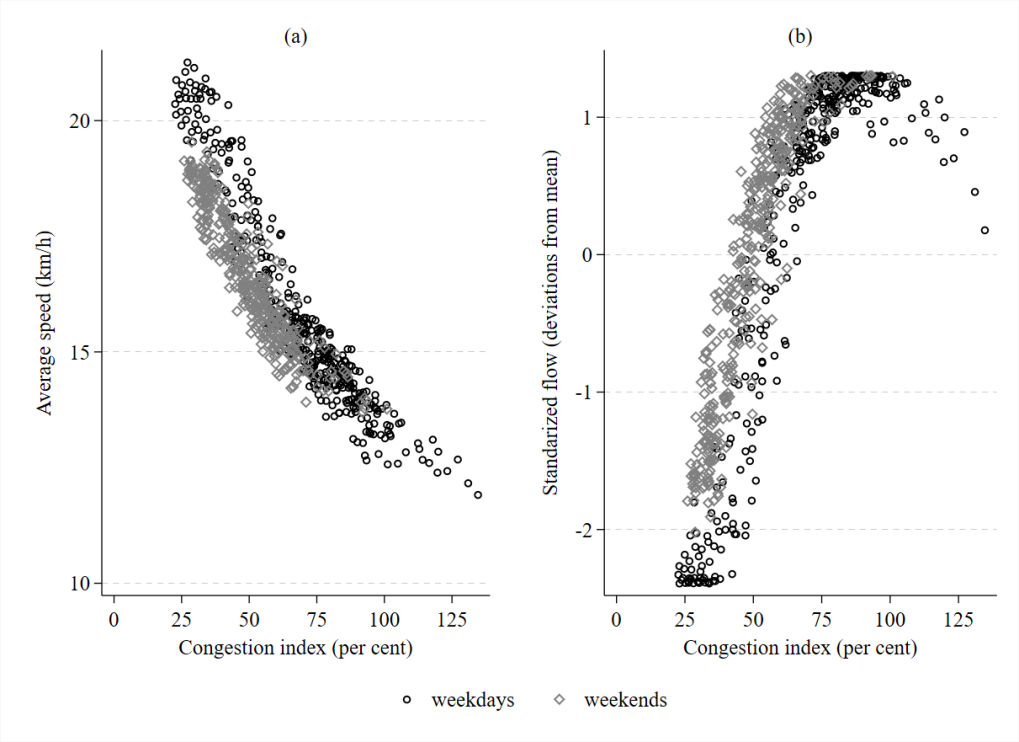

Figure 2.10. (a) Average speed vs. road congestion in Mexico City; (b) Estimated standardized flow, based on Geroliminis and Daganzo (2008) vs. road congestion in Mexico City. *Source:* Prepared by the authors using data retrieved from Uber Movement, © 2022 Uber Technologies, Inc, https://movement.uber.com

Finally, we assume an average traffic flow of 321 vehicles per hour, with a standard deviation of 129 (the same as for road lane segments in Yokohama) in order to calculate the risk of severe accidents based on our congestion index. We use the definition of risk proposed by Lindberg (2001), dividing the number of severe accidents (calculated using the estimated equations in Figure 2.7) by the estimated flow for each level of congestion.

As seen in Figure 2.11, the risk of a severe road accident decreases with congestion only up to a certain point. From that point risk rises as traffic flow falls with congestion. This effect is observed mainly for weekdays. For weekends, the relationship seems to be mostly negative. That is, the greater the congestion, the lesser the speed and risk of severe road accidents.

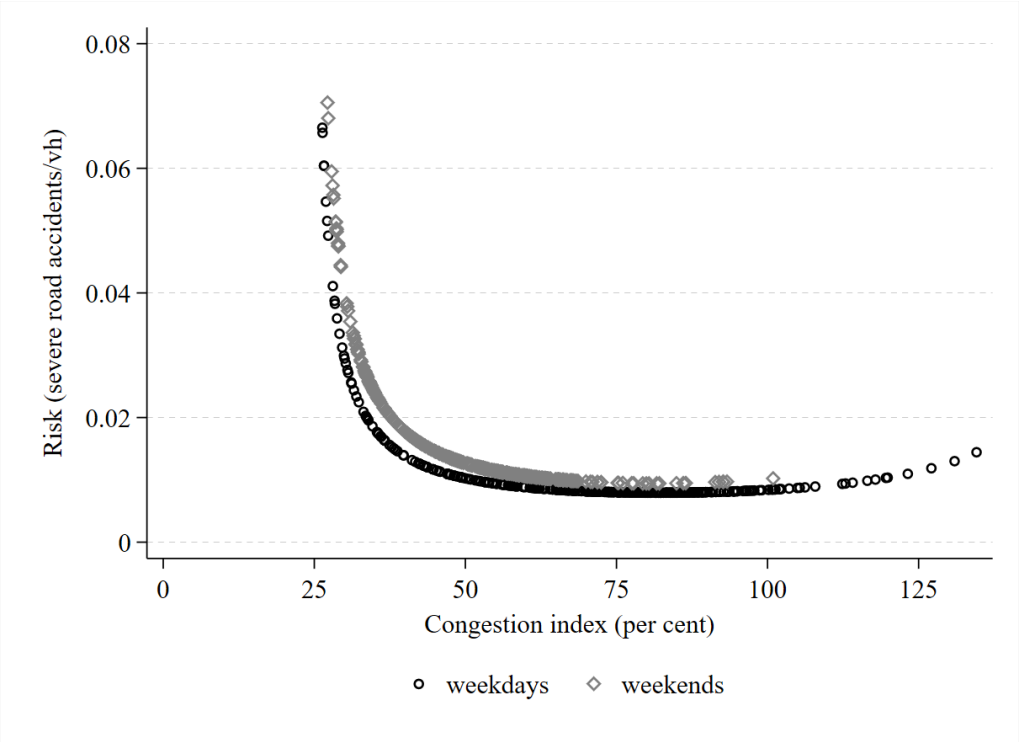

Figure 2.11. Rough measure of risk vs. road congestion in Mexico City. *Source:* Prepared by the authors using data retrieved from Uber Movement, © 2022 Uber Technologies, Inc, https://movement.uber.com

Therefore, our work is inherently related to the accident externality of driving. Consistent with the hypothesis of Edlin and Karaca-Mandic (2006) and Jansson (1994), the risk of severe accidents falls with congestion. That is, akin to Tang and van Ommeren (2022), our results suggest that congestion dilutes the accident externality of driving. However, very high levels of congestion are needed to see a reduction in the frequency of severe road accidents.

For the relevant range in which the congestion index fluctuates most of the day, the effect of the traffic volume externality coupled with the positive relationship between congestion and severe accidents involving vulnerable users predominate. This explains the positive relationship and the differences in functional form depending on the day of the week that we find.

Sun et al. (2016) provide a hypothesis that supports the positive relation between congestion and severe road accidents that we find. Congestion causes a greater interaction between vehicles due to more frequent lane changes, increasing the risk for other road users such as pedestrians, cyclists, and motorcyclists—which we consider in our analysis. However, congestion causing drivers to take alternative non-familiar roads (Albalate & Fageda, 2021) or being more likely to have a rear-end crash (Shi et al., 2016) cannot be discarded as other possible explanations.

2.7. Conclusions

We find a positive relationship between congestion and severe road accidents in Mexico City. Hence, transport policy efforts aiming to lower congestion provide benefits in terms of a reduction of the economic and social costs caused by road accidents. Transportation authorities in highly congested cities such as Mexico City should be more concerned about congestion. They should consider planning, implementing, and evaluating policies to alleviate it because benefits can be substantial.

Our results indicate that reducing weekdays congestion by one standard deviation (17.74 p.p.) from the 2019 average level (59.17%) would lead to an expected reduction of between 1,182 and 3,181 (5.5% to 14.8%) severe road accidents per year. Similarly, reducing weekends congestion by one standard deviation (10.93 p.p.) from the 2019 average level (43.25%) could prevent 535 severe road accidents per year in Mexico City (5.8%). In sum, between 1,717 and 3,716 severe road accidents per year can be prevented if congestion is reduced by roughly 30%.

Congestion patterns for weekdays and weekends exhibit significant differences and so, should be studied separately. To our knowledge, our work is the first to address this distinction allowing both intercept and slope to differ depending on the day of the week. While the relationship between congestion and severe road accidents is linear for weekends, it can be either linear or quadratic (inversed U-shaped) for weekdays. As the functional form for weekdays varies with the method and hours of the day considered, further research that considers this distinction is needed.

Furthermore, we find a positive relationship between congestion and severe road accidents for both vulnerable road users and car occupants during weekdays. For weekends, only vulnerable users are affected with increased congestion. Moreover, the positive relationship seems to be driven mainly by the central region of Mexico City. This suggests opportunities for transportation policy. To reduce the number of accidents, policymakers should evaluate alternatives that reduce the vehicular flow towards the city center, such as adaptive entrance controls (Daganzo, 2006), charges for driving in the center of the city (Green et al., 2016) or a system of ex post insurance premiums that charge the external cost of accidents to those who are involved in one (Jansson, 1994). Alternatively, policymakers may consider the expansion or construction of new subway lines which—apart from reducing traffic flow—restrict interactions among road users leading to a reduction in the number of severe road accidents.

Future studies can test if the positive relation between congestion and road accidents found in this study can also be explained by the indirect effect of congestion on nearby areas using the space or space-time specification of the congestion index that we proposed here, along with a spatial lag model. That is, they can test if drivers cause more accidents by taking alternative roads to avoid traffic congestion, as hypothesized by Albalate and Fageda (2021).

We conclude that the risk of severe road accidents falls with congestion. Hence, congestion lowers the accident externality of driving. However, a fall in the frequency of severe road accidents requires extremely high levels of congestion. As congestion is positively related with traffic flows during most of the hours of the day, each additional car on the road leads to a—less than proportional—increment in the number of severe road accidents in Mexico City.

Finally, this work shows that transportation authorities in congested cities from developing countries can rely on the growing available open datasets obtained from crowd-sources, especially if they don't have administrative data on traffic flows. At the same time, it is recommended that these cities invest on improving their administrative databases collecting traffic flows for their road network as such information can be used for improving the security and mobility of their inhabitants.

References

Albalate, D., & Fageda, X. (2021). On the relationship between congestion and road safety in cities. *Transport Policy*, *105*, 145-152. https://doi.org/10.1016/j.tranpol.2021.03.011

Arbia, G. (2014). *A primer for spatial econometrics: With applications in R*. Basingstoke: Palgrave Macmillan. https://doi.org/10.1057/9781137317940

Arceo, E., Hanna, R., & Oliva, P. (2016). Does the effect of pollution on infant mortality differ between developing and developed countries? Evidence from Mexico City. *The Economic Journal*, *126*(591), 257-280. https://doi.org/10.1111/ecoj.12273

Calatayud, A., Sánchez González, S., Bedoya Maya, F., Giraldez, F., & Márquez, J. M. (2021). *Congestión urbana en América Latina y el Caribe: Características, costos y mitigación*. Washington, DC, USA: Inter-American Development Bank. http://dx.doi.org/10.18235/0003149

Cameron, A. C., & Trivedi, P. K. (2010). *Microeconometrics using Stata* (Revised ed.). College Station, Texas: StataCorp LP.

Chen, Y., & Whalley, A. (2012). Green infrastructure: The effects of urban rail transit on air quality. *American Economic Journal: Economic Policy*, *4*(1), 58-97. http://dx.doi.org/10.1257/pol.4.1.58

Daganzo, C. F. (2006). Urban gridlock: Macroscopic modeling and mitigation approaches. *Transportation Research Part B: Methodological*, *41*(1), 49-62. https://doi.org/10.1016/j.trb.2006.03.001

Dickerson, A., Peirson, J., & Vickerman, R. (2000). Road accidents and traffic flows: An econometric investigation. *Economica*, *67*(265), 101-121. Retrieved from http://www.jstor.org/stable/2555219

Driscoll, J. C., & Kraay, A. C. (1998). Consistent covariance matrix estimation with spatially dependent panel data. *The Review of Economics and Statistics*, *80*(4), 549–560. https://doi.org/10.1162/003465398557825

Edlin, A. S., & Karaca-Mandic, P. (2006). The Accident Externality from Driving. *Journal of Political Economy*, *114*(5), 931-955. https://doi.org/10.1086/508030

Geroliminis, N., & Daganzo, C. F. (2008). Existence of urban-scale macroscopic fundamental diagrams: Some experimental findings. *Transportation Research Part B: Methodological*, *42*(9), 759–770. https://doi.org/10.1016/j.trb.2008.02.002

Green, C. P., Heywood, J. S., & Navarro, M. (2016). Traffic accidents and the London Congestion Charge. *Journal of Public Economics*, *133*, 11-22. https://doi.org/10.1016/j.jpubeco.2015.10.005

Hilbe, J. M. (2014). *Modeling count data*. New York, NY: Cambridge University Press. https://doi.org/10.1017/CBO9781139236065

Hoechle, D. (2006). *XTSCC: Stata module to calculate robust standard errors for panels with cross-sectional dependence*. Statistical Software Components, Boston College Department of Economics. https://ideas.repec.org/c/boc/bocode/s456787.html

IMCO, & Sin Tráfico. (2019). *El costo de la congestión, vida y recursos perdidos*. Retrieved from https://imco.org.mx/costo-la-congestion-vida-recursos-perdidos/

INEGI. (2010). *Manual de cartografía estadística*. Retrieved from https://www.inegi.org.mx/contenidos/temas/mapas/mg/metadatos/manual_cartografia_censal.pdf

INEGI. (2020). *Marco Geoestadístico Ciudad de México*. Retrieved from https://www.inegi.org.mx/app/biblioteca/ficha.html?upc=889463807469

Jann, B. (2019). *HEATPLOT: Stata module to create heat plots and hexagon plots*. Statistical Software Components, Boston College Department of Economics. https://ideas.repec.org/c/boc/bocode/s458598.html

Jansson, J. O. (1994). Accident Externality Charges. *Journal of Transport Economics and Policy*, *28*(1), 31-43. Retrieved from https://www.jstor.org/stable/20053022

Kreindler, G. (2016). *Driving Delhi? Behavioural responses to driving restrictions*. International Growth Centre, Working paper C-35330-INC-1. Retrieved from https://www.theigc.org/wp-content/uploads/2016/11/Kreindler-2016-Working-paper.pdf

Kripfganz, S., & Schneider, D. C. (2016). *ardl: Stata module to estimate autoregressive distributed lag models*. 2016 Stata Conference, Stata Users Group. Retrieved from https://ideas.repec.org/p/boc/scon16/18.html

Lindberg, G. (2001). Traffic insurance and accident externality charges. *Journal of Transport Economics and Policy*, *35*(3), 399-416. Retrieved from https://www.jstor.org/stable/20053882

Noland, R. B., & Quddus, M. A. (2005). Congestion and safety: A spatial analysis of London. *Transportation Research Part A: Policy and Practice*, *39*(7-9), 737-754. https://doi.org/10.1016/j.tra.2005.02.022

Pasidis, I. (2019). Congestion by accident? A two-way relationship for highways in England. *Journal of Transport Geography*, *76*, 301-314. https://doi.org/10.1016/j.jtrangeo.2017.10.006

Pearson, M., Sagastuy, J., & Samaniego, S. (2017). *Traffic flow analysis using Uber movement data*. Retrieved from https://snap.stanford.edu/class/cs224w-2017/projects/cs224w-11-final.pdf

Pesaran, M. H. (2021). General diagnostic tests for cross-sectional dependence in panels. *Empirical Economics, 60*, 13–50. https://doi.org/10.1007/s00181-020-01875-7

Retallack, A. E., & Ostendorf, B. (2019). Current understanding of the effects of congestion on traffic accidents. *International Journal of Environmental Research and Public Health*, 16(18), 3400. https://doi.org/10.3390/ijerph16183400

Retallack, A. E., & Ostendorf, B. (2020). Relationship between traffic volume and accident frequency at intersections. *International Journal of Environmental Research and Public Health*, *17*(4), 1393. https://doi.org/10.3390/ijerph17041393

Romem, I., & Shurtz, I. (2016). The accident externality of driving: Evidence from observance of the Jewish Sabbath in Israel. *Journal of Urban Economics*, *96*, 36-54. https://doi.org/10.1016/j.jue.2016.07.004

Sánchez González, S., Bedoya-Maya, F., & Calatayud, A. (2021). Understanding the effect of traffic congestion on accidents. *Sustainability*, *13*(13), 7500. https://doi.org/10.3390/su13137500

Shefer, D. (1994). Congestion, air pollution, and road fatalities in urban areas. *Accident Analysis & Prevention*, *26*(4), 501-509. https://doi.org/10.1016/0001-4575(94)90041-8

Shi, Q., Abdel-Aty, M., & Lee, J. (2016). A Bayesian ridge regression analysis of congestion's impact on urban expressway safety. *Accident Analysis & Prevention*, *88*, 124-137. https://doi.org/10.1016/j.aap.2015.12.001

Small, K. A., & Chu, X. (2003). Hypercongestion. *Journal of Transport Economics and Policy*, *37*(3), 319-352. Retrieved from http://www.jstor.org/stable/20053940

Sun, J., Li, T., Li, F., & Chen, F. (2016). Analysis of safety factors for urban expressways considering the effect of congestion in Shanghai, China. *Accident Analysis & Prevention*, *95*, 503-511. https://doi.org/10.1016/j.aap.2015.12.011

Tang, C. K., & van Ommeren, J. (2021). Accident externality of driving: Evidence from the London Congestion Charge. *Journal of Economic Geography*, *22*(3), 547-580. https://doi.org/10.1093/jeg/lbab012

Taylor, M. A., Woolley, J. E., & Zito, R. (2000). Integration of the global positioning system and geographical information systems for traffic congestion studies. *Transportation Research Part C: Emerging Technologies*, *8*(1-6), 257-285. https://doi.org/10.1016/S0968-090X(00)00015-2

TomTom International BV. (2019). *Traffic index ranking*. Retrieved from https://www.tomtom.com/traffic-index/ranking/

Uber Technologies, Inc. (2022). *Uber Movement: Travel Times Calculation Methodology*. Retrieved from https://movement.uber.com/

Walters, A. A. (1961). The theory and measurement of private and social cost of highway congestion. *Econometrica*, *29*(4), 676–699. https://doi.org/10.2307/1911814

Wang, C., Quddus, M. A., & Ison, S. G. (2009). Impact of traffic congestion on road accidents: A spatial analysis of the M25 motorway in England. *Accident Analysis & Prevention*, *41*(4), 798–808. https://doi.org/10.1016/j.aap.2009.04.002

Wooldridge, J. M. (2012). *Introductory Econometrics: A Modern Approach* (5th. ed.). Mason, OH: South-Western Cengage Learning.

Appendix

Table A2.1. Marginal effect of congestion on severe road accidents from vulnerable users and car occupants: SUR models by days of the week

	a) Vulnerable users					
	All days		Weekdays		Weekends	
Congestion index	0.0085***	0.0193***	0.0040*	0.0243***	0.0148***	0.0308***
	(0.0021)	(0.0061)	(0.0021)	(0.0079)	(0.0040)	(0.0116)
Congestion index²	-	-0.0001*	-	-0.0001***	-	-0.0001
		(0.0000)		(0.0000)		(0.0001)
R^2	0.8859	0.8867	0.9359	0.9374	0.8094	0.8105
Observations	768	768	384	384	384	384
	b) Car occupants					
	All days		Weekdays		Weekends	
Congestion index	0.0058***	0.0070	0.0071***	0.0155**	0.0040	-0.0066
	(0.0020)	(0.0057)	(0.0018)	(0.0066)	(0.0040)	(0.0119)
Congestion index²	-	-0.0000	-	-0.0000	-	0.0001
		(0.0000)		(0.0000)		(0.0001)
R^2	0.8175	0.8175	0.9290	0.9294	0.4565	0.4575
Observations	768	768	384	384	384	384
Corr. residuals	0.1438	0.1437	0.2088	0.2012	0.1270	0.1308
Breusch–Pagan test	15.89***	15.85***	16.734***	15.552***	6.191**	6.567**

Notes: All models include unit and time fixed effects. They also incorporate a constant and a set of daylight and rain control variables. Bootstrap standard errors from 400 replications are reported within parentheses. Figures presented with rounding to 4 decimal places. *p<0.1, **p<0.05, ***p<0.01. *Source:* Prepared by the authors using the "sureg" command in Stata.

Table A2.2. Marginal effect of congestion on severe road accidents from vulnerable users and car occupants: Cross-sectional OLS models with urban AGEBs as the unit of observation

	a) All			
	Weekdays		Weekends	
Congestion index	0.0341	0.0564*	0.0569**	-0.0360
	(0.0281)	(0.0331)	(0.0278)	(0.0752)
Congestion index²		-0.0001		0.0005
		(0.0001)		(0.0005)
Adjusted R^2	0.5446	0.5446	0.4464	0.4515
Observations	2406	2406	2405	2405
	b) Vulnerable users			
	Weekdays		Weekends	
Congestion index	0.0323**	0.0623***	0.0472**	-0.0195
	(0.0142)	(0.0180)	(0.0187)	(0.0509)
Congestion index²		-0.0001***		0.0000
		(0.0000)		(0.0004)
Adjusted R^2	0.4700	0.4711	0.3016	0.3149
Observations	2406	2406	2405	2405
	c) Car occupants			
	Weekdays		Weekends	
Congestion index	0.0033	-0.0040	0.0121	-0.0111
	(0.0178)	(0.0188)	(0.0109)	(0.0262)
Congestion index²		0.0000		0.000
		(0.0001)		(0.0002)
Adjusted R^2	0.5267	0.5265	0.4527	0.4533
Observations	2406	2406	2405	2405

Notes: The count of all severe road accidents for the period 2016-2019 were assigned to each urban AGEB based on their locations. For comparability, we divide the total number of accidents by the area of each AGEB. To assign the congestion index to each AGEB, we averaged congestion indexes on each AGEB with respect to their set of neighbors and then over all hours and quarters from the period 2016-2019. Each regression considers the following control variables: density (total length divided by area of the AGEB) of motorway, trunk, primary, secondary, tertiary, and residential roads; density (count divided by area of the AGEB) of trolley bus stops, bus rapid transit stations ("Metrobus") and subway stations; inhabited dwelling per square kilometer; and density of intersections of different types of roads. Robust standard errors within parentheses. Figures presented with rounding to 4 decimal places. *p<0.1, **p<0.05, ***p<0.01. *Source:* Prepared by the authors.

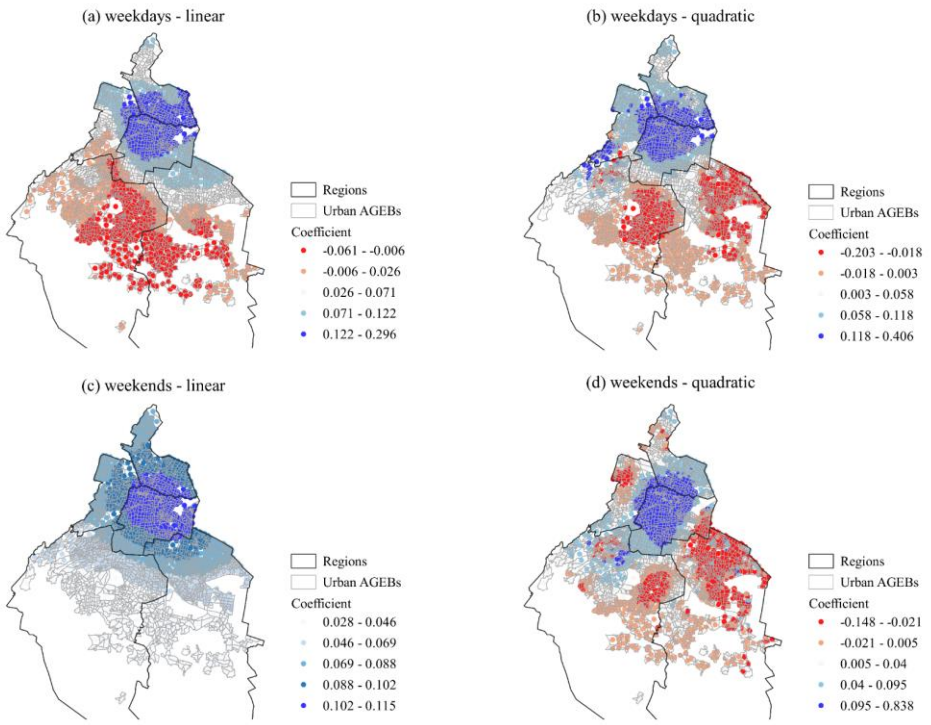

Figure A2.3. Estimated coefficients from a geographically weighted regression (GWR) for severe road accidents from vulnerable users in the period 2016-2019. *Notes:* We only include the results for vulnerable users, since this is the only group for which the congestion coefficient is statistically significant in Table A2.2 from the Appendix. The count of all severe road accidents for the period 2016-2019 were assigned to each urban AGEB based on their locations. For comparability, we divide the total number of accidents by the area of each AGEB. To assign the congestion index to each AGEB, we averaged congestion indexes on each AGEB with respect to their set of neighbors and then over all hours and quarters from the period 2016-2019. Each regression considers the following control variables: density (total length divided by area of the AGEB) of motorway, trunk, primary, secondary, tertiary, and residential roads; density (count divided by area of the AGEB) of trolley bus stops, bus rapid transit stations ("Metrobus") and subway stations; inhabited dwelling per square kilometer; and density of intersections of different types of roads. *Source:* Prepared by the authors using the package "spgwr" in R and QGIS 3.22.

Chapter 3. Behavioral responses to environmental emergency alerts and temporary driving restrictions: Evidence from cyclists in Mexico City

Executive Summary

Environmental emergencies are activated when ozone or particulates concentrations reach levels that pose a serious health risk to the population. In Mexico City, the authority issues a massive press release that includes precautionary recommendations (i.e., alerts) promoting the adoption of avoidance behaviors. For example, it recommends avoiding cycling and other vigorous outdoor activities. Emergencies also include a set of mandatory measures to reduce the emission of pollutants. For instance, about 35% of private cars have a temporary use restriction.

This combination of alerts and driving restrictions during environmental emergencies could result in a dilemma for some groups, such as cyclists who own restricted cars. On the one hand, alerts promote a reduction of cycling activity to avoid higher health costs. On the other hand, driving restrictions push them to use their bicycles and reduce emissions. Moreover, cyclist who own unrestricted cars have incentives to drive more, taking advantage of the reduced road congestion. Hence, it is interesting to ask the following. How do cyclists respond to environmental emergency alerts and temporary driving restrictions? Which behavioral response predominates: avoidance behavior or transport mode substitution? How does cyclists' trip purpose and characteristics influence their behavioral response?

A case study for Sydney (Australia) suggests that environmental alerts are effective to reduce cycling activity during highly polluted days, primarily for those who cycle for leisure (Saberian et al., 2017). Moreover, two case studies for Mexico City and Santiago (Chile) suggests that the combination between alerts and mandatory temporary driving restrictions can push individuals—specially, those who commute during rush hours—towards less polluting modes of transportation, such as subway, bus rapid transit or bicycle sharing systems (de Buen Kalman, 2021; Rivera, 2021). These previous articles used high frequency anonymized administrative records, collected at counters with fixed locations in cycle paths and stations. Therefore, they lack the information to accurately distinguish leisure from commuting trips. Likewise, their case studies—or periods analyzed—have not allowed them to estimate the differentiated cyclist' behavioral response to alerts and driving restrictions.

This chapter provides answers to the above questions in Mexico City. We partner with Strava Metro to obtain an hourly aggregated and anonymized dataset with all bicycle trips from the nearly twelve thousand people who track and—publicly—share their trips though the Strava application. These data allow us to observe—even at the road segment level—the location, duration, distance, and purpose of cycling trips registered in Mexico City during the period from January 2019 to March 2023. Hence, it is equivalent to having a counter that distinguishes commuting from leisure trips at each road segment.

Although environmental alerts and driving restrictions are closely linked, they do not necessarily occur simultaneously. For instance, alerts can be activated city-wide (with driving restrictions), or just regionally (with no driving restrictions). We harness the arbitrariness and specific design of the guidelines established in the latest update the Atmospheric Environmental Emergencies Program (PCAA) to carefully disentangle the effects of precautionary recommendations and temporary driving restrictions on cycling activity according to its purpose.

We estimate a panel fixed effects model to study how alerts and driving restrictions affect hourly cycling activity in the municipalities of Mexico City during the period from January 2019 to March 2023. In contrast with previous studies, our analysis distinguishes the behavioral response from commuting and leisure cyclist to both alerts and driving restrictions. Furthermore, it evaluates the heterogeneity of the results according to the cyclist' income level.

We find that environmental alerts are effective, yet limited, persuading cyclists to reduce their cycling activity during highly polluted days. Although cycling activity is reduced 9-27% in response to the precautionary recommendations, most cyclists in Mexico City continue to exercise during emergencies even with elevated levels of pollution. Moreover, we confirm that driving restrictions are effective, yet regressive. While commuters with higher incomes (and greater availability of vehicles) increase their cycling activity by 6-9% in response to driving restrictions, the response of commuters with lower incomes is almost three times greater. That is, they increase their cycling activity between 17-26%. While higher-income commuters continue to drive thanks to their greater availability of cars, lower-income commuters are pushed to opt for cleaner means of transportation—as bicycles—during environmental emergencies, at a higher cost for their health.

The results are relevant in terms of environmental and transportation policy in Mexico City. Considering that environmental emergencies are a rare event, policymakers could promote more avoidance behavior sending real-time air quality alerts through applications such as Strava and Ecobici, which are extensively used by cyclists before their trips. Further, policymakers could attenuate the regressivity of temporary driving restriction, reducing public transportation fares during environmental emergencies. However, a solution to the root of the problem would require evaluating market alternatives to reduce congestion in the city. For instance, establishing congestion charges for traveling by car to the city center.

Full text

3.1. Introduction

When air quality conditions in Mexico City worsen to the point of posing an exceedingly high risk to public health, the authority issues a massive press release declaring a state of environmental emergency. The activation of an emergency is accompanied by a series of precautionary recommendations that the population at risk—such as cyclists—can follow to

reduce their exposure to pollution. Moreover, environmental emergencies include the temporary tightening of driving restrictions that have been permanently imposed by the *Hoy No Circula* (HNC) program. These measures are colloquially known as "double" HNC. However, they force almost six times as many private vehicle owners to reschedule their activities or use other unrestricted transportation alternatives.

Cyclists in Mexico City could respond to these emergencies with avoidance behaviors, heeding to the precautionary recommendations issued by the authority. For instance, rescheduling their trips or opting for other less exposed means of transportation. However, at least some of these cyclists could also be temporarily restricted to drive their cars. Therefore, they must face the dilemma between traveling using their bicycles—ignoring the precautionary recommendations—or using the car—disobeying, facing, or circumventing the economic sanctions that are imposed due to the temporary driving restrictions—to safeguard their health. Of course, they could also use public transport.

The existing literature has highlighted the importance of considering trips' purpose to determine the predominant behavioral response between avoidance behavior and transport mode substitution. For instance, Saberian et al. (2017) find that environmental alerts have been effective in Sydney (Australia) deterring cyclists from exposure during highly polluted days, especially those who make trips outside of peak hours for discretionary purposes. On the other hand, de Buen Kalman (2021) and Rivera (2021) show that when environmental alerts are combined with mandatory temporary driving restrictions, these are effective in pushing individuals—specifically, those who commute during rush hours—to temporarily abandon their cars and opt for cleaner means of transportation such as bike-sharing systems in Mexico City, or mass transportation systems (metro and bus rapid transit) in Santiago (Chile).

Despite its importance, previous studies have not been able to distinguish accurately between leisure and commuting at the trip level. Additionally, they have focused either on the specific role of environmental alerts (Saberian et al., 2017), or the joint effect of environmental alerts and temporary driving restrictions (de Buen Kalman, 2021; Rivera, 2021). That is, they have not been able to decompose the effects of alerts and restrictions depending on whether the trips are related to leisure or commuting.

We fill the two gaps using administrative data recorded by Mexico City cyclists through the Strava application. These data allow us to observe—even at the road segment level—the location, duration, distance, and purpose of cycling trips registered in the application during the period from January 2019 to March 2023. Moreover, we take advantage of the arbitrary and specific design of the guidelines established for the Atmospheric Environmental Emergencies Program (PCAA) in Mexico City to carefully disentangle the effects of precautionary recommendations (i.e., environmental alerts) and temporary driving restrictions on cycling activity according to its purpose.

Our results complement those obtained by de Buen Kalman (2021) and Saberian et al. (2017). Consistent with Saberian et al. (2017), we find that cyclists in the aggregate respond to environmental emergencies with avoidance behavior. That is, they reduce their cycling activity by 9-27%, complying with the precautionary recommendations issued by the authority during these episodes. On the other hand, in line with de Buen Kalman (2021), we find that temporary driving restrictions are effective in pushing commuters to adopt cleaner means of transportation increasing cycling activity by 8-13%.

Importantly, the greater granularity of Strava data—compared to that employed by de Buen Kalman (2021) and Saberian et al. (2017)—allows us to explore the heterogeneity of these responses by cyclists' income level. We find that, despite their effectiveness, temporary driving restrictions are a regressive measure. While a good portion of high-income commuters takes advantage of their greater availability of cars to continue driving during environmental emergencies, even benefiting from less congestion, driving restrictions impose a greater burden on low-income commuters, forcing them to make their trips in cleaner modes of transportation—such as bicycles—at a higher cost to their health.

3.2. Related literature

To face the external health costs of environmental pollution, individuals—as utility-maximizing agents—undertake defensive behaviors, either avoiding pollution exposure or purchasing protective equipment and medications that reduce the severity of its damages (Williams, 2019). Avoidance behavior includes reducing the frequency (and/or intensity) of outdoor activities during highly polluted days, particularly those of a discretionary nature that are carried out for recreational purposes such as taking a bicycle ride (de Buen Kalman, 2021; Liang et al., 2023; Saberian et al., 2017; Zhao et al., 2018), visiting or camping in natural parks (Gellman et al., 2022; Keiser et al., 2018), going to parks or zoos (Noonan, 2014; Zivin & Neidell, 2009), and attending sport events (Yoo, 2021). Conversely, defensive expenditures include purchases of specialized facemasks (Wang & Zhang, 2023; Zhang & Mu, 2018), indoor air purifiers (Barwick et al., 2023; Ito & Zhang, 2020), as well as cough and sinus medications, and other remedies that help improve breathing (Du, 2023).

The costs that individuals incur to protect themselves from pollution—whether by making extra expenses or foregoing the utility of performing some activities—are not distributed evenly across the population (Williams, 2019). Evidence shows that sensitive groups—such as elders and those with previous diagnoses of respiratory diseases—avoid exposure to high levels of pollution to a greater extent (Barwick et al., 2023; Noonan, 2014; Williams, 2019; Xu et al., 2021). According to Borbet et al. (2018), these individuals receive medical services more frequently, which raises their awareness about the adverse effects of pollution on health. Therefore, as suggested by Welch et al. (2005), they have a greater predisposition to heed public health recommendations.

Policymakers have recognized that information plays a fundamental role in the economic decisions of individuals, and consequently have procured its dissemination as a strategy to promote a greater participation in defensive behaviors. These efforts—with the potential to reduce mortality attributable to pollution—have included the deployment of real-time air quality monitoring and diffusion programs, accompanied in some cases by environmental alerts systems (Barwick et al., 2023; Huang et al., 2023). Air quality alerts are issued in diverse cities such as Atlanta, Beijing, Chicago, Los Angeles, Mexico City, Santiago, San Francisco, Salt Lake City, Stuttgart, and Sydney when pollution reach (or are predicted to reach) levels that pose a health risk to the population. They usually recommend individuals, particularly the most vulnerable, to refrain from doing outdoor activities, in special those that require a greater physical effort, such as cycling (Saberian et al., 2017).

Studies of cycling activity in Sydney in Australia (Saberian et al., 2017), or Chengdu and Beijing in China (Liang et al., 2023; Zhao et al., 2018), confirm that cyclists engage in avoidance behavior in the face of pollution. Saberian et al. (2017) were the first to estimate the effect of air quality alerts on cycling activity, carefully distinguishing it from the effect of air quality itself. That is, they estimate that, keeping other thing equal (including air quality), alerts reduce cycling activity about 15-35%. Furthermore, according to Liang et al. (2023) and Saberian et al. (2017), the response of cyclists is greater for leisure trips than commuting. However, even though they used administrative records from the dockless bike-sharing system in Chengdu and the bike counters in the Sydney cycle path network, respectively, none of them have data that distinguishes explicitly the purpose of the trip. Hence, they arrive to this conclusion indirectly by assuming that commuting and leisure are more likely to occur during certain hours of the day and certain days of the week. Our article fills this gap using data from Strava that allows us to distinguish between leisure and commuting at the trip level.

In some cities, air quality alerts also recommend to voluntarily reduce the use of private vehicles. However, they have shown limited effectiveness with daily traffic volume reductions of just 2.5-3.5% in the San Francisco Bay Area (Cutter & Neidell, 2009), 0.3-0.5% in northern Utah (Caplan, 2023), and a null effectiveness for Atlanta (Noonan, 2014). These recommendations can even have counter effects—as in the case of Stuttgart (Dangel & Goeschl, 2022) and Salt Lake City (Tribby et al., 2013) —with overall increases in traffic volume of up to 2-4%, due to the displacement of trips from the city center to the periphery. Furthermore, evidence from the San Francisco Bay Area and Chicago points to a null overall effect on the use of rapid train systems, although in both cases there were significant temporary increases in ridership during peak hours (Cutter & Neidell, 2009; Welch et al., 2005).

A plausible reason for the limited effectiveness of voluntary information programs in reducing automobile use is the conflict between the private and public interests of drivers. As suggested by Caplan (2023), Noonan (2014), and Tribby et al. (2013), self-interest leads

individuals to choose means of transportation that reduce their exposure to pollution and travel times (such as the automobile), while altruistic motivations encourage individuals to replace their driving for a less polluting mode of transport (such as the bicycle or public transport). As noted by Welch et al. (2005), these programs generally do not include an economic incentive and therefore depend on the effectiveness of the communication process to persuade individuals.

In cities such as Santiago and Mexico City, recommendations on reducing vehicle use on highly polluted days are mandatory. License plate based temporary driving restrictions are imposed on a portion of the vehicle fleet, including polluting cars and cleaner vehicles (Rivera, 2021). Unlike voluntary information programs, these harsh policies seek to discourage the use of restricted vehicles by imposing fines. For instance, fines in Mexico City can exceed $175 US dollars.

An extensive literature has documented the lack of effectiveness of HNC to reduce pollution and encourage the substitution of automobiles with less polluting means of transport, suggesting that individuals take different behavioral measures to avoid the restrictions (Davis, 2008, 2017; Eskeland & Feyzioglu, 1997; Gallego et al., 2013; Guerra & Millard-Ball, 2017; Guerra et al., 2022; Guerra & Reyes, 2022).

Initially, the literature attributed the lack of effectiveness of HNC to the fact that households (mainly those with middle income) responded to the policy by acquiring a second (more polluting) vehicle (Davis, 2008; Eskeland & Feyzioglu, 1997; Gallego et al., 2013). More recently, Guerra and Millard-Ball (2017) dissent with this explanation, attributing the lack of effectiveness of HNC to the high percentage of private vehicles exempt from the restrictions. According to our calculations, 93.8 percent of vehicles are exempt on weekdays.

Guerra and Millard-Ball (2017) argue that there is a battery of relatively cheaper alternatives that drivers appeal to avoid the restrictions. For instance, as demonstrated by Oliva (2015), almost 10% of car owners have resorted to bribery to pass the emissions test, and thus obtain a verification hologram that exempt them from HNC. Moreover, according to Guerra and Reyes (2022), drivers have adjusted their behavior to circumvent the restrictions: replacing their old vehicles with cars eligible to be exempt from HNC (especially, those with higher incomes), rescheduling their discretionary trips to non-restricted hours, driving on less policed streets, and ultimately bribing traffic officers if they are caught avoiding the restrictions.

In contrast with the lack of effectiveness of HNC, de Buen Kalman (2021) and Rivera (2021) show that environmental alerts combined with mandatory temporary driving restrictions can be effective in reducing the number of trips in private vehicles, and persuade inhabitants to resort to other less polluting means of transport such as the subway, bus rapid transit or bicycle sharing systems.

Although de Buen Kalman (2021) discusses and recognizes the role of environmental alerts in moderating cycling activity in Mexico City, these are not explicitly included in their empirical model. In fact, de Buen Kalman (2021) considers environmental alerts and temporary driving restrictions as two simultaneous events. We are careful to distinguish both measures in accordance with the guidelines from the Atmospheric Environmental Emergencies Program (PCAA), focusing on a different study period in which temporary driving restrictions were tightened, restricting 13.8 more private vehicles.

Our work is the first to carefully disentangle the effect of temporary driving restrictions from the precautionary recommendations issued by the authority to cyclists following the activation of environmental emergencies in accordance with their trips' purpose. It is also the first to estimate the magnitude of the behavioral response of cyclists to precautionary recommendations during environmental emergencies in Mexico City.

3.3. Environmental emergencies and driving restrictions in Mexico City

An environmental emergency is a temporary episode that is activated when ozone or particulates concentrations reach levels that can harm public health or the environment (Government of Mexico City, 2019b). The Megalopolis Environmental Commission (CAMe) oversees the activation and suspension of environmental emergencies in accordance with the guidelines established in the Atmospheric Environmental Emergencies Program (PCAA). This program defines the actions needed to reduce the emission of pollutants and protect the health of the inhabitants of the Valley of Mexico.

To announce the activation or suspension of an environmental emergency, CAMe issues a press release that is widely disseminated in mass media. As established by Government of Mexico City (2019b), the announcement includes precautionary recommendations and mandatory measures for schools, government institutions, vehicles, commercial and service establishments, major plants from the manufacturing industry, as well as the general population that lives or transits in the Metropolitan Area of the Valley of Mexico (ZMVM)[1].

The PCAA dates to May 1986 (Government of Mexico City, 2019a). However, the first environmental emergency was activated until February 1988 (Government of Mexico City, 2023a). In its beginnings, the PCAA only considered ozone concentrations and contemplated three phases. The program now incorporates guidelines to activate environmental emergencies in response to threaten concentrations of PM_{10} and $PM_{2.5}$ particles which were established in May 1988 and May 2019, respectively.

Moreover, environmental regulation in Mexico City has become more stringent over time. There has been a decrease in the Air Quality Index (AQI) values required for the activation

[1] The ZMVM includes Mexico City and the surrounding municipalities from the State of Mexico. The number of surrounding municipalities included has changed over time, going from 18 to 59 on May 29, 2019 (Government of Mexico City, 2019b)

of environmental emergencies, as well as in the maximum permissible concentrations of ozone and particulates. Since April 2016, phase 1 emergencies are activated when the AQI for ozone or PM_{10} particles are between 151 and 200 points (Government of Mexico City, 2019a). An AQI equal to 100 corresponds to the maximum permissible concentration level defined by the Ministry of Health for each pollutant. Hence, it represents an hourly ozone concentration of 0.095 ppm. In the case of PM_{10}, it corresponds to a 24-hour average concentration of 75 $\mu g\ /\ m^3$. Therefore, phase 1 emergencies are activated with concentrations between 0.155 and 0.204 ppm for ozone, and between 215 and 354 $\mu g\ /\ m^3$ in the case of PM_{10} (Government of Mexico City, 2018).

As mentioned before, $PM_{2.5}$ particles began to be considered recently, on May 29, 2019. This occurred after numerous fires in the Valley of Mexico triggered the most severe environmental emergency in recent history, which lasted 4 days and caused the suspension of classes for the first time[2]. The activation of phase 1 emergencies for this pollutant now requires 24-hour average concentrations between 97.5 and 150.4 $\mu g\ /\ m^3$ (Government of Mexico City, 2018).

While environmental emergencies for ozone are applied city-wide, phase 1 emergencies for particles can be activated either in the whole Valley of Mexico or just regionally. Municipalities of the ZMVM are grouped into five regions, according to their geographical location: center, northeast, northwest, southeast, and southwest[3]. If the activation levels for PM_{10} or $PM_{2.5}$ are reached in just one of these regions, emergencies are only applied for that specific region. In contrast, if the activation levels are reached in two or more regions, emergencies for particles are activated city-wide (Government of Mexico City, 2019b).

Table 3.1 shows the frequency and severity of environmental emergencies since the beginning of the PCAA. Eighty-six percent of these episodes are activated by high concentrations of ozone. Environmental emergencies are activated most frequently during winter and spring (from December to May) between 12:00 and 6:00 p.m. with an average duration of 47 hours (Government of Mexico City, 2023a). Although their seasonal pattern coincides with that of thermal inversions, Arceo et al. (2016) find that the contribution of thermal inversions to higher ozone concentrations is negligible compared to other pollutants, such as carbon monoxide and PM_{10} particles. In contrast, seven out of the twelve environmental emergencies caused by the high concentrations of PM_{10} and $PM_{2.5}$ particles were activated on December 25th or January 1st. This happens because, in Mexico as in other

[2] "Terminan 4 días de contingencia; el miércoles presentarán nuevos protocolos", *Lilián Hernández (Excelsior)*, May 18, 2019. Available at https://www.excelsior.com.mx/comunidad/terminan-4-dias-de-contingencia-el-miercoles-presentaran-nuevos-protocolos/1313745

[3] Regional classification for the 16 municipalities of Mexico City: Center (Iztacalco, Benito Juárez, Cuauhtémoc, and Venustiano Carranza); Northeast (Gustavo A. Madero); Northwest (Azcapotzalco and Miguel Hidalgo); Southeast (Tláhuac, Iztapalapa, Xochimilco, and Milpa Alta); and Southwest (Coyoacán, La Magdalena Contreras, Cuajimalpa de Morelos, Álvaro Obregón, and Tlalpan).

parts of the world, there is a deep-rooted tradition of celebrating festivities—such as Christmas and New Year—with fireworks (Retama et al., 2019).

Table 3.1. Frequency and severity of environmental emergencies in the Valley of Mexico

	Pre-emergencies			Emergencies								
				Phase 1					Phase 2	Avg. max. concentration		
				City-wide			Regional			O_3	PM_{10}	$PM_{2.5}$
Years	O_3	PM_{10}	$PM_{2.5}$	O_3	PM_{10}	$PM_{2.5}$	PM_{10}	$PM_{2.5}$	O_3	(1 h)	(24 h)	(24 h)
1986–88	-	-	-	2	-	-	-	-	0	0.361	-	-
1989–93	-	-	-	18	-	-	-	-	5	0.352	-	-
1994–98	74	5	-	16	1	-	-	-	0	0.312	371	-
1999–03	89	5	-	4	0	-	2	-	0	0.300	443	-
2004–08	5	3	-	0	0	-	1	-	0	-	344	-
2009–13	15	4	-	0	0	-	0	-	0	-	-	-
2014–18	13	1	-	13	0	-	3	-	0	0.173	237	-
2019–23*	4	2	3**	15	0	1***	1	3	0	0.162	264	112

Notes: Ozone (O_3) concentrations are measured in part per million (ppm). Particulates concentrations are micrograms per cubic meter ($\mu g/m^3$). Pre-emergencies include the preventive phase of environmental emergencies registered since May 29, 2019. * With data up to March 31, 2023. ** It includes an extraordinary air quality alert declared on May 12, 2019. *** Extraordinary emergency for both O_3 and $PM_{2.5}$. Source: Prepared with information from Government of Mexico City (2016a, 2023a), and Mexico City Ministry of Environment (SEDEMA).

A preventive emergency phase for the three pollutants was reincorporated in the latest update of the PCAA on May 29, 2019[4]. Pre-emergencies seek to apply preventive measures that could avoid more severe episodes like phase 1 emergencies. Nonetheless, the activation values that were initially established have been followed with discretion in practice[5]. These episodes have been activated in only eight occasions, mainly during holidays such as Christmas and New Year, with an average duration of 160 minutes. The latest update of the PCAA also includes a combined phase for ozone and particles. Additionally, it considers—as before—a phase 2 environmental emergency for each pollutant, which requires more than 200 AQI points to activate. However, the criteria necessary for the activation of these latter phases have not been met recently.

As we study the period from January 2019 to March 2023, we concentrate on phase 1 emergencies[6]. Similar to Santiago (Rivera, 2021), emergencies in Mexico City include a combination of precautionary recommendations that individuals may follow to avoid pollution exposure to protect their health, such as avoiding vigorous outdoor activities from

[4] Pre-emergencies were first introduced in 1997, substituting phase 3 emergencies. They operated until April 2016.

[5] "¿Y la protección de la salud?", *Angélica Simón (Greenpeace)*, July 25, 2019. Available at https://www.greenpeace.org/mexico/noticia/2831/y-la-proteccion-de-la-salud/

[6] In Table A3.1 from the Appendix, we present a detailed description of the precautionary recommendations and mandatory measures enforced during these phase 1 emergencies.

13:00 to 19:00 hrs. during ozone emergencies, as well as mandatory measures that are imposed with the aim of reducing pollutant emissions mostly applicable to the transportation sector, for instance, temporarily restricting driving of eligible vehicles.

A substantial share of private cars is eligible to these temporary driving restrictions, particularly the most polluting ones. To qualify for exemption (or liability), car owners must submit their vehicles to a mandatory emission test and visual inspection every six months. An authorized verification center must determine if vehicles are approved or rejected based on emission limits established by Mexico City Ministry of Environment (Oliva, 2015). The approval of this verification results in the assignment of one out of the five hologram stickers that must be placed on the car front windshield (i.e., "exempt", "00", "0", "1", and "2").

Electric, full hybrid and plug-in hybrid vehicles, as well as motorcycles, are exempt from driving restrictions[7]. New and semi-new vehicles that demonstrate a superior energy-efficiency, for example gasoline-powered cars with a fuel economy of at least 16 km/l are eligible to receive the "00" hologram valid for 2 years[8]. Mild hybrid cars and other natural gas or gasoline-powered relatively new vehicles (model year greater to 2005) that pass the emissions test receive the "0" hologram valid for 6 months. Older—and more pollutant—automobiles, such as those with model year 1994 to 2005 or previous are assigned holograms "1" and "2", respectively (Government of Mexico City, 2023b).

Table 3.2. Percent of private cars subject to driving restrictions in Mexico City

	Permanent HNC		HNC for COVID-19	Temporary driving restrictions	
Hologram	Weekdays	Saturdays	Weekdays (April 23 to June 15, 2020)	Before May 29, 2019	After May 29, 2019
00 and 0	0.0	0.0	13.8	0.0	13.8
1	4.1	10.3	4.1	10.3	10.3
2	2.0	10.2	2.0	10.2	10.2
All	6.2	20.5	20.0	20.5	34.4

Notes: Vehicles rejected during the verification process, as well as those with foreign plates without a verification hologram, are considered as if they had a "2" hologram. Driving restrictions during health emergency for COVID-19 also included exempt electric and hybrid vehicles. Source: Own estimates based on the guidelines for the programs HNC (Government of Mexico City, 2014, 2020b) and PCAA (Government of Mexico City, 2016b, 2019b), together with the actual holograms obtained by 1.3 million private cars during the second semester of 2018, available at https://datos.cdmx.gob.mx/dataset/verificacion-automotriz-segundo-semestre-2018

Temporary driving restrictions are applied on the day after the activation of environmental emergencies from 5:00 to 22:00 hours based on a combination of the verification hologram

[7] A list of electric and hybrid vehicle models eligible to be exempt from driving restrictions is available at https://verificentros.sedema.cdmx.gob.mx/Listado/Exentos

[8] Vehicles eligible for the "00" hologram are listed at https://verificentros.sedema.cdmx.gob.mx/Listado/

assigned to the vehicle and the last digit of the license plate[9]. Restrictions are not implemented when the phase 1 emergency is declared regionally. Prior to the last update of the PCAA, these restrictions concentrated on the most polluting cars (i.e., those with holograms "1" and "2"), restricting the circulation of approximately 21% of the private automobiles. After May 29, 2019, temporary restrictions also include cleaner cars. With this important modification, almost 35% of private vehicles in Mexico City are restricted during highly polluted days (see Table 3.2).

It is important to note that the temporary driving restrictions are applied in addition to the permanent restrictions defined by the HNC program. As shown in Table 3.2, temporary measures defined by the PCAA restrict much more than twice as many vehicles on weekdays. Consequently, the response of car owners to these temporary restrictions increases abruptly (see Figure 3.1).

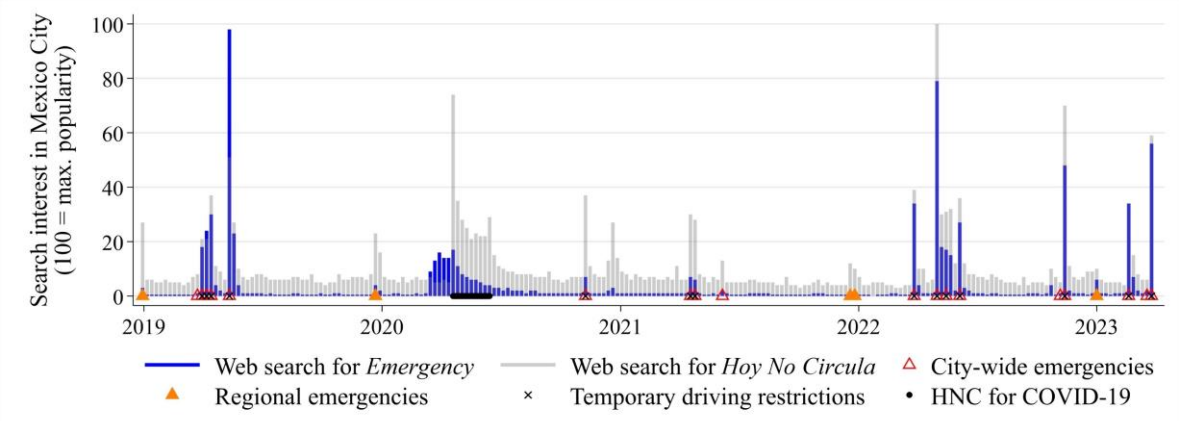

Figure 3.1. Search interest for "*Emergency*" and "*Hoy No Circula*" in Mexico City. Source: Prepared with data from Google Trends. Data available at https://trends.google.es/trends/explore?date=2018-12-30%202023-03-31&geo=MX-DIF&q=Contingencia,Hoy%20no%20circula

Driving restrictions were also extended extraordinarily during the COVID-19 health emergency. These measures restricted the circulation of private vehicles in accordance with the last digit of their license plate, regardless of their verification hologram (Government of Mexico City, 2020b). Therefore, they included 20% of private cars, also including exempt electric and hybrid vehicles. The extraordinary HNC for COVID-19 was applied on weekdays (5:00 to 22:00 hrs.) from April 23 to June 15, 2020.

3.4. Theoretical framework

We can predict the expected behavioral responses of individuals to the precautionary recommendations and temporary driving restrictions imposed during environmental emergencies according to their trip purpose based on the theoretical framework developed

[9] Unusually, for the only occasion, temporary driving restrictions imposed on April 17 and 18, 2019 were applied from 9:00 to 18:00 hours.

by Cutter and Neidell (2009). However, it is necessary to consider two critical changes to adapt this framework to the policy context described in the guidelines from the PCAA in Mexico City, as well as to the objective of this study.

First, unlike *Spare the Air* (STA), the voluntary information program studied by Cutter and Neidell (2009) in the San Francisco Bay Area, temporary driving restrictions in Mexico City are mandatory for about 34% of private vehicles. According to article 47 in the transit regulations of Mexico City, drivers who fail to comply with the temporary driving restrictions and are caught driving by a transit officer must pay a fine of between $2,075 and $3,112 Mexican pesos (equivalent to $117 and $175 US dollars, respectively)[10]. Additionally, local authorities detain the vehicle, and the owner must pay the costs of towing and storing it.

Second, unlike Cutter and Neidell (2009)—who consider public transportation as an option to replace car trips—we study the substitution between car and bicycle trips. This is relevant when distinguishing between the purpose of trips. While commuting trips by bicycle can replace a trip by car (or public transport), a leisure trip by bike cannot be substituted.

This theoretical framework highlights the importance of considering the purpose of trips to carefully distinguish the effect of precautionary recommendations and temporary driving restrictions on cycling activity. Furthermore, it motivates the analysis of the heterogeneity in the response of cyclists according to their income level.

3.4.1. Leisure trips

Similar to the case of public transportation users who make discretionary trips considered by Cutter and Neidell (2009), the utility of making a leisure trip by bicycle for an individual i, $U_{i,b}^{L}$ during an environmental emergency ($\mathbb{1}_{Emergency} = 1$) decreases due to a higher health cost for the individual H_i,

$$\Delta U_{i,b}^{L} | \mathbb{1}_{Emergency} = -\Delta^{+} H_i \leq 0, \qquad \mathbb{1}_{Emergency} = 1. \tag{1}$$

Thus, consistent with Saberian et al. (2017), we would expect leisure cyclists—especially those who engage in vigorous exercise or belong to vulnerable groups—to respond reducing their cycling activity, avoiding their exposure to pollution in accordance with the precautionary recommendations issued by the authority.

In addition, we would not expect to observe a positive effect of temporary driving restrictions on leisure cycling trips because they do not replace car trips. However, it is possible to observe a negative effect if leisure cycling activity is complemented by car use. This is possible if, for example, individuals drive their cars to transport themselves and their bicycles to parks and other places intended for exercise. In any case, both effects are

[10] The current transit regulations of Mexico City are available at https://www.ssc.cdmx.gob.mx/organizacion-policial/subsecretaria-de-control-de-transito/reglamento-de-transito

reinforced, and we would expect a significant overall reduction in leisure cycling activity during environmental emergencies.

3.4.2. Commuting trips

The utility of individuals who choose to make their trips by car during environmental emergencies $U_{i,d}^{C}$ is reduced due to the probability of being detained and fined for driving a restricted vehicle. However, following Cutter and Neidell (2009), given that up to 34% of private vehicles stop circulating in Mexico City due to the temporary driving restrictions, individuals' utility would also increase due to a reduction in their travel times $t_{i,d}$ attributed to less road congestion. Thus,

$$\Delta U_{i,d}^{C}|\mathbb{1}_{Emergency} = -\left[\mathbb{1}_{HNC} \times \Pr\{Traffic\ Detention\} \times U_{i,d}(\$175 + c)\right] - \Delta^{-} t_{i,d} \qquad (2)$$

where $\mathbb{1}_{HNC}$ is an indicator function that takes the value of 1 if the vehicle of individual i is subject to the temporary driving restrictions, and $U_{i,d}(\$175 + c)$ corresponds to the utility equivalent for the sum of a \$175 fine and the additional costs derived from the retention of the vehicle by the authority. Consistent with Gallego et al. (2013), temporary driving restrictions can be effective if they are applied sporadically. That is, for some individuals the disutility associated with the possibility of being penalized for violating the restrictions may be large enough to discourage them from driving during environmental emergencies. In contrast, owners of unrestricted vehicles (about 66% of total vehicles) would have an additional incentive to continue driving due to less traffic congestion.

Identical to the case of public transport commuters considered by Cutter and Neidell (2009), individuals who choose to make their commuting trips by bicycle instead of using their automobiles during environmental emergencies increase their utility because they value contributing to the reduction of pollution. In the words of Cutter and Neidell (2009), they receive an "environmental warm glow", G_i. However, they also face an increase in their health costs, H_i.

$$\Delta U_{i,b}^{C}|\mathbb{1}_{Emergency} = G_i - \Delta^{+} H_i \qquad (3)$$

Following Cutter and Neidell (2009), the probability that an individual changes their mode of transportation from car to bicycle to make commuting trips during environmental emergencies ($\mathbb{1}_{Emergency} = 1$) increases to the extent that $\Delta U_{i,b}^{C}\left|\mathbb{1}_{Emergency}\right. > \Delta U_{i,d}^{C}\left|\mathbb{1}_{Emergency}\right.$. This is,

$$G_i - \Delta^{+} H_i > \left|\Delta^{-} t_{i,d}\right| - \left[\mathbb{1}_{HNC} \times \Pr\{Traffic\ Detention\} \times U_{i,d}(\$175 + c)\right]. \qquad (4)$$

We can make some assumptions about the relative size of the terms in inequality (4) to predict the most likely response between driving a car or riding a bicycle for individuals who commute during environmental emergencies according to their characteristics. To do this,

we consider three important traits highlighted by the literature: income level, health vulnerability and altruistic behavior.

Consistent with the results of Gallego et al. (2013), and Guerra and Reyes (2022), we consider the importance of income to moderate the response of individuals to driving restrictions. We classify higher-income individuals as those whose benefits from the reduced driving travel time outweighs their disutility of facing the potential monetary costs of penalties imposed for driving during environmental emergencies, $\left|\Delta^{-} t_{i,d}\right| > \left[\mathbb{1}_{HNC} \times \Pr\{Traffic\ Detention\} \times U_{i,d}(\$175 + c)\right]$. That is, individuals with a high opportunity cost for their time who have a greater probability of getting around the restrictions either by facing the sanctions (legally or illegally) or by reducing their probability of being sanctioned. For instance, by driving more kilometers to travel along routes with less police enforcement (Guerra et al., 2022; Guerra & Reyes, 2022); by bribing technicians to obtain an hologram subject to fewer driving restrictions (Oliva, 2015); or by having at their disposal a greater number of additional exempt vehicles and/or cars subject to fewer restrictions (Guerra et al., 2022; Guerra & Reyes, 2022). We reverse the inequality to characterize individuals with a lower income.

Health-vulnerable commuters are those whose sacrifice—reflected in their higher health costs—are large enough to exceed the utility obtained if they decided to replace driving their cars with bike commutes to contribute to the reduction of pollution during environmental emergencies, $\Delta^{+} H_i > G_i$. We would expect the number of commuters in this group to be substantially small when compared to the non-vulnerable ones, because commuting trips are made by younger individuals during times of the day with lower concentrations of pollutants. According to Guerra et al. (2020), the probability of commuting by bicycle in Mexico reaches its maximum at the age of 45, and reduces considerably after the age of 60, when individuals begin to stop being part of the economically active population. We assume that for non-vulnerable commuters, $\Delta^{+} H_i < G_i$.

Finally, we incorporate the importance of altruistic behavior highlighted by Caplan (2023), Noonan (2014), and Tribby et al. (2013). We assume that self-interested individuals give more weight to the savings in travel time they can obtain by driving their vehicle than to the utility they would obtain by contributing publicly, reducing their polluting emissions by using a bicycle during environmental emergencies. That is, $\left|\Delta^{-} t_{i,d}\right| > G_i$. In contrast, we assume that altruistic individuals place more value on their contributions to reduce polluting emissions, even if this decision takes more time than driving their vehicles during environmental emergencies.

In Table 3.3, we combine inequality (4) with the restrictions defined to categorize individuals according to their income level, health vulnerability, and altruistic behavior to predict the most likely response of commuters—between driving a car or riding a bicycle—in response to the activation of an environmental emergency in Mexico City.

Table 3.3. Transportation mode (car or bicycle) that commuters most likely choose in the event of an environmental emergency according to their income level, health vulnerability, and altruistic behavior.

a) Lower income

		Self-interested	Altruistic
Vulnerable	Restricted ($\mathbb{1}_{HNC} = 1$)	Ambiguous	Ambiguous
	Non-restricted ($\mathbb{1}_{HNC} = 0$)	Drive car	Drive car
Non-vulnerable	Restricted ($\mathbb{1}_{HNC} = 1$)	Ride bicycle	Ride bicycle
	Non-restricted ($\mathbb{1}_{HNC} = 0$)	Drive car	Ride bicycle

b) Higher income

		Self-interested	Altruistic
Vulnerable	Restricted ($\mathbb{1}_{HNC} = 1$)	Drive car	Drive car
	Non-restricted ($\mathbb{1}_{HNC} = 0$)	Drive car	Drive car
Non-vulnerable	Restricted ($\mathbb{1}_{HNC} = 1$)	Drive car	Ambiguous
	Non-restricted ($\mathbb{1}_{HNC} = 0$)	Drive car	Ambiguous

Note: Predictions based on an extension of the theoretical model developed by Cutter and Neidell (2009).

First, we predict that health-vulnerable commuters reduce their cycling activity by opting for means of transport that expose them less to pollution (such as the automobile) to reduce their health costs, complying with the precautionary recommendations issued by the authority during environmental emergencies. It should be noted that in the case of health-vulnerable individuals with lower incomes, this behavioral response could be in conflict with temporary driving restrictions.

Consistent with Liang et al. (2023) and Saberian et al. (2017), we expect to observe a weaker avoidance behavior response than that shown by individuals who travel for leisure for two reasons. First, as indicated by Cutter and Neidell (2009), the health cost faced by commuters is lower than that faced by leisure cyclists. This occurs because ozone concentrations in Mexico City are higher from 13:00 to 19:00 hrs. (that is, outside of morning peak commuting hours). Second, commuters have less flexibility to cancel or reschedule their trips to work (de Buen Kalman, 2021; Cutter & Neidell, 2009).

Next, we expect non-vulnerable lower-income commuters to increase their use of bicycles due to temporary driving restrictions. Moreover, consistent with Caplan (2023), Noonan (2014), and Tribby et al. (2013), the response of non-vulnerable commuters to environmental emergencies in the absence of an economic incentive will depend of their altruistic traits. The most altruistic commuters will be more likely to choose riding their bicycles, while those with greater self-interest will prefer to drive their cars.

Finally, it is important to highlight that—as pointed out by Gallego et al. (2013), and Guerra and Reyes (2022)—income level seems to be the most important dimension to determine the degree to which temporary driving restrictions are effective—in the short

term—to persuade commuters to opt for less polluting alternative means of transport, such as bicycles. While commuters with a lower income face the greatest burden to reduce pollution during environmental emergencies, most higher-income commuters are likely to continue driving their cars. However, there is a possibility that a small group of higher-income and more altruistic commuters can also contribute reducing their polluting emissions by riding a bicycle during environmental emergencies.

3.5. Data

3.5.1. Cycling activity

We have hourly records of cyclists' activities in Mexico City for the period Jan 2019 - Mar 2023. These records come from two sources. First, we partnered with Strava Metro to obtain an hourly aggregated and anonymized count of all bicycle trips tracked and—publicly—shared in Strava for each road segment in Mexico City[11]. Strava is a platform where users can track and share—either publicly or privately—their daily trips with their phones or GPS devises. Nearly twelve thousand people currently share their cycling activities in Mexico City. Cyclist and pedestrians around the world use Strava to monitor and compare their performances, connect with friends, and find new routes[12].

An important advantage of Strava Metro data is that before aggregating trips by road segment, they are classified by type of activity according to their purpose, either as commute or leisure. For Strava, a commuting trip is any utilitarian trip that substitutes the use of cars or public transit[13]. For example, a trip to work or school. Leisure trips refers to all non-commuting trips, such as those conducted for recreational or exercise purposes.

We multiply the number of bicycle trips in each segment by its length in kilometers to obtain the total distance traveled per hour in each segment, distinguishing by type of activity. As expected, commuting trips have a different hourly pattern than leisure trips (see Figure 3.2). The volume and distance of activities conducted for leisure is greater during weekends, reaching their peak at 9:00 a.m. These activities are similar during weekdays, although they start earlier. In contrast, commuting trips are more common during weekdays with two prominent peaks at 8:00 a.m. and 6:00 p.m., associated with workday schedules. Moreover, they exhibit a completely different pattern during weekends.

[11] Strava Metro is an initiative that seeks to leverage the substantial number of activities tracked by Strava users to enhance safety, accessibility, and efficiency of bicycle and pedestrian travels in cities around the world. As the raw data is property of Strava, Inc., those who need to access the data we use for Mexico City—or some other city—must apply for a Strava Metro partnership at https://metro.strava.com/

[12] A detailed description of Strava features is available at https://www.strava.com/features

[13] "Tracking the rise of bike commuting around the world", *Erik Sunde (Strava Metro)*, Feb 8, 2019. Available at https://medium.com/strava-metro/tracking-the-rise-of-bike-commuting-around-the-world-5bada94585c5

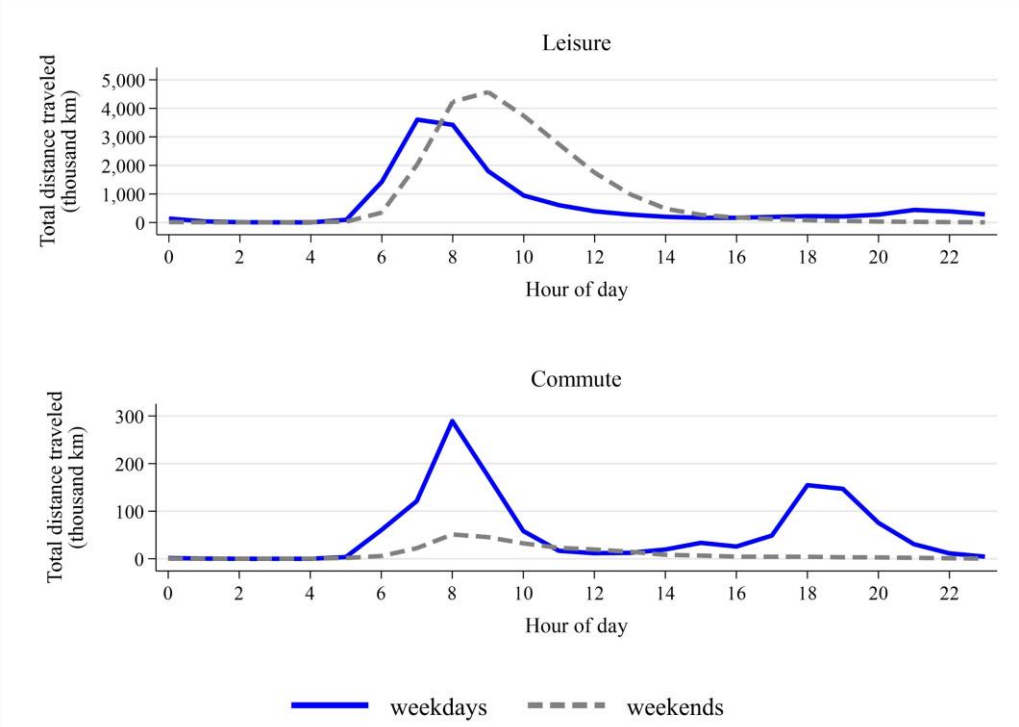

Figure 3.2. Total distance traveled per hour by Strava cyclists in Mexico City (Jan 2019 – Mar 2023). Source: Prepared considering all bicycle trips tracked and publicly shared in Strava with data from Strava Metro.

As an alternative data source, we calculate the total distance traveled per hour by users of Ecobici, Mexico City's bike-sharing system[14]. Ecobici allows its users to arrange unlimited trips between stations with a duration of no more than 45 minutes from 05:00 to 00:30 hours. In August 2022, the Ecobici system had 480 stations located in the municipalities of Benito Juárez, Cuauhtémoc, and Miguel Hidalgo[15]. From that month, the system entered a renewal phase that included, among other things, updating the bicycle inventory, and an expansion of the bike-sharing stations network. In 1 year, the number of stations increased to 503 with 4,800 bicycles available, reaching nearly sixty thousand users with an annual subscription[16,17]. The current rate scheme ranges from $188 MXN pesos for a 1-day pass (about $11 US dollars) to $521 MXN pesos per annual subscription (about $29 US dollars), allowing its users to subscribe for 1, 3, 7 or 365 days.

[14] Monthly Ecobici datasets are open and can be downloaded at https://ecobici.cdmx.gob.mx/datos-abiertos/

[15] The exact location of bike-sharing stations can be found at https://datos.cdmx.gob.mx/dataset/ubicacion-de-estaciones-de-ecobici-sistema-anterior

[16] "ECOBICI llega a 3.8 millones de viajes en la Ciudad de México", *Government of Mexico City*, Jun, 5, 2023. Available at https://gobierno.cdmx.gob.mx/noticias/ecobici-llega-a-3-8-millones-de-viajes-en-la-ciudad-de-mexico/

[17] "Se cumple el primer año de la transformación ECOBICI", *Ecobici*, Aug 13, 2023. Available at https://ecobici.cdmx.gob.mx/se-cumple-el-primer-ano-de-la-transformacion-ecobici/

To obtain the total distance traveled in Ecobici, we multiply the hourly trip count for each pair of origin-destination stations by the travel distance on the shortest cycling route between them. Travel distance was estimated from the linear distance between the origin and destination station. That is, we took a random sample of 1,800 origin-destination Ecobici station pairs, estimating the relationship between the distance traveled on the shortest route by bicycle (obtained using Google Maps) and the linear distance between them[18].

Our decision to use travel distances, instead of counts, is twofold. First, travel distance captures both frequency and intensity. This is important as cyclists can avoid pollution exposure either by completely abstaining from cycling, or by simply reducing exposure time, taking shorter trips. In fact, according to Liang et al. (2023) and (Zhao et al., 2018), cyclists who continue riding during highly polluted days are more likely those that take shorter trips. Second, we opted to use distances instead of counts so we could compare our Strava and Ecobici data. Nonetheless, it is important to keep in mind that Ecobici has about five times more users than Strava.

About 80% of Ecobici trips are made for commuting purposes (Government of Mexico City, 2020a). This explains the similarity between the cycling activity in Ecobici and the commuting trips by Strava cyclists during weekdays. During these days, when commuting trips predominate, the distance traveled by Ecobici users is greater than on Strava. However, this reverses during weekends when leisure trips increase (see Figures 3.2 and 3.3).

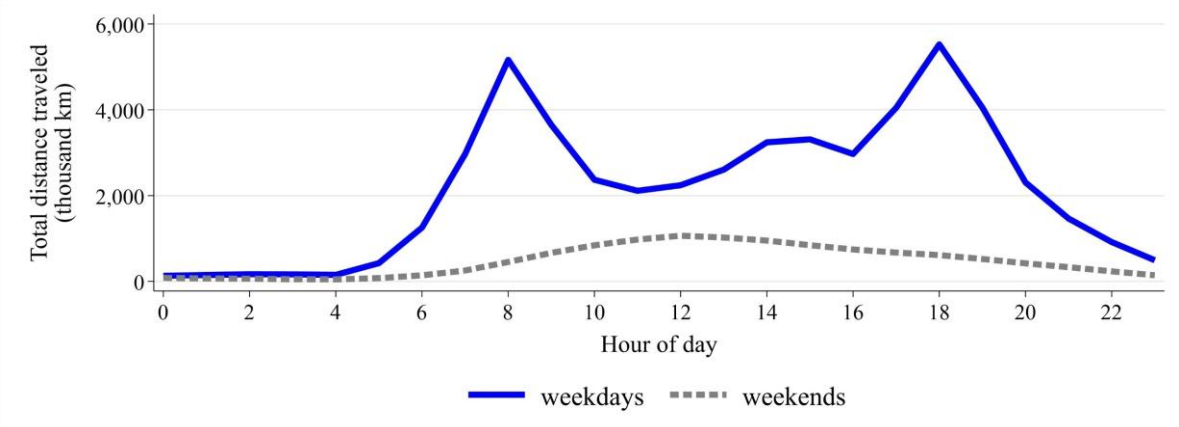

Figure 3.3. Total distance traveled per hour by Ecobici users in Mexico City (Jan 2019 – Mar 2023). Source: Prepared using data from Ecobici.

Ecobici users ride on bike lanes. They prefer this mode of transportation mainly for convenience or time saving motives, rather than for altruistic reasons that represent a broader

[18] The fitted regression line is given by $TravelDistance = 0.257 + 1.2247 \times LinearDistance$, with $R^2 = 0.9664$. Figure A3.2 from the Appendix shows a scatter plot between the travel and linear distances of the 1,800 Ecobici station pairs considered. When origin and destination stations are the same for a given trip, we calculate the distance traveled using its duration and the average speed of Ecobici trips.

benefit for the society (such as concerns for the environment). About 41% of Ecobici users report having their own car, and only 21% use their own bicycle as a means of transportation (Government of Mexico City, 2020a).

Most cycling activity in Mexico City takes place between 5:00 and 22:00 hours (see Figures 3.2 and 3.3). Therefore, we limit our analysis to trips made in these hours. This criterion is consistent with previous articles. For example, de Buen Kalman (2021) only considers the hours when the Ecobici system is in operation, while Liang et al. (2023) limit their analysis to daytime, from 07:00 to 19:00 hours.

Further, we disaggregate the distance traveled per hour by municipality. In Strava, the municipality represents the place where the cycling activity took place, while in Ecobici, it corresponds to the municipality where the trip began. This disaggregation is relevant because cycling infrastructure changes considerably depending on the municipality (see Figure 3.4). For instance, little more than half of cycle paths are concentrated in municipalities close to the city center (Cuauhtémoc, Benito Juárez and Miguel Hidalgo). Moreover, as shown in Table 3.4, it is precisely in these municipalities where most cycling activity can be observed throughout the day in Mexico City.

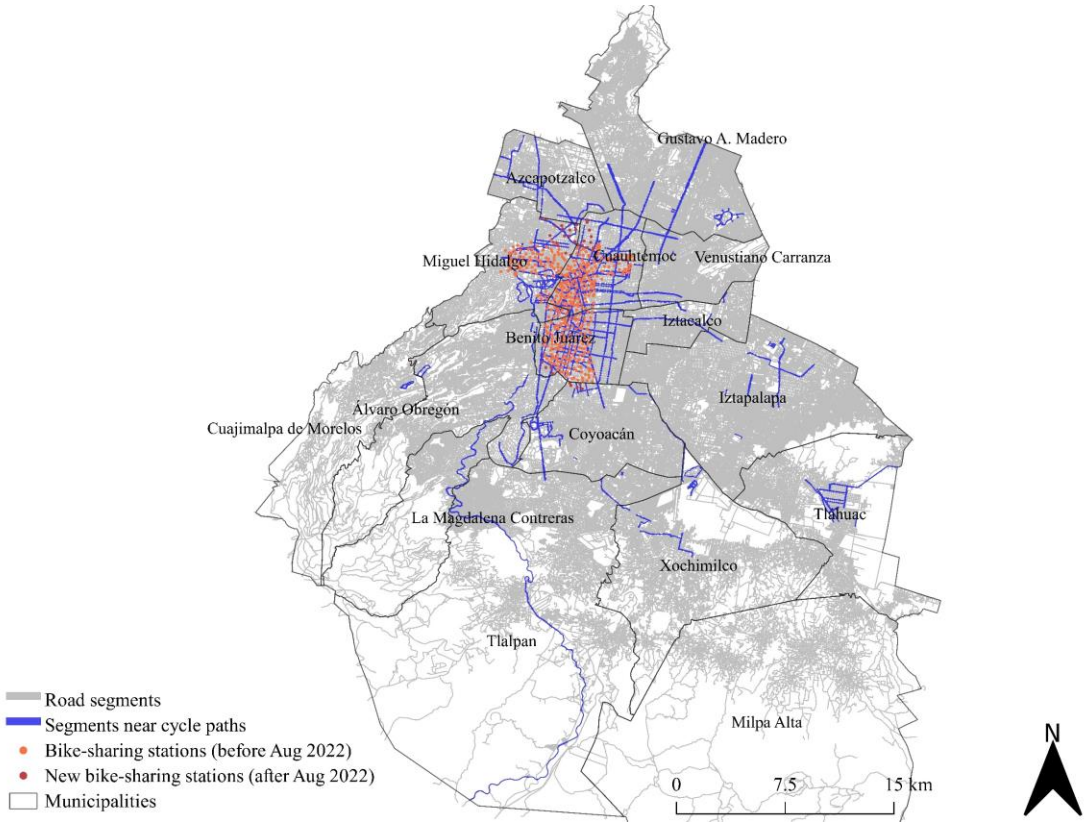

Figure 3.4. Location of cycling infrastructure in Mexico City. Note: Ecobici stations updated as of July 6, 2023. Source: Prepared using data from Strava and Mexico City Ministry of Transport.

In summary, separating our data by municipality and trip purpose as shown in Table 3.4, we can identify three different profiles of cyclists in Mexico City. First, the numerous Ecobici users, who frequently make commuting short trips of around 2.5 km during weekdays, starting and ending their trips at different stations, using the available cycling infrastructure. Next, with a similar profile but in smaller numbers, are Strava users who publicly share their commuting activities. These cyclists use their own bike—or a shared bicycle from the Ecobici system—to make short weekdays trips of roughly 2.1 km during peak hours. Akin to Ecobici users, most of them ride on cycle paths in municipalities near to the city center.

Table 3.4. Mean distance traveled per hour in the municipalities of Mexico City (km)

	Strava				Ecobici	
	Leisure		Commute		Trips started during	
Municipality	All segments	Near cycle paths	All segments	Near cycle paths	Weekends	Weekdays
Center						
Benito Juárez	79	62	14	12	330	592
Cuauhtémoc	108	82	16	14	823	1,447
Iztacalco	53	3	1	0	-	-
Venustiano Carranza	13	3	1	1	-	-
Northeast						
Gustavo A. Madero	22	8	1	1	-	-
Northwest						
Azcapotzalco	5	2	1	0	-	-
Miguel Hidalgo	264	98	9	5	257	600
Southeast						
Iztapalapa	17	0	2	0	-	-
Milpa Alta	27	-	0	-	-	-
Tláhuac	3	1	0	0	-	-
Xochimilco	28	2	1	0	-	-
Southwest						
Álvaro Obregón	89	33	3	2	-	-
Coyoacán	248	42	5	2	3	3
Cuajimalpa	278	1	2	0	-	-
La Magdalena C.	34	3	0	0	-	-
Tlalpan	101	9	2	0	-	-
All	86	23	4	3	447	836
Activity count (2019 - Mar 2023)	1,796,291		1,202,078		10,594,830	49,702,434
Km per activity	25.2		2.1		2.5	2.5

Notes: This table considers cycling activities from 5:00 to 22:00 hrs. Segments near cycle paths include those located closer than twenty-five meters from any of the 565.5 km of bicycle road infrastructure in Mexico City. Figures presented with rounding to the nearest integer. Source: Prepared using data from Strava Metro and

Ecobici. A shapefile with the location and characteristics of the bicycle road infrastructure in Mexico City updated as of July, 2023 is available at https://datos.cdmx.gob.mx/dataset/infraestructura-vial-ciclista

Finally, there are Strava cyclists who go outdoors to exercise, or ride for recreational purposes. These cyclists take longer trips of around 25.2 km, more frequently on weekends. They tend to use different routes in municipalities that do not necessarily have cycling infrastructure. Unlike commuting trips, only 30% of leisure trips are conducted near cycle paths.

3.5.2. Environmental emergencies and temporary driving restrictions

As we explained in Section 3.3, environmental emergencies and temporary driving restrictions are closely linked in Mexico City. For this reason, de Buen Kalman (2021) considered them as simultaneous or identical events. However, it is important to disentangle the separate impact of environmental emergencies from the temporary driving restrictions given that both measures could be in conflict for some cyclists. This will allow us to determine whether avoidance behavior or transport mode substitution predominates among cyclists in the city.

We take advantage of the fact that starting from May 29, 2019, the PCAA clearly states in its guidelines that temporary driving restrictions are applied the day after the activation of city-wide environmental emergencies from 5:00 a.m. to 10:00 p.m. (Government of Mexico City, 2019b)[19]. These restrictions are lifted the same day when environmental emergencies are suspended at 10:00 p.m. Hence, even if driving restrictions are applied for most hours during an emergency, as considered by de Buen Kalman (2021), there are also hours in which only one of the events is active, either the emergency or the temporary driving restriction. For example, the last city-wide environmental emergency for ozone we considered was activated on March 25, 2023, at 4:00 p.m., and was suspended on March 27 at 6:00 p.m. Meanwhile, additional temporary driving restrictions were applied on March 26 and 27 from 5:00 a.m. to 10:00 p.m.

In contrast to de Buen Kalman (2021), our work also considers that temporary driving restrictions are not implemented when emergencies are declared regionally. Furthermore, we conduct an analysis at the municipal level—instead of an aggregated analysis for the entire Mexico City—recognizing that precautionary recommendations for cyclist issued by the authority during regional emergencies only apply to the municipalities where the activation limit is reached. Moreover, precautionary recommendations for cyclists during city-wide ozone emergencies only apply from 13:00 to 19:00 hrs., when ozone concentrations are

[19] Nonetheless, this was already the way in which driving restrictions were applied in practice before the last update of the PCAA. This can be confirmed in the press releases issued by CAMe, available at https://www.gob.mx/comisionambiental/archivo/prensa?idiom=en

higher. In the case of regional emergencies for particles, these recommendations extend for all hours during the environmental emergency.

In Figure 3.5, we present a diagram that details the relationship between pre-emergencies, emergencies, and temporary driving restrictions that occurred during the hours we analyzed in this study. CAMe recommended cyclists to avoid riding during 200 out of the 26,367 hours that we studied from January 2019 to March 2023. For their part, non-exempt private vehicles were subject to temporary driving restrictions for 1.3% of the hours (341 hours).

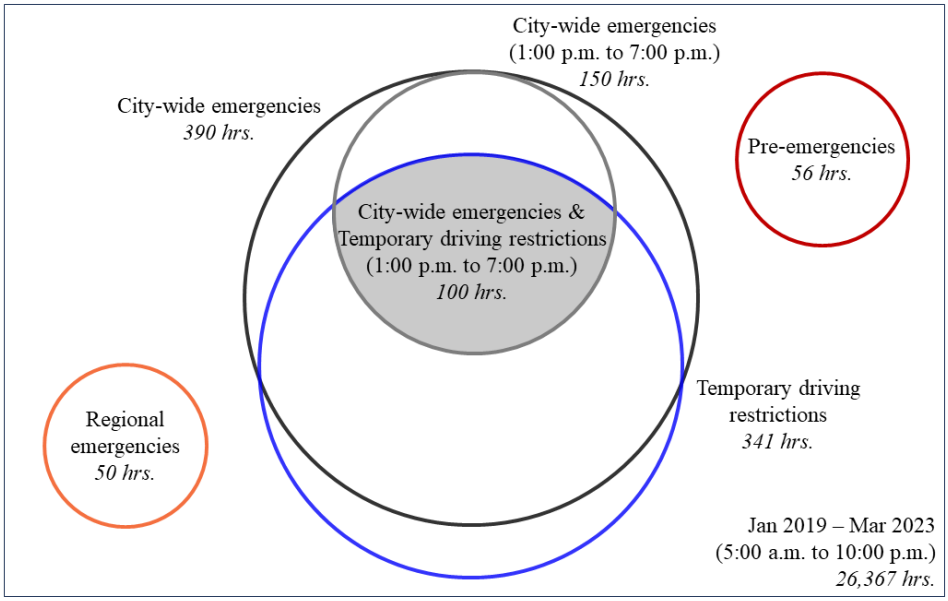

Figure 3.5. Relationship between pre-emergencies, emergencies, and temporary driving restrictions in Mexico City. Source: Prepared with information from Government of Mexico City (2019b, 2023a).

Following de Buen Kalman (2021) and Rivera (2021), we consider the issuance of precautionary recommendations and the enforcement of temporary driving restrictions as exogenous events, out of the control of Strava and Ecobici users. Cyclists cannot anticipate, modify nor prevent their issuance because both the AQI levels at which environmental emergencies are activated, as well as the schedules subject to both measures were arbitrarily established by the authority in the PCAA guidelines. Moreover, regular drivers cannot predict if during a particular hour in the future their vehicles will be subject to temporary driving restrictions because the selection is made conditional on the issuance of an environmental emergency along with their verification hologram and the last digit of their license plates.

As expected, the purpose of trips made by bicycle seems to be fundamental for understanding the behavioral responses of cyclists during environmental emergencies (see Table 3.5). While the hourly average distance traveled for recreational purposes in the municipalities of Mexico City decreases during environmental emergencies, commuting cycling activity on Strava increases. Similarly, consistent with the results of de Buen Kalman

(2021), the cycling activity of Ecobici users increases during environmental emergencies. Mean differences, although illustrative, do not allow us to attribute these changes to the different measures applied during environmental emergencies. Later, in Section 3.6 we propose an empirical strategy that will allow us to distinguish the effects of precautionary recommendations and temporary driving restrictions on cycling activity depending on trip purpose.

Table 3.5. Hourly mean for variables in the municipalities of Mexico City

	During emergencies?			During emergencies?	
	No	Yes		No	Yes
Cycling activity (km)					
Strava – Leisure	85.36	74.10	Ecobici – Weekends	444.50	666.43
	(0.47)	(3.14)		(2.94)	(45.77)
Strava – Commute	3.62	5.21	Ecobici – Weekdays	832.05	1,049.25
	(0.02)	(0.20)		(3.49)	(29.36)
Air Quality Index (AQI)					
Regional	71.19	103.96	PM_{10}	54.32	85.35
	(0.03)	(0.28)		(0.04)	(0.24)
O_3	35.94	65.03	$PM_{2.5}$	64.24	89.89
	(0.05)	(0.55)		(0.02)	(0.25)
Weather					
Temperature (°C)	18.45	21.65	Wind speed (m/s)	3.53	3.78
	(0.01)	(0.06)		(0.00)	(0.03)
Relative humidity (%)	47.10	35.26	Rain (mm)	1.51	0.36
	(0.03)	(0.21)		(0.01)	(0.02)
Thermal inversions					
Frequency (%)	8.56	12.07	Thickness (m)	248.23	157.19
	(0.04)	(0.41)		(1.10)	(7.62)
Intensity (°C)	1.12	0.71			
	(0.00)	(0.02)			

Notes: City-wide and regional emergencies are considered. Emergencies contemplate the period between the activation and suspension declared by CAMe. Standard errors are in parenthesis. Figures presented with rounding to two decimal places.

3.5.3. Air quality and weather

Cyclists' decision to go out and travel by bicycle, whether for commuting or leisure, is influenced by external factors such as air quality and climate conditions (de Buen Kalman, 2021; Liang et al., 2023; Saberian et al., 2017; Zhao et al., 2018). Therefore, it is essential to make comparisons under equivalent climatic and air quality conditions. In this subsection we describe the external factors that we consider for our analysis.

During our study period, an Air Quality Index (AQI)—previously known as the Metropolitan Air Quality Index (IMECA)—was reported by Mexico City Ministry of Environment (SEDEMA) to continuously communicate inhabitants about the air quality

conditions in Mexico City. The AQI expressed the concentrations of criterion pollutants as a function of the maximum permissible values defined by Mexican environmental health standards, which were normalized to represent an AQI equal to 100. To ease the communication process, the index is segmented into six categories. Each category is assigned a specific color, along with a level of health risk and a series of precautionary actions recommended for the most vulnerable population (Government of Mexico City, 2018)[20]. The AQI has a certain relationship with the PCAA, given that activation levels for environmental emergencies coincide exactly with the transition from a "bad" to the "very bad" AQI category.

The AQI is reported hourly for every one of the monitoring stations that integrate the Atmospheric Monitoring System of Mexico City and each of the criterion pollutants: ozone (O_3), nitrogen dioxide (NO_2), sulfur dioxide (SO_2), carbon monoxide (CO), and particulates ($PM_{2.5}$ and PM_{10}). SEDEMA also publishes the maximum regional AQI for each pollutant.

Given that some states in Mexico did not have a communication tool such as the AQI in Mexico City and/or they informed the population about air quality according to their own discretionary criteria, the Ministry of the Environment and Natural Resources (SEMARNAT) design a similar index than the AQI, homologated for the whole country. As of February 20, 2020, all entities and municipalities in Mexico have now the obligation to calculate and disseminate this latter index, denominated *Índice Aire y Salud* (hereafter, Air and Health Index)[21]. SEDEMA complied with this new regulation but decided to continue disseminating the AQI simultaneously during our study period. This decision was intended to allow the population to become familiar with the new index because they were already very familiar with the AQI (CAMe, 2020). According to Borbet et al. (2018), about 61% of the inhabitants of Mexico City had already heard or read about the AQI for their regions.

For this reason, we chose to use the AQI as the indicator of air quality that cyclists regularly consulted in Mexico City during our study period. Specifically, we consider the

[20] According to Government of Mexico City (2018), the 6 categories considered by the AQI are: Good (low health risk, AQI: 00-50); Regular (moderate health risk, AQI: 51-100); Bad (high health risk, AQI: 101-150); Vey bad (very high health risk, AQI: 151-200); Extremely bad (extremely high health risk, AQI: 201-300); and Dangerous (health hazard for all the population, AQI: 301-500).

[21] The Air and Health Index has similarities with the AQI. It is also a tool to ease the communication about health risks associated with the air quality conditions at a given time and place that is accompanied with a series of precautionary recommendations for the population at risk (SEMARNAT, 2019). However, according to (CAMe, 2020) it also differs on relevant issues: (i) It is not expressed on a unitless scale relative to the maximum permissible values defined by Mexican environmental health standards, but in the units of concentrations for each pollutant; (ii) It uses a different categorization and is timelier warning about high concentrations of particulates; (iii) It distinguishes its precautionary recommendations for the most vulnerable population and the population in general; and (iv) It is independent of the PCAA, since none of its defined thresholds between categories coincide with the activation level of environmental emergencies.

hourly regional AQI. To do this, we assign each municipality the highest hourly AQI score among the different pollutants in the region where the cycling activity took place.

In the case of climate factors, we assign hourly values of temperature, relative humidity and wind speed to each municipality based on the records of 13 stations that are part of the Atmospheric Monitoring System of Mexico City. To do this, we employ an inverse distance weighted average, considering the linear distances between the monitoring stations and the centroid of each municipality. Each of the thirteen monitoring stations we considered reported more than 70% of the available hours in our study period. Meanwhile, we assigned each municipality the average daily rainfall measured in millimeters from the records of sixty-two hydrometric stations administered by the National Water Commission (CONAGUA), according to the municipality where these stations were located.

As shown in Table 3.5, air quality worsens substantially during environmental emergencies, primarily due to high ozone concentrations. This worsening of air quality is well captured by the regional AQI we consider in our analysis. Furthermore, during environmental emergencies the temperature is higher, there is less rain and less humidity.

3.5.4. Thermal inversions

Including the AQI to control for air quality conditions is essential to identify the response of cyclists to the recommendations and restrictions imposed by the authority during environmental emergencies. However, the AQI is potentially endogenous due to its simultaneity with cycling activity (Liang et al., 2023; Saberian et al., 2017). Cyclists can avoid pollution either by postponing or canceling their outdoor activities, or by switching to other modes of transportation that reduce their exposure. As argued by Saberian et al. (2017) and Noonan (2014), this change can be towards more polluting means of transport such as the automobile, generating a simultaneity between both variables.

Moreover, our measure of air quality may contain measurement errors either from its calculation and reporting at the monitoring stations or introduced unintentionally when we aggregated the index regionally or attributed it to each municipality. For this reason, previous authors have chosen to instrument air quality to solve the potential problem of endogeneity, measurement error and the possible omission of relevant non-observable factors that change over time (Arceo et al., 2016; Liang et al., 2023; Saberian et al., 2017).

Following Arceo et al. (2016) and Liang et al. (2023), we use thermal inversions as an instrumental variable for air quality. During the season from October to May, when the temperature, humidity and rainfall are lower in Mexico City, thermal inversions cause the air layers closest to the surface to be colder. As explained by Ezcurra (2009), the above prevents the vertical movement of the air layers, making it difficult for pollutants to disperse in the atmosphere. In the words of Liang et al. (2023), thermal inversions function as a natural “plug” that traps contaminants near the surface.

In response to a request for public information, SEDEMA provided us with a daily record with the characteristics of the thermal inversions registered on the surface of Mexico City during our study period. Unlike Arceo et al. (2016) and Liang et al. (2023) who consider the weekly and daily frequency of thermal inversions, we distinguish the hours of the day in which a thermal inversion occurred. That is, we identify the hours prior to the "breakup" of the inversion, when pollutants were prevented to disperse appropriately.

Furthermore, as Liang et al. (2023), we contemplate the intensity of thermal inversions, which according to García-Guadalupe et al. (2012) corresponds to the temperature differential between the base and top of the inversion layer. Following Arceo et al. (2016), we also include the thickness of the inversion layer measured in meters. As shown in Table 3.5, thermal inversions occurred more frequently during the hours in which environmental emergencies were active, although they registered a lower average intensity and thickness.

Thermal inversions meet the three essential requirements of a valid instrument described by Angrist and Pischke (2014). First, thermal inversions have a positive causal effect on the Air Quality Index (AQI). As seen in Figure 3.6, during the hours with thermal inversions the AQI mean is 5.36 points higher in the municipalities of Mexico City. This represents a statistically significant increase of 7.3%. Moreover, the marginal effect of thermal inversions on the AQI does not change substantially when we add additional controls (see Table A3.3 from the Appendix).

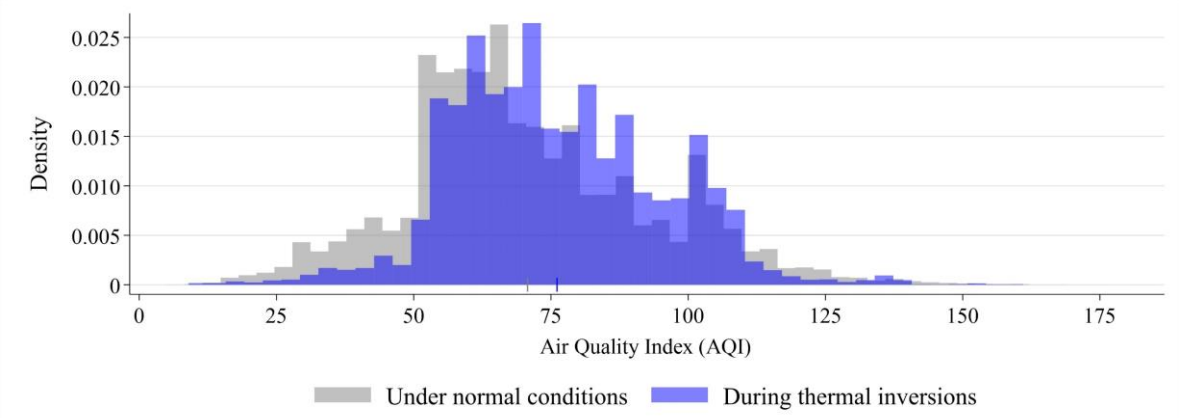

Figure 3.6. Histogram of the hourly Air Quality Index (AQI) in the municipalities of Mexico City. Notes: We considered records from 5:00 a.m. to 10:00 p.m. from Jan 2019 to Mar 2023. Source: Prepared with data from Mexico City Ministry of Environment (SEDEMA).

The above suggests compliance with the second requirement for a valid instrument. Thermal inversions occurred in the hours of the analyzed period as if they would have been assigned randomly. That is, the occurrence of a thermal inversion is independent of any omitted factor that could be relevant to determine either cycling activity or air quality conditions in Mexico City. Finally, thermal inversions affect cycling activity only through their causal effect on air quality. As argued by Arceo et al. (2016), thermal inversions do not

generate a risk to the health of the population by themselves, but in the presence of high concentrations of pollutants that cannot be dispersed with normality in the atmosphere.

3.5.5. Other relevant controls

To avoid the omitted variable bias, we control for several factors that may influence the cycling activity in Mexico City and are correlated with its other determinants, such as with the air quality conditions.

First, we control for festivities that are usually celebrated using fireworks. Cycling activity changes during these days because individuals plan and assist to festivities instead of their regular jobs and/or studies. In addition, the concentrations of pollutants increase due to fireworks (Retama et al., 2019). As shown in Figure A3.4 from the Appendix, in Mexico City this occurs every year during the celebration of Mexico's Independence Day (early morning of September 16), the feast of the *Virgen de Guadalupe* (December 12), Christmas and New Year (early mornings of December 25 and January 1). Following Caplan (2023), we construct an indicator variable that takes the value of 1 in a 3-day window around these festivities (i.e., it includes the day before and after the event).

Next, we control for the policy changes that were implemented as of March 2020 in response to the COVID-19 health emergency. In Mexico, strict confinement measures were established from March 23 to May 30, 2020. This strategy was denominated *Jornada Nacional de Sana Distancia* (JNSD). These measures included the suspension of non-essential activities, classes, and mass events, together with a series of precautionary recommendations to reduce the risk of contagion, applicable mainly for elders[22]. Additionally, as we explain in Section 3.3, the Government of Mexico City applied extraordinary driving restrictions, extending the application of HNC to more private vehicles during the weekdays from April 23 to June 15, 2020. We include both measures using two binary variables that take the value of 1 during the hours in which either the JNSD or the extraordinary HNC for COVID-19 were in effect.

As of June 1, 2020, the JNSD was replaced by an epidemiological risk semaphore that assigned a color (green, yellow, orange, and red) to each state in Mexico according to its risk of COVID-19 contagion. The colors were associated with increasingly restrictive measures on mobility[23]. The epidemiological risk semaphore was disseminated weekly for almost 2 years, until May 1, 2022. In our analysis we consider the daily color of the semaphore for Mexico City. Specifically, we included three binary variables that indicate whether the

[22] The main recommendations and measures contemplated by the JNSD are described in https://www.gob.mx/cms/uploads/attachment/file/541687/Jornada_Nacional_de_Sana_Distancia.pdf

[23] The methodology for estimating the epidemic risk for each state, along with its subsequent classification into one of the four semaphore colors can be consulted at https://coronavirus.gob.mx/semaforo/

semaphore was yellow, orange, or red, respectively. In addition, we added as a control variable the number of confirmed cases of COVID-19 in Mexico City.

Additionally, we control the effects of the expansion and renewal of the Ecobici bike sharing system by including an indicator variable that takes the value of 1 as of August 2022. The inclusion of this variable is relevant because a supply shift of bike sharing stations (and shared bicycles) could have affected Ecobici's own cycling activity, as well as the number of activities recorded on Strava. This is because Strava records can include cycling activities conducted on privately own and shared bicycles.

Finally, we consider the non-working days contemplated by educational institutions of basic education, and the *Universidad Nacional Autónoma de México* (UNAM), the largest public university in Mexico located in Mexico City. We obtained this information from the official calendars of both institutions. These control variables also consider the extraordinary suspension of classes conducted on May 16 and 17, 2019 due to the high concentrations of ozone and particles. Similarly, we control for official mandatory non-working days according to the Labor Law.

3.6. Empirical strategy

Our purpose is to evaluate the effectiveness of the precautionary recommendations issued by the authority to cyclists during environmental emergencies in Mexico City, as well as the effect of the associated temporary driving restrictions on cycling activity distinguishing between commuting and leisure trips. To do this, we employ an identification strategy based on Liang et al. (2023) and Saberian et al. (2017).

We estimate the following fixed effects panel model for the municipalities of Mexico City during the period from January 2019 to March 2023 and between 05:00 and 22:00 hrs.,

$$Cycling_{it} = \beta_1 PreEmergency_{it} + \beta_2 Emergency_{it} + \beta_3 DrivingRestriction_t + \gamma_1 AQI_{it} + \boldsymbol{W}_{it}\delta + \boldsymbol{X}_{it}\theta + \alpha_i + \tau_t + \epsilon_{it} \quad (5)$$

where $Cycling_{it}$ is the total kilometers traveled by bicycle in municipality i at hour t, distinguishing the cycling activity by the purpose of the trips—leisure or commuting—if these were recorded and shared publicly on Strava, or, by the day of the week of the trips—weekends or weekdays—if these were made in Ecobici.

Our main explanatory variables are $Emergency_{it}$ and $DrivingRestriction_t$. $Emergency_{it}$ is an indicator variable that takes the value of 1 if the authority recommended cyclists to avoid riding outdoors in municipality i at hour t. As explained in Subsection 3.5.2, these precautionary recommendations were in effect throughout the city from 13:00 to 19:00 hrs. during ozone environmental emergencies, and throughout the day in the municipalities where particulates regional emergencies were declared. On the other hand, $DrivingRestriction_t$ is an indicator variable that takes the value of 1 during the hours in

which a substantial share of private vehicles (34.4% after May 29, 2019) was temporarily restricted from circulating on the roads of Mexico City. As detailed in Subsection 3.5.2, temporary driving restrictions start being applied the day following the activation of an ozone environmental emergency from 5:00 to 22:00 hrs. They are suspended on the same day that the ozone environmental emergencies at 22:00 hrs.

We want to compare the frequency and intensity of cycling activity in each municipality and hour of the day in the presence and absence of precautionary recommendations for cyclists or temporary driving restrictions, keeping other things equal. Therefore, we include a set of relevant control variables that we explain below.

First, we include $PreEmergency_{it}$ and AQI_{it} controls. $PreEmergency_{it}$ takes the value of 1 if the authority recommended cyclists to avoid exposure to pollution in municipality i at hour t during the preventive phase of environmental emergencies, and 0 otherwise. As explained in Section 3.3, pre-emergencies are less frequent and long-lasting than emergencies, and in the case of Mexico City, they have been activated with a certain degree of arbitrariness. For its part, AQI_{it} is the hourly regional AQI corresponding to municipality i.

Second, we consider a vector of climate controls $\boldsymbol{W}_{it}$ that includes temperature, relative humidity, wind speed and precipitation recorded in municipality i at hour t. Additionally, we consider $\boldsymbol{X}_{it}$, a vector of relevant control variables that are described in detail in Subsection 3.5.5. These variables control for factors such as the expansion of the Ecobici bike sharing system starting in August 2022, as well as the mobility restrictions that were imposed in response to the COVID-19 health emergency in Mexico City. They also control the days off from work and school, as well as the annual festivities that are celebrated using fireworks.

Finally, we include a series of unit and time fixed effects. Unit fixed effects α_i control for the characteristics of each municipality that remained unchanged during the period from January 2019 to March 2023. Time fixed effects τ_t control for changes in cycling activity that were recorded in a given hour and day of the week or in a specific month and year across all municipalities in Mexico City.

As we detailed in Subsection 3.5.4, $Cycling_{it}$ is determined simultaneously along with the air quality conditions, measured by the AQI_{it}. Following Saberian et al. (2017), the simultaneity between our dependent variable and the Air Quality Index (AQI) together with the close relationship between the AQI level and the activation of environmental emergencies in Mexico City, would bias our estimated parameters of interest, $\hat{\beta}_2$ and $\hat{\beta}_3$.

Akin to Liang et al. (2023) and Saberian et al. (2017), we address this problem substituting AQI_{it} in equation (5) with the fitted values from a first stage where we include $ThermalInversion_t$ as an exogenous explanatory variable. That is,

$$\widehat{AQI}_{it} = \phi_1 ThermalInversion_t + \boldsymbol{W}_{it}\delta + \boldsymbol{X}_{it}\theta + \alpha_i + \tau_t \qquad (6)$$

where $ThermalInversion_t$ is a binary variable that indicates if during hour t there was a thermal inversion on the surface of Mexico City.

3.7. Results

3.7.1. Main results

We present our results in Table 3.6, expressing the estimated coefficients as a percentage of the dependent variable to facilitate their interpretation and comparison[24]. To determine the level of significance, we perform inference from cluster standard errors at the municipality level for the baseline model of equation (5) in columns 1 and 2. When we instrument the AQI using equation (6) in columns 3 to 10, we use standard errors obtained resampling by cluster, hereafter referred as cluster bootstrap (CB) standard errors[25].

In line with predictions of the theoretical model that we present in Section 3.4, cyclists in Mexico City respond to precautionary recommendations issued by the authority, avoiding exposure to pollution during environmental emergencies. Consistent with the conclusions of Liang et al. (2023) and Saberian et al. (2017), leisure cyclists are more likely to respond with avoidance behavior. As shown in column 3 of Table 3.6, Strava cyclists who ride for recreational purposes reduce their activities by 24% while those who take commuting trips do so by 19.9%.

These figures are within the range of response to environmental alerts reported by Saberian et al. (2017) for cyclists in Sydney, Australia. However, we find that the difference in the response of cyclists according to the purpose of their trips is much smaller than that suggested by Saberian et al. (2017) and Liang et al. (2023). These authors reported a response 2 to 3 times higher for trips made outside of peak hours, plausibly for discretionary purposes. It is necessary to remember that, unlike previous studies, Strava data gives us the advantage of distinguishing more precisely the purpose of each trip.

Table 3.6. Percentage change of cycling activity caused by environmental emergencies and temporary driving restrictions

	Main results			Robustness checks						
	(1)	(2)	(3)	(4)	(5)	(6)	(7)	(8)	(9)	(10)
Strava – Leisure										
Emergency	-9.0**	-19.5***	-24.0***	-16.5***	-25.6***	-27.5***	-24.3***	-25.2***	-	-
Temp. driving restriction	-6.4	-3.8	-5.8	-6.3*	-3.0	-5.4	-5.4	-4.0	-	-
Strava – Commute										

[24] The original estimated coefficients—expressed in kilometers—together with estimation details, including standard errors, number of observations, and the goodness-of-fit of model, are presented in Table A3.5 from the Appendix.

[25] As shown in Table A3.6 from the Appendix, the significance levels of our estimates have minimum changes if we use instead the wild cluster bootstrap (WCB) method to perform inference, considering that our number of clusters is small (MacKinnon et al., 2023).

Emergency	-15.7*	-17.7	-19.9**	-16.8**	-18.4**	-16.3**	-20.8**	-18.1	-	-
Temp. driving restriction	10.5**	12.9**	11.0**	10.9**	8.3**	10.5**	11.7**	8.0	-	-
Ecobici – Weekends										
Emergency	13.7	15.1	13.9	14.3	14.2	22.7	14.2	-	16.7	-4.3
Temp. driving restriction	-1.1	0.6	0.4	-1.4	-0.1	1.4	0.1	-	1.1	-4.2
Ecobici – Weekdays										
Emergency	0.5	-4.6***	-5.3***	-5.1***	-6.8***	6.2**	-4.9***	-	-5.1***	-9.1***
Temp. driving restriction	-4.5*	0.9	0.8	0.6	3.1***	-0.6	0.7	-	0.5	5.3
After May 29, 2019		✓	✓	✓	✓	✓	✓	✓	✓	✓
Instrumenting AQI			✓	✓	✓	✓	✓	✓	✓	✓
Robustness checks:										
Excludes 2020				✓						
Shorter driving restrictions					✓					
Non-linear temperature						✓				
Additional instruments							✓			
Segments near cycle paths								✓		
One-way trips									✓	
Round trips										✓

Notes: Estimates are reported rounded to one decimal place and represent a percentage change with respect to the average of the corresponding dependent variable. Columns (1) and (2) are obtained estimating equation (5), performing inference with standard errors clustered at the municipality level. Estimates from column (3) to (10), further instrumented the hourly AQI with an indicator variable for thermal inversions, using cluster bootstrap (CB) standard errors from 400 replications for inference. The symbols ***, **, and * indicate significance at the 1%, 5%, and 10% levels, respectively.

As anticipated by the theoretical model, the distinction of the purpose of the trip is also relevant to determine the response of cyclists to the temporary driving restrictions that are imposed starting the day after the activation of environmental emergencies. While Strava commuter cyclists respond to the restrictions by increasing their activity by 11%, leisure cyclists do not show significant changes in their activity (see column 3 of Table 3.6). This last result is consistent with the 12-16% increase in the number of Ecobici users for peak hours that de Buen Kalman (2021) attributes to temporary driving restrictions enforced on the period between 2016 and mid-2019.

Taken together, the behavioral response of cyclists to both measures according to their trips purposes explains the general reduction in cycling activity for leisure cyclists, and the corresponding increase in the case of commuting activities that are observed in Table 3.5. It is necessary to remember that temporary driving restrictions were applied in slightly more than twice as many hours as the precautionary recommendations issued by CAMe (see Figure 3.5). Therefore, the effect of the substitution of the mode of transport caused by temporary driving restrictions predominates in the case of cyclists who travel for commuting purposes.

The results presented so far are based on what happened after the last update of the PCAA (still in force), on May 29, 2019. When we only consider this period, the response of cyclists to the precautionary recommendations and driving restrictions imposed by the authority increases in absolute value (see columns 1 and 2 of Table 3.6). In the case of temporary driving restrictions, this change is not surprising as the latest update of the PCAA is more rigorous, temporarily restricting 13.8% more private vehicles, particularly less polluting vehicles with verification holograms "0" and "00" (see Table 3.2). Therefore, our work is also distinguished from that of de Buen Kalman (2021)—whose analysis extends only until June 30, 2019—focusing on a period with more stringent driving restrictions triggered by environmental emergencies.

The greater propensity of cyclist to respond to environmental emergencies with pollution avoidance behavior after the last update of the PCAA could be explained by the occurrence of the most severe environmental emergency in recent years between May 14 and 17, 2019. This emergency combined high concentrations of ozone and particulates, causing the extraordinary suspension of classes on May 16 and 17, and generating the greatest interest in web searches for the term "Emergency" in Mexico City during our study period (see Figure 3.1). Consistent with the argument of Arceo et al. (2016) and Barwick et al. (2023), it would seem as if this event made the harmful effects of pollution more visible, reducing the cost of acquiring information, and increasing the subsequent avoidance behaviors.

Just as Strava cyclists, Ecobici users who make trips on weekdays respond to the authority's precautionary recommendations, reducing their activities in 5.3% during environmental emergencies (see column 3 of Table 3.6). This result is to be expected considering that both leisure and commuting cyclists respond to alerts in the same direction. Nonetheless, Ecobici user respond with less avoidance behavior.

Finally, in contrast to de Buen Kalman (2021), our results do not show a significant response from Ecobici users to temporary driving restrictions. In line with the predictions of the theoretical model, it is possible that this result arises from the conflict between the responses of users who conduct commuting and leisure trips on Ecobici. The above is confirmed by observing the importance of the purpose of the activity in the sign and significance of the effect of temporary driving restrictions in the case of cycling activity on Strava. We found this result even though the majority of Ecobici trips are made for weekday commuting purposes, with a similar pattern to that of weekdays commuting trips by Strava cyclists. In sum, this result supports the advantage of having a data source that allows us to distinguish the purpose of each trip accurately.

3.7.2. Robustness checks

The results we present for our preferred specification in column 3 of Table 3.6 are robust to different changes. As a first exercise, we exclude observations from 2020 to evaluate whether the controls we included to isolate the effects of the COVID-19 health emergency

are effective. Our main results retain their sign and significance; however, we estimate that Strava cyclists reduce their activity by only 17% due to the precautionary recommendations issued by the authority during environmental emergencies (see column 4 of Table 3.6).

Secondly, the guidelines established in the PCAA indicate that temporary driving restrictions must be suspended on the same day that the environmental emergency at 10:00 p.m. (Government of Mexico City, 2019b). However, the authority also considers the possibility of discretionarily suspending these measures in advance. In its press releases, CAMe generally suspends all measures at the same time than environmental emergencies, including temporary driving restrictions. In column 5 of Table 3.6 we show that our main results remain almost unchanged if we adopt this convention.

Following Liang et al. (2023) and Saberian et al. (2017), we allow for the existence of non-linear effects of temperature on cycling activity. We include the quadratic and cubic terms for the temperature variable in the estimates that we present in column 6 of Table 3.6. Our results are robust to this change.

In line with Arceo et al. (2016) and Liang et al. (2023), we show that our results hold if we consider the intensity and thickness of thermal inversions as additional instruments of the air quality conditions, measured by the AQI (see column 7 of table 3.6). That is, for this robustness check we obtain the fitted values for AQI in a first stage using equation (7) instead of equation (6),

$$\widehat{AQI}_{it} = \phi_1 ThermalInversion_t + \phi_2 (ThermalInversion_t \times Intensity_t) + \phi_3 (ThermalInversion_t \times Thickness_t) + \boldsymbol{W}_{it}\delta + \boldsymbol{X}_{it}\theta + \alpha_i + \tau_t. \quad (7)$$

As we show in Table 3.4, cyclists who conduct activities for recreational purposes use cycle paths to a lesser extent than those who make commuting trips. If we limit our study to trips made near a bike lane—akin to Saberian et al. (2017)—we observe that this distinction does not seem to be relevant for leisure cyclists, since their behavioral response to precautionary recommendations during environmental emergencies is practically the same (see column 8 of Table 3.6). In contrast, when performing this exercise for commuting cycling activity, the magnitude of the estimated coefficients remains almost unchanged, but they are no longer statistically significant. Consistent with the predictions of the theoretical model, this last result could be masking the key role of income in moderating the response of cyclists to temporary driving restrictions given that bike infrastructure is in the highest-income areas of Mexico City (see Figure 3.7).

Finally, in columns 9 and 10 of Table 3.6 we separate the Ecobici trips that start and end in a different station from those that start and end at the same point. This distinction is relevant because around 80% of Ecobici trips are made on weekdays; starting and ending in

different stations, most likely for commuting purposes[26]. Our results indicate that the main cycling activity in Ecobici is reduced by 9.1% due to the precautionary recommendations issued by CAMe during environmental emergencies.

3.7.3. Heterogeneous results by income level

In this subsection, we explore the heterogeneity of our main results considering the income level of the places where commuting cycling activity takes place. We only use Strava data, taking advantage of its greater granularity that allows us to spatially classify trips at the road segment level and distinguish their purpose.

According to the theoretical framework that we present in Section 3.4, income is the main factor moderating the response of commuters to temporary driving restrictions. In our adaptation of the model developed by Cutter and Neidell (2009), income determines whether the possibility of receiving an economic punishment is large enough to overcome the reduction in time that commuters would obtain if they violate the restrictions and drive during environmental emergencies, leveraging the lowest level of road congestion. Therefore, it is a determining factor for the effectiveness of temporary driving restrictions.

To incorporate this key factor in our analysis, we classify cycling activity on Strava according to the urban marginalization level (GMU) of the geographical area where the cycling activity was registered. We compared the behavioral response of cyclists who rode their bikes in areas with very low GMU (i.e., higher-income commuters) against the response of those who rode their bikes in other geographic areas (i.e., commuters with a lower income). It is important to remember that Strava commuters make very short trips—just 2.1 km in distance—that replace the use of public transportation and/or car. Given the similarity of their profile with Ecobici users, it is very likely that they also choose this mode of transport for convenience or time saving motives. For this reason, it is highly plausible that the trips of commuters registered in Strava take place near to where they live.

The urban marginalization level (GMU) is a multidimensional indicator that measures the degree to which the population in a particulate geographic area participates and has access to essential goods and services such as basic education, health care, decent housing, and the availability of goods associated with greater purchasing power, such as refrigerator, cell phone and internet service (CONAPO, 2021). This indicator was designed by the National Population Council (CONAPO) based on the Census of Population and Housing 2020. Figure

[26] This distinction is also relevant because our method for estimating the distance traveled on trips for each case is different. While for single trips (i.e., trips that start and end at different stations) we use the distance between stations, our estimate for the case of round trips (i.e., trips that start and end at the same stations) is based on the duration of the trip and the average speed at which we estimate Ecobici users circulate in Mexico City, which is almost 12 km/h.

3.7 shows the spatial distribution of the GMU in Mexico City. As can be seen, cycling infrastructure is concentrated in geographical areas with a lower degree of marginalization.

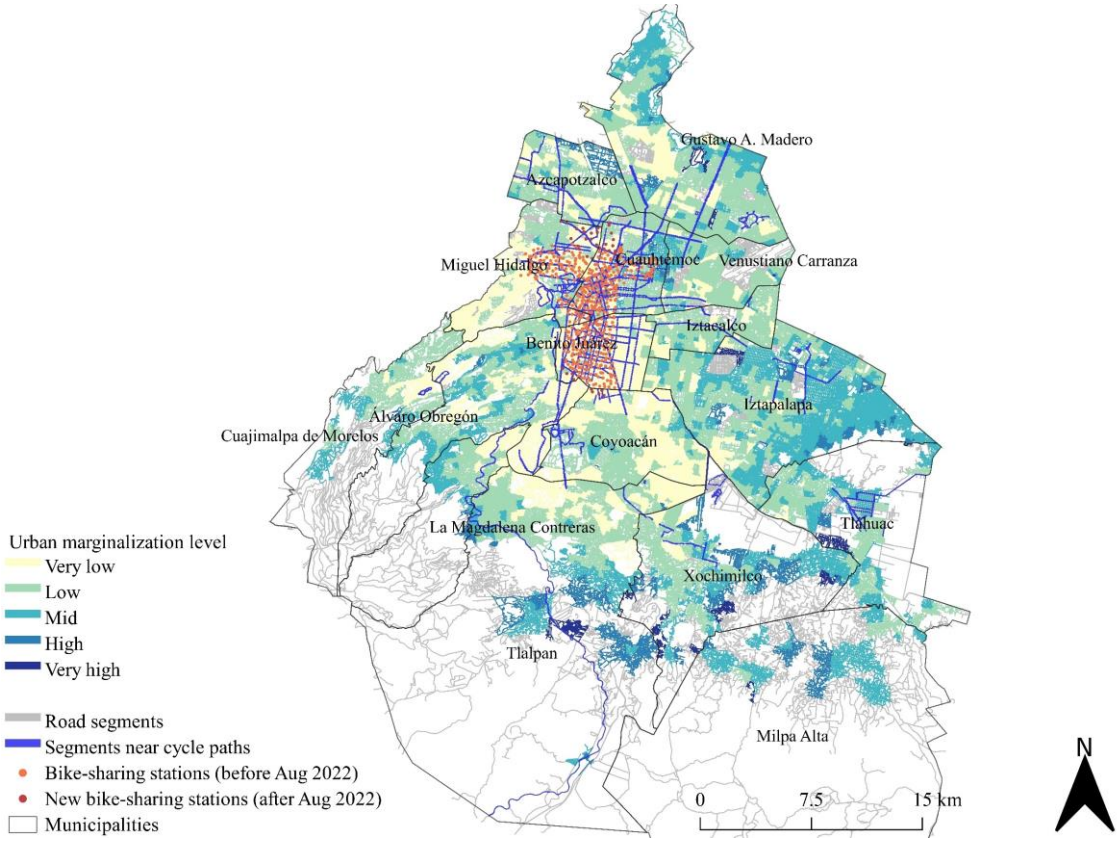

Figure 3.7. Urban marginalization level (GMU 2020) in Mexico City. Source: Prepared using data from the National Population Council (CONAPO) and Mexico City Ministry of Transport.

Consistent with the predictions of the theoretical model—and the conclusions of Gallego et al. (2013), and Guerra and Reyes (2022)—commuters with lower income receive the greatest burden of driving restrictions, resorting to a greater extent to alternative means of transportation—such as bicycles—during environmental emergencies. While lower-income commuters increase their cycling activity by 17.2%, those with higher incomes do so by only 7.2% (see Table 3.7).

Furthermore, in contrast with Zhao et al. (2018), our results for commuting cycling activity indicate that cyclists with lower incomes respond with more avoidance behavior when faced with pollution. That is, commuting cyclists with lower incomes comply to a greater extent with the precautionary recommendations issued by the authority, reducing their activity by 27.7% during environmental emergencies, while those with higher incomes reduce it—non-significantly—by 14.5%. Thus, despite their greater aversion to pollution, lower-income commuters are pushed to use their bicycles for transportation, incurring a greater health cost due to temporary driving restrictions.

Table 3.7. Percentage change of commuting cycling activity caused by environmental emergencies and temporary driving restrictions according to the income level in the geographic area where it was recorded

	Urban marginalization		Social gap level		Share of HH with vehicles		Vehicles per 1,000 people	
	Higher (Other)	Lower (Very low)	Higher (Other)	Lower (Very low)	Lower (< 51%)	Higher (≥ 51%)	Lower (< 185)	Higher (≥ 185)
Emergency	-27.7***	-14.5	-34.0***	-17.4	-30.2**	-16.5	-33.2**	-15.3
Temp. driving restriction	17.2**	7.1*	26.2**	8.2*	17.2*	9.2**	24.9**	6.3*

Notes: Figures are reported rounded to one decimal place and represent a percentage change with respect to the average of the corresponding dependent variable. Each estimate is based on the specification adopted in column (3) of Table 3.6, instrumenting the hourly AQI with an indicator variable for thermal inversions on the surface of Mexico City. We limit the observations to what occurred after May 29, 2019, from 05:00 to 22:00 hours. To perform inference, we use cluster bootstrap (CB) standard errors from 400 replications. The symbols ***, **, and * indicate significance at the 1%, 5%, and 10% levels, respectively.

To assess the robustness of our results, we use three additional indicators as income proxies. First, we use the social gap level (GRS) estimated by the National Council for Evaluation of Social Development Policy (CONEVAL) with data from the Census of Population and Housing 2020. The GRS considers the same dimensions as the GMU but uses a different methodology and combination of indicators to build the index (CONEVAL, 2021). For instance, instead of considering the availability of cell phone and internet service, the GRS considers whether households have a washing machine. As shown in Figure A3.7 from the Appendix, the spatial distribution of the GRS is very similar to that of the GMU.

Next, we employ the results of the Census of Population and Housing 2020 (INEGI, 2021) to compare the response of cyclists who rode their bikes in geographical areas where more than half of the inhabited private properties had their own vehicle (i.e., commuters with a higher income) versus the response of those who did it in areas with a lower percentage of vehicles (i.e., lower-income commuters). Finally, we use data from the most recent transportation survey applied to households in the ZMVM (INEGI, 2017) to distinguish geographic areas according to the number of vehicles per 1,000 inhabitants. The spatial distribution of these two indicators is presented in Figures A3.8 and A3.9 from the Appendix.

As shown in Table 3.7, our results hold when we take any of the four alternative income indicators. In line with Guerra and Reyes (2022), it seems that the greater availability of vehicles exempted or subject to fewer driving restrictions (either permanent or temporary), allow higher-income commuters to avoid environmental policies, even benefiting from a reduction in their travel times during environmental emergencies.

3.8. Conclusions

In this work we evaluate the effectiveness of the precautionary recommendations and temporary driving restrictions that are applied in accordance with the guidelines established

by the Atmospheric Environmental Emergencies Program (PCAA) to reduce polluting emissions and protect the health of the population when the concentrations of pollutants reach extremely high levels in Mexico City. Our study contributes to the existing literature by carefully distinguishing the effect of both measures, and by using for the first time a database that allows us to distinguish the behavioral responses of cyclists according to the purpose of their trips. Our work is also informative about the importance of cyclists' income level in moderating their responses to the program, leading to relevant implications for environmental and transportation policy in Mexico City.

We found that the PCAA is effective in reaching its target audience, persuading cyclists to change their behavior, reducing their cycling activity during the hours when it is recommended to avoid vigorous outdoor activities to reduce exposure to pollution and the associated health costs. Consistent with Saberian et al. (2017), our results indicate that cycling activity is reduced in a range of 9-27% due to the precautionary recommendations issued by CAMe during environmental emergencies in Mexico City.

However, as pointed out by Borbet et al. (2018), there is still a gap between awareness and action. Although the effects of the precautionary recommendations are substantial, most cyclists in Mexico City continue to exercise during environmental emergencies even with elevated levels of pollution. Considering that environmental emergencies are a rare event (they occurred in less than 2% of the hours analyzed in the period from January 2019 to March 2023), there is still plenty of room to inform and persuade cyclists to adopt more avoidance behaviors during environmental emergencies to benefit their health. A relatively inexpensive alternative that should be evaluated could include sending real-time air quality alerts through applications such as Strava and Ecobici, extensively used by cyclists just before starting their trips.

Consistent with de Buen Kalman (2021), we find that the temporary driving restrictions contemplated by the PCAA are effective in persuading commuters to reduce their polluting emissions, pushing them toward cleaner means of transportation such as bicycles. Our results indicate that commuter cyclists increase their cycling activity in a range of 8-13% in response to temporary driving restrictions. Considering that nearly 28% more private vehicles are subject to weekday driving restrictions due to environmental emergencies, the elasticity with respect to commuting cycling activity is between 0.29 and 0.46. That is, commuting cycling activity increases 2.9-4.6% (between 18 and 30 additional commuting trips in the case of Strava[27]) for every 10% of vehicles that are restricted from circulating on the roads of Mexico City during environmental emergencies, holding everything else constant.

However, our work demonstrates that the effectiveness of temporary driving restrictions is achieved at the expense of lower-income commuters. In line with the conclusions of

[27] Considering that Strava commuting trips travel an average distance of 2.1 km and that temporary driving restrictions are applied on average for 23 hours during environmental emergencies.

Gallego et al. (2013), and Guerra and Reyes (2022), we find that temporary driving restrictions are a regressive measure in Mexico City. While commuters with higher incomes (and greater availability of vehicles) increase their cycling activity by 6-9%, the response of commuters with lower incomes is almost three times greater, increasing their cycling activity between 17-26%.

Thus, while at least a group of the higher-income commuters—who contribute to the polluting emissions that trigger environmental emergencies—continues to drive thanks to their greater availability of vehicles, a portion of the lower-income commuters—who receive the greatest burden of driving restrictions—are forced to opt for cleaner means of transportation during environmental emergencies, at a greater cost for their health.

An alternative to reduce the regressivity of the measures imposed in the PCCA can contemplate the reduction of public transport fares during environmental emergencies as done in Stuttgart (Dangel & Goeschl, 2022). According to the price elasticity estimated by Davis (2021), a 100% reduction in the price of the Mexico City metro ticket would result in an increase in ridership of 25%. However, just as with temporary driving restrictions, this alternative would only serve as a containment measure that is far from solving the root problem. To do so, authorities could evaluate market alternatives such as the congestion charges that have been applied in London since 2003 (Green et al., 2016).

Finally, it is important to highlight and recognize the theoretical model developed by Cutter and Neidell (2009). Our results show that, with small modifications, this simple model manages to accurately predict what we found empirically for the case of Mexico City. Therefore, we recommend taking it as a basis in future studies to evaluate the a-priori effect of different variants of programs such as the STA in the San Francisco Bay Area, or the PCAA in Mexico City.

References

Angrist, J. D., & Pischke, J.-S. (2014). *Mastering 'metrics: The path from cause to effect*. Princeton University Press.

Arceo, E., Hanna, R., & Oliva, P. (2016). Does the effect of pollution on infant mortality differ between developing and developed countries? Evidence from Mexico City. *The Economic Journal*, *126*(591), 257-280. https://doi.org/10.1111/ecoj.12273

Barwick, P. J., Li, S., Lin, L., & Zou, E. (2023). From fog to smog: The value of pollution information. *NBER Working Paper Series*, 26541. https://doi.org/10.3386/w26541

Borbet, T. C., Gladson, L. A., & Cromar, K. R. (2018). Assessing Air Quality Index awareness and use in Mexico City. *BMC Public Health*, *18*, 538. https://doi.org/10.1186/s12889-018-5418-5

CAMe. (2020). *Air and Health Index: Characteristics and application*. Mexico City. Retrieved from https://www.gob.mx/comisionambiental/articulos/indice-de-calidad-del-aire-y-salud-caracteristicas-y-aplicacion

Caplan, A. J. (2023). Missing the warning signs? The case of "yellow air day" advisories in northern Utah. *Environmental and Resource Economics, 85*, 479–522. https://doi.org/10.1007/s10640-023-00773-7

CONAPO. (2021). *Urban marginalization index 2020*. Retrieved from https://www.gob.mx/cms/uploads/attachment/file/828844/urbana.pdf

CONEVAL. (2021). *Social gap index 2020: Main results.* Mexico City. Retrieved from https://www.coneval.org.mx/Medicion/Documents/IRS_2020/Nota_principales_resultados_IRS_2020.pdf

Cutter, W. B., & Neidell, M. (2009). Voluntary information programs and environmental regulation: Evidence from 'Spare the Air'. *Journal of Environmental Economics and Management*, *58*(3), 253-265. https://doi.org/10.1016/j.jeem.2009.03.003

Dangel, A., & Goeschl, T. (2022). Air quality alerts and don't drive appeals: Cautionary evidence from Germany. *AWI Discussion Paper Series, 718*. https://doi.org/10.11588/heidok.00032164

Davis, L. W. (2008). The effect of driving restrictions on air quality in Mexico City. *Journal of Political Economy*, *116*(1), 38-81. https://doi.org/10.1086/529398

Davis, L. W. (2017). Saturday Driving Restrictions Fail to Improve Air Quality in Mexico City. *Scientific Reports, 7,* 41652. https://doi.org/10.1038/srep41652

Davis, L. W. (2021). Estimating the price elasticity of demand for subways: Evidence from Mexico. *Regional Science and Urban Economics, 87,* 103651. https://doi.org/10.1016/j.regsciurbeco.2021.103651

de Buen Kalman, R. (2021). Can't drive today? The impact of driving restrictions on bikeshare ridership in Mexico City. *Transportation Research Part D: Transport and Environment, 91,* 102652. https://doi.org/10.1016/j.trd.2020.102652

Du, X. (2023). Symptom or Culprit? Social Media, Air Pollution, and Violence. *CESifo Working Papers No. 10296*. https://dx.doi.org/10.2139/ssrn.4380957

Eskeland, G. S., & Feyzioglu, T. (1997). Rationing can backfire: The "day without a car" in Mexico City. *The World Bank Economic Review, 11*(3), 383–408. https://doi.org/10.1093/wber/11.3.383

Ezcurra, E. (2009). Las inversiones térmicas. *Ciencias,* (22). Retrieved from https://www.revistas.unam.mx/index.php/cns/article/view/11206

Gallego, F., Montero, J.-P., & Salas, C. (2013). The effect of transport policies on car use: Evidence from Latin American cities. *Journal of Public Economics, 107,* 47-62. https://doi.org/10.1016/j.jpubeco.2013.08.007

García-Guadalupe, M. E., Ramírez-Sánchez, H. U., Ulloa Godínez, H., Arias, S., & Pérez, A. (2012). Las inversiones térmicas y la contaminación atmosférica en la Zona Metropolitana de Guadalajara (México). *Investigaciones Geográficas,* (58), 9-29. https://doi.org/10.14198/INGEO2012.58.01

Government of Mexico City. (2014). *Ordinance by which the Hoy No Circula program is issued in the Federal District*. Mexico City: Gaceta Oficial Distrito Federal. Retrieved from https://www.sedema.cdmx.gob.mx/storage/app/media/programas/hoy-no-circula/decreto-programa-hoy-no-circula-segundo-semestre-2016.pdf

Government of Mexico City. (2016a). *History of environmental pre-emergencies in Mexico City and its surroundings.* Ministry of Environment, Mexico City. Retrieved from http://www.aire.cdmx.gob.mx/descargas/ultima-hora/calidad-aire/pcaa/pcaa-historico-precontingencias.pdf

Government of Mexico City. (2016b). *Notice announcing the Atmospheric Environmental Emergencies Program in Mexico City*. Ministry of Environment. Mexico City: Gaceta Oficial de la Ciudad de México. Retrieved from https://data.consejeria.cdmx.gob.mx/portal_old/uploads/gacetas/9084adeae18b748216271dc1b25792c4.pdf

Government of Mexico City. (2018). *Notice announcing the environmental standard NADF-009-AIRE-2017, which establishes the requirements to prepare the Air Quality Index in Mexico City*. Ministry of Environment. Mexico City: Gaceta Oficial de la Ciudad de México. Retrieved from https://data.consejeria.cdmx.gob.mx/portal_old/uploads/gacetas/b319229ffe56762edeba326d02ef83d0.pdf

Government of Mexico City. (2019a). *Modification of Atmospheric Environmental Emergencies Program*. Ministry of Environment, Mexico City. Retrieved from http://www.aire.cdmx.gob.mx/descargas/ultima-hora/calidad-aire/pcaa/pcaa-modificaciones.pdf

Government of Mexico City. (2019b). *Notice announcing the Atmospheric Environmental Emergencies Program in Mexico City*. Ministry of Environment. Mexico City: Gaceta Oficial de la Ciudad de México. Retrieved from https://data.consejeria.cdmx.gob.mx/portal_old/uploads/gacetas/25a1ef7295458ade0faad3daebb31f05.pdf

Government of Mexico City. (2020a). *Ecobici Survey 2020*. Mexico City Ministry of Transportation, Mexico City. Retrieved from https://ecobici.cdmx.gob.mx/wp-content/uploads/2022/07/encuesta_2020_rv4_2.pdf

Government of Mexico City. (2020b). *Fourth Agreement by which extraordinary actions are determined in Mexico City to address the Declaration of Phase 3 of the health emergency due to force majeure, with the purpose of avoiding contagion*. Mexico City: Gaceta Oficial de la Ciudad de México. Retrieved from https://data.consejeria.cdmx.gob.mx/portal_old/uploads/gacetas/7b1dd0fb767629e618b9bab5ad294a59.pdf

Government of Mexico City. (2023a). *History of environmental emergencies in Mexico City and its surroundings*. Ministry of Environment, Mexico City. Retrieved from http://www.aire.cdmx.gob.mx/descargas/ultima-hora/calidad-aire/pcaa/pcaa-historico-contingencias.pdf

Government of Mexico City. (2023b). *Notice announcing the Mandatory Vehicle Verification Program for the second semester of 2023*. Ministry of Environment. Mexico City: Gaceta Oficial de la Ciudad de México. Retrieved from https://data.consejeria.cdmx.gob.mx/portal_old/uploads/gacetas/df2e4d42390f65c04e681ed0c6f7a616.pdf

Gellman, J., Walls, M., & Wibbenmeyer, M. (2022). Wildfire, smoke, and outdoor recreation in the western United States. *Forest Policy and Economics*, *134*, 102619. https://doi.org/10.1016/j.forpol.2021.102619

Guerra, E., & Millard-Ball, A. (2017). Getting around a license-plate ban: Behavioral responses to Mexico City's driving restriction. *Transportation Research Part D: Transport and Environment*, *55*, 113-126. https://doi.org/10.1016/j.trd.2017.06.027

Guerra, E., & Reyes, A. (2022). Examining behavioral responses to Mexico City's driving restriction: A mixed methods approach. *Transportation Research Part D: Transport and Environment*, *104*, 103191. https://doi.org/10.1016/j.trd.2022.103191

Guerra, E., Sandweiss, A., & Park, D. S. (2022). Does rationing really backfire? A critical review of the literature on license-plate-based driving restrictions. *Transport Reviews*, *42*(5), 604-625. https://doi.org/10.1080/01441647.2021.1998244

Guerra, E., Zhang, H., Hassall, L., Wang, J., & Cheyette, A. (2020). Who cycles to work and where? A comparative multilevel analysis of urban commuters in the US and Mexico. *Transportation Research Part D: Transport and Environment*, *87*, 102554. https://doi.org/10.1016/j.trd.2020.102554

Green, C. P., Heywood, J. S., & Navarro, M. (2016). Traffic accidents and the London Congestion Charge. *Journal of Public Economics*, *133*, 11-22. https://doi.org/10.1016/j.jpubeco.2015.10.005

Huang, J., Xing, J., & Zou, E. (2023). (Re)scheduling pollution exposure: The case of surgery schedules. *Journal of Public Economics*, *219*, 104825. https://doi.org/10.1016/j.jpubeco.2023.104825

INEGI. (2017). *Origin-Destination Survey in Households of the Metropolitan Zone of the Valley of Mexico (EOD) 2017*. Retrieved from https://en.www.inegi.org.mx/programas/eod/2017/#microdata

INEGI. (2021). *Census of Population and Housing 2020*. Retrieved from Main results by the AGEB and urban block: https://en.www.inegi.org.mx/programas/ccpv/2020/#microdata

Ito, K., & Zhang, S. (2020). Willingness to pay for clean air: Evidence from air purifier markets in China. *Journal of Political Economy*, *128*(5), 1627-1672. https://doi.org/10.1086/705554

Keiser, D., Lade, G., & Rudik, I. (2018). Air pollution and visitation at U.S. national parks. *Science Advances*, *4*(7). https://doi.org/10.1126/sciadv.aat1613

Liang, Y., Wang, D., Yang, H., Yuan, Q., & Yang, L. (2023). Examining the causal effects of air pollution on dockless bike-sharing usage using instrumental variables. *Transportation Research Part D: Transport and Environment*, *121*, 103808. https://doi.org/10.1016/j.trd.2023.103808

MacKinnon, J. G., Nielsen, M. Ø., & Webb, M. D. (2023). Cluster-robust inference: A guide to empirical practice. *Journal of Econometrics*, *232*(2), 272-299. https://doi.org/10.1016/j.jeconom.2022.04.001

Noonan, D. S. (2014). Smoggy with a chance of altruism: The effects of ozone alerts on outdoor recreation and driving in Atlanta. *The Policy Studies Journal*, *42*, 122-145. https://doi.org/10.1111/psj.12045

Oliva, P. (2015). Environmental regulations and corruption: Automobile emissions in Mexico City. *Journal of Political Economy*, *123*(3), 686-724. https://doi.org/10.1086/680936

Retama, A., Neria-Hernández, A., Jaimes-Palomera, M., Rivera-Hernández, O., Sánchez-Rodríguez, M., López-Medina, A., & Velasco, E. (2019). Fireworks: A major source of inorganic and organic aerosols during Christmas and New Year in Mexico City. *Atmospheric Environment: X*, *2*, 100013. https://doi.org/10.1016/j.aeaoa.2019.100013

Rivera, N. M. (2021). Air quality warnings and temporary driving bans: Evidence from air pollution, car trips, and mass-transit ridership in Santiago. *Journal of Environmental Economics and Management, 108*, 102454. https://doi.org/10.1016/j.jeem.2021.102454

Roodman, D., MacKinnon, J. G., Nielsen, M. Ø., & Webb, M. D. (2019). Fast and wild: Bootstrap inference in Stata using boottest. *The Stata Journal*, 19(1), 4-60. https://doi.org/10.1177/1536867X19830877

Saberian, S., Heyes, A., & Rivers, N. (2017). Alerts work! Air quality warnings and cycling. *Resource and Energy Economics*, *49*, 165-185. https://doi.org/10.1016/j.reseneeco.2017.05.004

SEMARNAT. (2019). *Guidelines for obtaining and communicating the Air Quality and Health Risk Index*. Mexico City: Diario Oficial de la Federación. Retrieved from https://www.dof.gob.mx/nota_detalle.php?codigo=5579387&fecha=20/11/2019

Tribby, C. P., Miller, H. J., Song, Y., & Smith, K. R. (2013). Do air quality alerts reduce traffic? An analysis of traffic data from the Salt Lake City metropolitan area, Utah, USA. *Transport Policy*, *30*, 173-185. https://doi.org/10.1016/j.tranpol.2013.09.012

Wang, Z., & Zhang, J. (2023). The value of information disclosure: Evidence from mask consumption in China. *Journal of Environmental Economics and Management*, *122*, 102865. https://doi.org/10.1016/j.jeem.2023.102865

Welch, E., Gu, X., & Kramer, L. (2005). The effects of ozone action day public advisories on train ridership in Chicago. *Transportation Research Part D: Transport and Environment*, *10*(6), 445-458. https://doi.org/10.1016/j.trd.2005.06.002

Williams, A. M. (2019). Understanding the micro-determinants of defensive behaviors against. *Ecological Economics*, *163*, 42-51. https://doi.org/10.1016/j.ecolecon.2019.05.007

Xu, Y., Liu, Y., Chang, X., & Huang, W. (2021). How does air pollution affect travel behavior? A big data field study. *Transportation Research Part D: Transport and Environment*, *99*, 103007. https://doi.org/10.1016/j.trd.2021.103007

Yoo, G. (2021). Real-time information on air pollution and avoidance. *Population and Environment*, *42*, 406–424. https://doi.org/10.1007/s11111-020-00368-0

Zhang, J., & Mu, Q. (2018). Air pollution and defensive expenditures: Evidence from particulate-filtering facemasks. *Journal of Environmental Economics and Management*, *92*, 517-536. https://doi.org/10.1016/j.jeem.2017.07.006

Zhao, P., Li, S., Li, P., Liu, J., & Long, K. (2018). How does air pollution influence cycling behaviour? Evidence from Beijing. *Transportation Research Part D: Transport and Environment*, *63*, 826-838. https://doi.org/10.1016/j.trd.2018.07.015

Zivin, J. G., & Neidell, M. (2009). Days of haze: Environmental information disclosure and intertemporal avoidance behavior. *Journal of Environmental Economics and Management*, *58*(2), 119-128. https://doi.org/10.1016/j.jeem.2009.03.001

Appendix

Table A3.1. Main recommendations and mandatory measures to protect public health and reduce emissions from vehicles during emergencies in the Valley of Mexico (2019-2023).

	Pollutant that caused emergency			
	Before May 29, 2019		After May 29, 2019	
	O_3	PM_{10}	O_3	PM^{*}
a) Health				
Precautionary recommendations				
▪ Stay informed about air quality.	✓	✓	✓	✓
▪ Avoid outdoor activities, especially those that require vigorous effort or are executed by vulnerable groups[**].	✓	✓	✓	✓
▪ No smoking, especially indoors.	✓	✓	✓	✓
▪ Postpone massive outdoor events[**].			✓	✓
▪ Keep doors and windows closed. Use air conditioning in recirculation mode.				✓
Mandatory measures				
▪ Suspend outdoor activities organized by public and private institutions[**].			✓	
b) Transportation				
Precautionary recommendations				
▪ Reduce the use of private vehicles, carpool, and use the public transport service.	✓	✓	✓	✓
▪ Allow remote work for employees.	✓	✓	✓	✓
Mandatory measures				
▪ Expedite traffic flow. Suspend public works and infrastructure maintenance that hinder traffic.	✓	✓	✓	✓
▪ Partially restrict driving to gasoline, diesel, and LP gas delivery vehicles[***].	✓	✓	✓	
▪ Restrict driving to non-exempt freight transport from 06:00 to 10:00 hrs.	✓	✓	✓	✓
▪ Allow driving to taxis (restricted by HNC) from 05:00 to 10:00 hrs.	✓	✓	✓	✓
▪ Restrict driving to all vehicles with verification hologram 2, and a portion of vehicles with hologram "1"[***].	✓	✓		
▪ Restrict driving to all vehicles with verification hologram "2", and a portion of vehicles with holograms "1", "0", and "00"[***].			✓	✓
▪ Restrict driving to non-exempt official administrative government vehicles.			✓	✓

▪ Monitor compliance and sanction vehicles that ignore driving restrictions.	✓	✓	✓	✓

Notes: The recommendations and required action included correspond to the phase 1 of environmental emergencies. These actions also include the partial suspension of economic activities from establishments identified as major sources of emissions—as well as those without emissions control equipment—in the commerce, services, and manufacturing sectors. *Including PM_{10} and $PM_{2.5}$. **In the case of ozone, these required actions and recommendations apply from 13:00 to 19:00 hrs. ***Driving restrictions are in addition to those imposed by the Hoy No Circula (HNC) program. They begin the day after the emergency is activated and end the day the emergency is suspended. The restriction applies from 05:00 to 22:00 hrs. Source: Adapted from Government of Mexico City (2016b, 2019b).

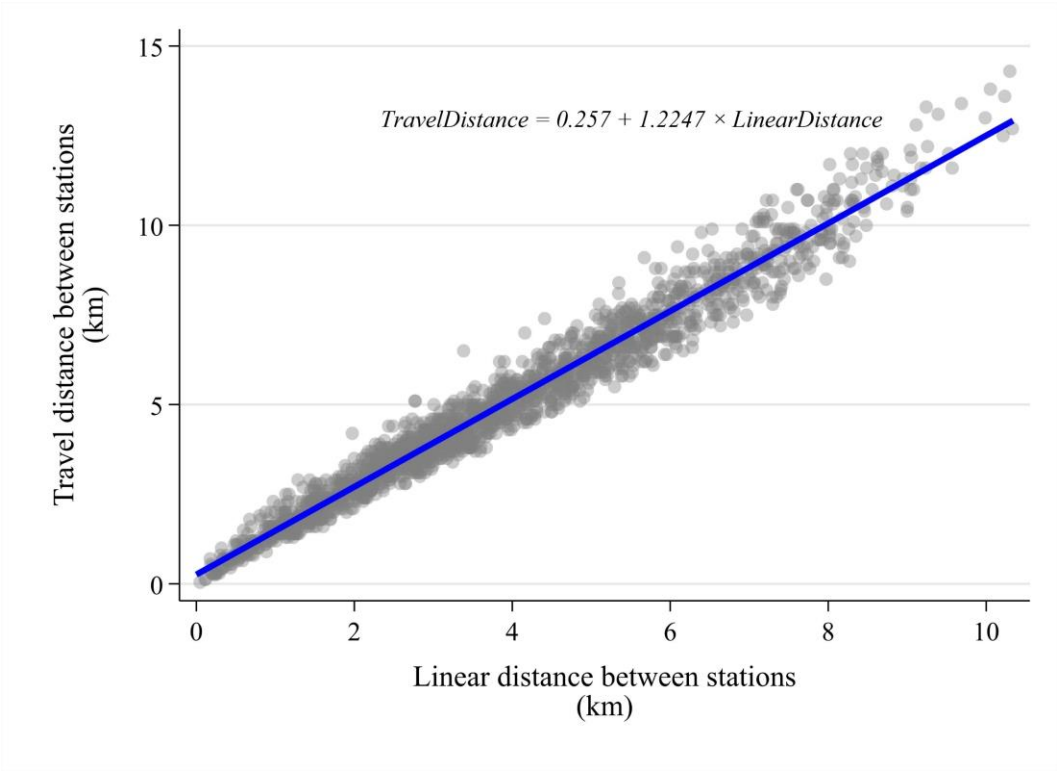

Figure A3.2. Traveled vs. linear distance between origin-destination Ecobici station pairs in Mexico City. Notes: Each point correspond to one out of the 1,800 random sampled pair of origin-destination bike-sharing stations. Travel distance was obtained searching for the shortest route by bicycle between each station pair using Google Maps. Source: Prepared combining data from Ecobici and Google Maps.

Table A3.3. The marginal effect of thermal inversions on the Air Quality Index (AQI)

	(1)	(2)	(3)	(4)	(5)	(6)	(7)
Thermal inversion	5.19***	5.30***	4.83***	4.34***	6.55***	2.60***	0.03
	(0.46)	(0.48)	(0.47)	(0.53)	(0.41)	(0.45)	(0.38)
Thermal inversion × Intensity						2.51***	2.34***
						(0.18)	(0.18)
Thermal inversion × Thickness							0.01***
							(0.00)
Mean AQI	71.26	69.79	70.09	69.79	70.53	69.79	69.79
R^2 (within)	0.42	0.40	0.42	0.42	0.41	0.40	0.40
N	416,160	375,904	278,528	375,904	70,482	375,904	375,904
From 05:00 to 22:00 hrs.	✓	✓	✓	✓	✓	✓	✓
After May 29, 2019		✓	✓	✓	✓	✓	✓
Robustness checks:							
Excluding 2020			✓				
Non-linear temperature				✓			
Municipalities Cuauhtémoc, B. Juárez and M. Hidalgo					✓		
Including characteristics of thermal inversion						✓	✓

Notes: Estimates are reported rounded to one decimal. Columns (1) to (5) are obtained estimating equation (6), while columns (6) and (7) are obtained from equation (7). Standard errors clustered at the municipality level are presented within parenthesis. The symbols ***, **, and * indicate significance at the 1%, 5%, and 10% levels, respectively.

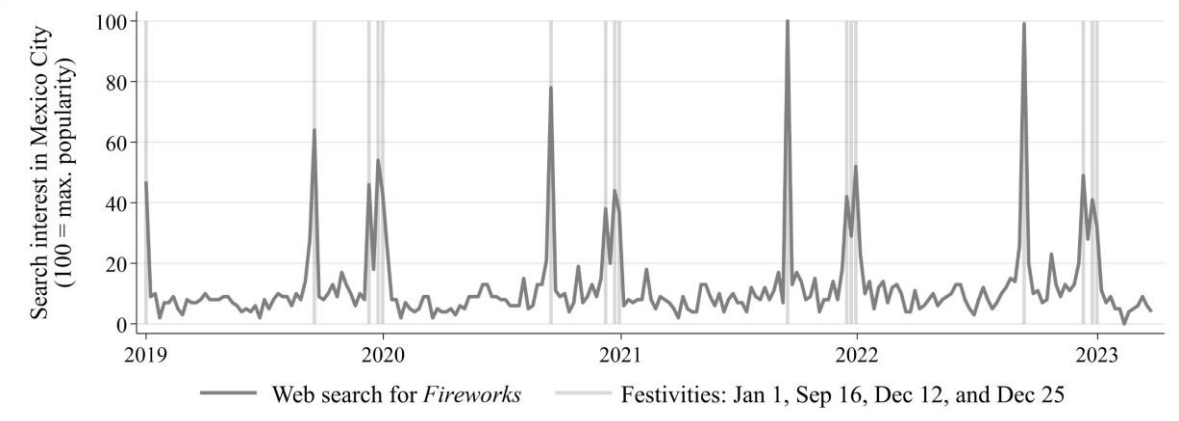

Figure A3.4. Search interest for "Fireworks" during festivities in Mexico City. Source: Adapted from Google Trends. Data available at https://trends.google.es/trends/explore?date=2018-12-30%202023-03-31&geo=MX-DIF&q=Cohetes

Table A3.5. The marginal effect of env. emergencies and temp. restrictions on cycling activity (km)

	Main results			Robustness checks						
	(1)	(2)	(3)	(4)	(5)	(6)	(7)	(8)	(9)	(10)
Strava – Leisure										
Emergency	-7.7**	-17.5***	-21.5***	-16.0***	-23.0***	-24.7***	-21.8***	-6.2***	-	-
	(3.2)	(5.9)	(5.4)	(3.8)	(5.9)	(8.3)	(5.5)	(2.2)		
Temporary driving restriction	-5.4	-3.4	-5.2	-6.1*	-2.7	-4.9	-4.8	-1.0	-	-
	(4.6)	(3.7)	(3.4)	(3.7)	(3.5)	(3.4)	(3.3)	(0.8)		
R^2 (within)	0.28	0.29	0.28	0.29	0.28	0.28	0.28	0.22	-	-
N (thousands)	421.9	381.6	375.9	278.5	375.9	375.9	375.9	352.4	-	-
Strava – Commute										
Emergency	-0.6*	-0.6	-0.7**	-0.7**	-0.7**	-0.6**	-0.8**	-0.5	-	-
	(0.3)	(0.4)	(0.3)	(0.3)	(0.3)	(0.3)	(0.3)	(0.3)		
Temporary driving restriction	0.4**	0.5**	0.4**	0.5**	0.3**	0.4**	0.4**	0.2	-	-
	(0.1)	(0.2)	(0.2)	(0.2)	(0.1)	(0.2)	0.2)	(0.1)		
R^2 (within)	0.13	0.13	0.13	0.14	0.13	0.13	0.13	0.13	-	-
N (thousands)	421.6	381.6	375.9	278.5	375.9	375.9	375.9	352.4	-	-
Ecobici – Weekends										
Emergency	61.2	66.4	61.4	67.6	62.8	99.9	62.5	-	63.9	-2.5
	(46.7)	(57.9)	(48.1)	(44.7)	(48.9)	(65.8)	(48.4)		(46.2)	(2.0)
Temporary driving restriction	-5.1	2.5	1.9	-6.4	-0.3	6.3	0.5	-	4.3	-2.4
	(20.2)	(22.1)	(17.3)	(18.4)	(17.2)	(15.9)	(17.7)		(12.6)	(5.7)
R^2 (within)	0.50	0.49	0.49	0.48	0.49	0.50	0.49	-	0.51	0.31
N (thousands)	23.7	21.6	20.9	15.7	20.9	20.9	20.9	-	20.9	20.9
Ecobici – Weekdays										
Emergency	4.1	-35.7***	-41.7***	-42.0***	-53.1***	48.7**	-38.5***	-	-36.8***	-4.9***
	(20.6)	(5.9)	(7.6)	(14.7)	(7.0)	(20.8)	(6.9)		(7.9)	(1.3)
Temporary driving restriction	-37.3*	6.8	6.6	5.0	24.6***	-4.4	5.1	-	3.7	2.9
	(12.5)	(7.8)	(8.4)	(8.8)	(7.5)	(7.9)	(8.1)		(7.0)	(2.5)
R^2 (within)	0.55	0.53	0.53	0.51	0.53	0.53	0.53	-	0.54	0.35
N (thousands)	59.5	54.1	53.6	40.5	53.6	53.6	53.6	-	53.6	53.6
After May 29, 2019		✓	✓	✓	✓	✓	✓	✓	✓	✓
Instrumenting AQI			✓	✓	✓	✓	✓	✓	✓	✓
Robustness checks:										
Excludes 2020				✓						
Shorter driving restrictions					✓					
Non-linear temperature						✓				
Additional instruments							✓			
Segments near cycle paths								✓		
One-way trips									✓	
Round trips										✓

Notes: Estimates are reported rounded to one decimal place and represent a marginal change expressed in kilometers. Columns (1) and (2) are obtained estimating equation (5). For these columns, we present standard errors clustered at the municipality level within parenthesis. Estimates from column (3) to (10), further instrumented the hourly AQI with an indicator variable for thermal inversions. We report cluster bootstrap (CB)

standard errors from 400 replications for these columns. The symbols ***, **, and * indicate significance at the 1%, 5%, and 10% levels, respectively.

Table A3.6. Percentage change of cycling activity caused by emergencies and temporary driving restrictions

	Main results			Robustness checks						
	(1)	(2)	(3)	(4)	(5)	(6)	(7)	(8)	(9)	(10)
Strava – Leisure										
Emergency	-9.0**	-19.5***	-24.0***	-16.5***	-25.6***	-27.5***	-24.3***	-25.2***	-	-
Temp. driving restriction	-6.4	-3.8	-5.8	-6.3	-3.0	-5.4	-5.4	-4.0	-	-
Strava – Commute										
Emergency	-15.7*	-17.7	-19.9**	-16.8**	-18.4**	-16.3**	-20.8**	-18.1	-	-
Temp. driving restriction	10.5**	12.9**	11.0**	10.9**	8.3*	10.5**	11.7**	8.0	-	-
Ecobici – Weekends										
Emergency	13.7	15.1	13.9	14.3	14.2	22.7	14.2	-	16.7	-4.3
Temp. driving restriction	-1.1	0.6	0.4	-1.4	-0.1	1.4	0.1	-	1.1	-4.2
Ecobici – Weekdays										
Emergency	0.5	-4.6***	-5.3**	-5.1*	-6.8***	6.2	-4.9**	-	-5.1**	-9.1**
Temp. driving restriction	-4.5*	0.9	0.8	0.6	3.1**	-0.6	0.7	-	0.5	5.3
After May 29, 2019		✓	✓	✓	✓	✓	✓	✓	✓	✓
Instrumenting AQI			✓	✓	✓	✓	✓	✓	✓	✓
Robustness checks:										
Excludes 2020				✓						
Shorter driving restrictions					✓					
Non-linear temperature						✓				
Additional instruments							✓			
Segments near cycle paths								✓		
One-way trips									✓	
Round trips										✓

Notes: Estimates are reported rounded to one decimal place and represent a percentage change with respect to the average of the corresponding dependent variable. They are the same estimates presented in Table 3.6, with the difference that in columns (3) to (10) we employ wild cluster bootstrap (WCB) inference from 9,999 bootstrap samples using the 'boottest' package in Stata (Roodman et al., 2019), considering that our number of clusters is small (MacKinnon et al., 2023). The symbols ***, **, and * indicate significance at the 1%, 5%, and 10% levels, respectively.

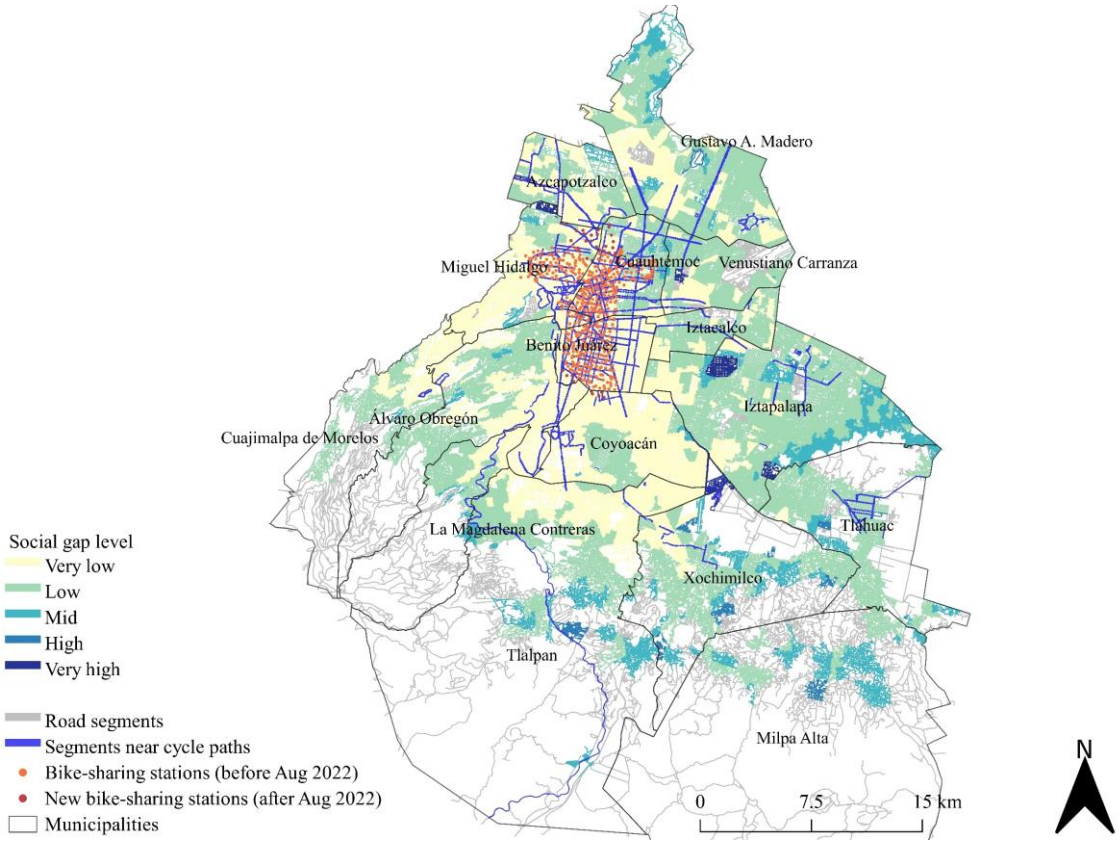

Figure A3.7. Social gap level (GRS 2020) in Mexico City. Source: Prepared using data from the National Council for the Evaluation of Social Development Policy (CONEVAL) and Mexico City Ministry of Transport.

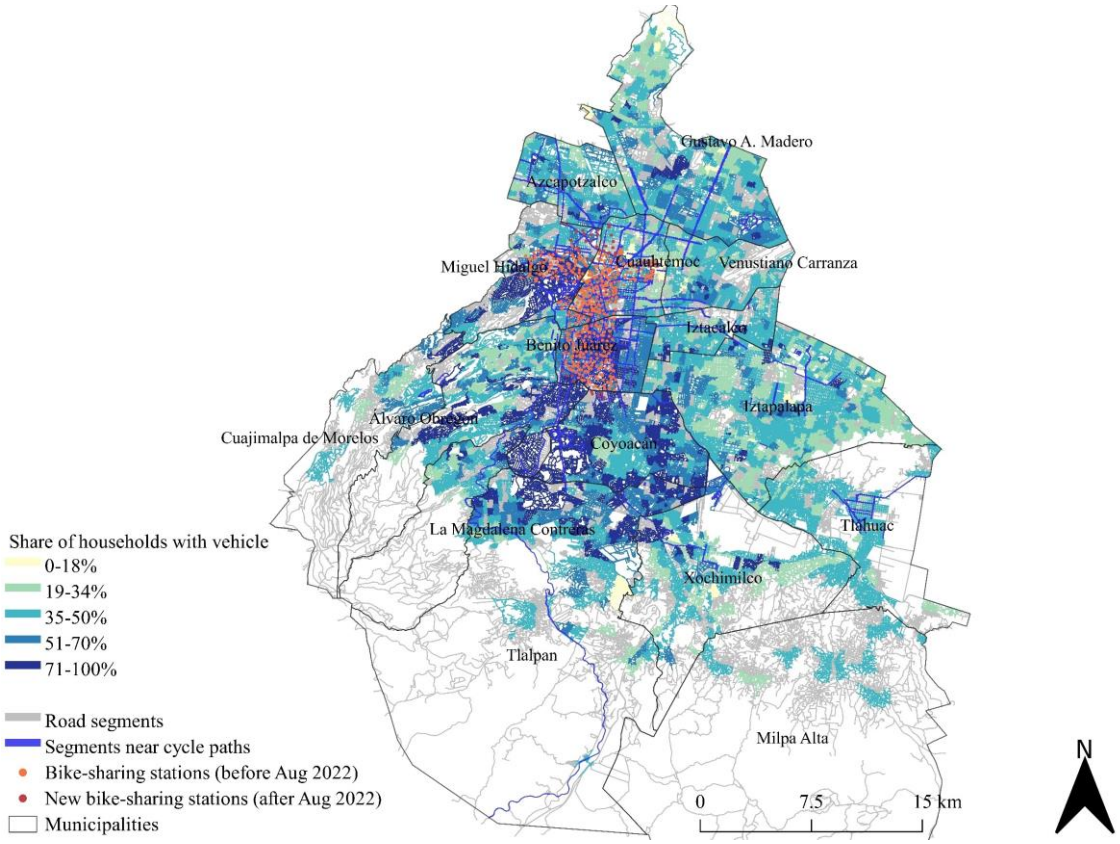

Figure A3.8. Share of households with vehicle in Mexico City. Source: Prepared using data from the Census of Population and Housing 2020 (INEGI, 2021) and Mexico City Ministry of Transport.

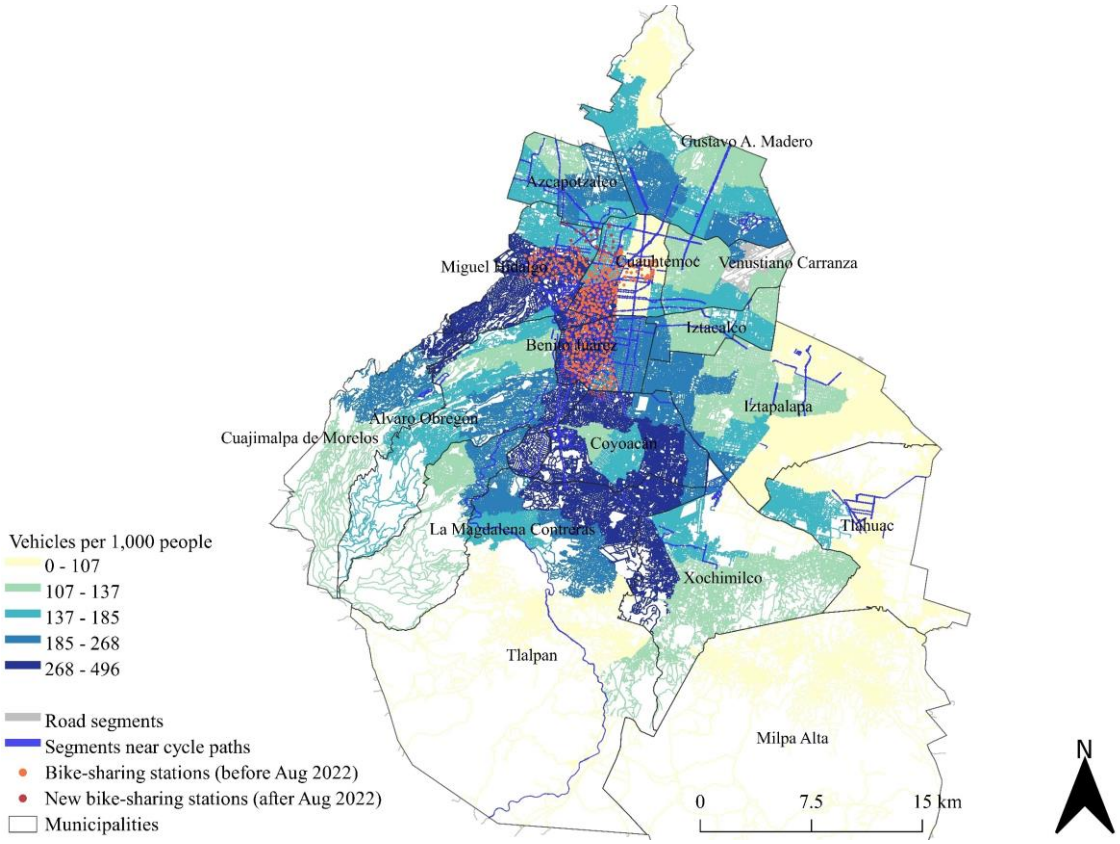

Figure A3.9. Vehicles per 1,000 people in Mexico City. Source: Prepared using data from a transportation household survey for the ZMVM (INEGI, 2017) and Mexico City Ministry of Transport.